

Solutions for Interharmonics in Variable Speed Drives for LNG Plants

By

Michel Verhulst

Master of Science Thesis

Delft University of Technology

August 26, 2011

Supervisor:

Dr. ir. Henk Polinder

Committee members:

Prof.dr. eng. J.A. Ferreira, Technical University of Delft, the Netherlands,

Dr.ir. H. Polinder, Technical University of Delft, the Netherlands,

Prof.dr. ir. H. Hellendoorn, Technical University of Delft, the Netherlands,

S. Copple, Principal Technical Expert Shell Projects and Technology, Shell Global Solutions International BV, the Netherlands

In corporation with Shell Global Solutions International BV

Abstract

Variable speed drives can cause components of any frequency known as interharmonics. Large variable speed drives in the order of tens of megawatts can replace Gas Turbines in driving cooling compressors in a Liquefied Natural Gas Plant. The drives used in this application are among the largest drives that are built today. As a consequence the effect of the interharmonics is also much larger than in other applications. These interharmonics can cause torques on the resonance frequencies of the Gas Turbine Generators used to produce the electric power. Without mitigation this can cause fatigue or even catastrophic failure of the shaft. Reliability is of utmost importance as every day a plant is down can cost tens of millions of Euros due to lost revenue.

First the basic principles including the creation and the effect of interharmonics are thoroughly researched. Hereafter different solutions, both new and existing, are researched. The most promising solution is to avoid constant excitation of the resonance by avoiding constant creation of the same interharmonic. This is first tested on small scale to find the most effective way to limit the torque caused by resonance. A model of a full scale plant is built to verify its effectiveness.

Acknowledgements

This thesis research was done in collaboration with Shell Global Solutions. I would like to thank them, and in particular Wim de Wilt and Steve Copple, my mentor and daily supervisor respectively, for the research topic and all the support during the research.

I would also like to thank the Power Engineering group from Delft University of Technology, and in particular my supervisor Henk Polinder, for the support during the research.

Furthermore I would like to thank the people at Siemens and Mott McDonald who took the time to discuss their views on this subject in great depth.

Table of Contents

Abstract.....	IV
Acknowledgements.....	V
Table of Contents.....	VI
Table of Figures.....	VIII
Abbreviations.....	XII
1 Introduction	1
2 Background	2
2.1 LNG	2
2.2 Harmonics and Interharmonics	5
2.3 Gas Turbine Generator Resonance.....	9
2.4 Converters	16
2.4.1 Voltage Source Inverters.....	16
2.4.2 Load Commutated Inverters	18
2.4.3 Pulse number	19
3 Possible Solutions	22
3.1 Passive Filters	23
3.2 Active Filters	24
3.3 Active Front End	26
3.4 Multi-level VSI.....	27
3.5 Multi-phase	30
3.6 Multi-pole	31
3.7 Increased motor speed.....	33
3.8 Damper	34
3.9 Speed through	35
3.10 Mechanical torques insertion.....	36
3.11 Firing pulse	37
3.12 Summary of solutions.....	42
4 System Simulation.....	43
4.1 Overview.....	43
4.2 Motor model	44
4.3 Generator model	48
4.4 LCI model	50

4.4.1	Rectifier.....	50
4.4.2	Inverter.....	54
4.4.3	DC-Link.....	57
4.4.4	Total system.....	58
4.5	Gas and Steam turbine model.....	62
4.6	Compressor Model.....	67
4.7	Grid.....	68
4.7.1	Transformer.....	68
4.7.2	Cables.....	70
4.7.3	Network.....	71
4.8	Controller.....	80
4.9	Validation.....	82
4.10	Results.....	84
5	Solution simulations.....	86
5.1	Constant sinusoidal frequency variations.....	86
5.2	Frequency variations: other waveforms.....	89
5.3	Dynamic frequency variations.....	90
5.4	Torque feedback.....	91
5.5	Effect of speed variations.....	93
5.6	Effect of firing angle variations.....	94
5.7	Total system result.....	95
6	Conclusion.....	97
Appendix 1	References.....	99
Appendix 2	Rectifier MATLAB code.....	102
Appendix 3	Inverter MATLAB Code.....	106

Table of Figures

Figure 1: Simplified LNG production	2
Figure 2: Traditional setup[3]	3
Figure 3: All electric setup[3]	3
Figure 4: Power consumption of Throttle Control and VSD [4]	4
Figure 5: Ideal AC side current	5
Figure 6: AC side current with DC ripple	6
Figure 7: Simple Campbell diagram of a 6 pulse converter connected to a 2 pole machine	7
Figure 8: Elaborate Campbell diagram of a 6 pulse converter connected to a 2 pole machine.....	8
Figure 9: Alstom GT26 Gas turbine rotor	9
Figure 10: Four mass model	9
Figure 11: Multi-mass model element	10
Figure 12: Multi-mass model	11
Figure 13: Multi-mass pulse time response	12
Figure 14: Multi-mass pulse frequency response	12
Figure 15: Continuous excitation on a resonance frequency	13
Figure 16: Continuous excitation near a resonance point	14
Figure 17: Slow Sweep passed a resonance point	14
Figure 18: Fast Sweep passed a resonance point	15
Figure 19: VSI setup (Diode rectifier, IGBT inverter)	16
Figure 20: LCI setup	18
Figure 21: 6-pulse rectifier	20
Figure 22: 12-pulse rectifier	20
Figure 23: 6-pulse rectifier waveform	20
Figure 24: 12-pulse rectifier waveform	20
Figure 25: 6-pulse rectifier spectrum	20
Figure 26: 12-pulse rectifier spectrum	20
Figure 27: 12-pulse LCI with two independent DC links	21
Figure 28: 12-pulse LCI with single DC Link	21
Figure 29: 12-pulse LCI with two mutually coupled DC links	21
Figure 30: C-type filter	23
Figure 31: Second order High Pass filter	23
Figure 32: Shunt Active Filter	24
Figure 33: Series Active Filter	24
Figure 34: LCI with DC ripple reinjection	25
Figure 35: VSI with Active Front End	26
Figure 36: Neutral Point Clamped VSI	27
Figure 37: Floating Symmetrical Capacitor VSI	28
Figure 38: Cascaded H-Bridge VSI	29
Figure 39: 2 Pole rotor	31
Figure 40: 4 Pole rotor	31
Figure 41: Allowed and forbidden speed bands	32
Figure 42: Mechanical damper	34

Figure 43: Continuous excitation	37
Figure 44: Constant excitation with 1.2Hz disturbance with a 10 second period	38
Figure 45: Continuous excitation with carrier inversion every five seconds	39
Figure 46: Continuous excitation with carrier inversion every second	39
Figure 47: 10-20Hz 0.1Hz sweep without carrier inversion.....	40
Figure 48: 10-20Hz 0.1Hz sweep with carrier inversion every second	40
Figure 49: Campbell diagram for a PWM VSI with 500Hz (fsw1) or 600Hz (fsw2) PWM carrier	41
Figure 50: Simulated system overview	43
Figure 51: dq system equivalent d circuit	44
Figure 52: dq system equivalent q circuit	44
Figure 53: Motor model.....	46
Figure 54: Generator model.....	48
Figure 55: LCI setup.....	50
Figure 56: Rectifier Simulink implementation	51
Figure 57: Grid voltage.....	52
Figure 58: Rectifier 1 output voltage	53
Figure 59: Rectifier 1 input current.....	53
Figure 60: Rectifier 2 output voltage	53
Figure 61: Rectifier 2 input current.....	53
Figure 62: Combined rectifier output voltage	53
Figure 63: Combined input current.....	53
Figure 64: Inverter Simulink implementation.....	55
Figure 65: Inverter 1 output current.....	56
Figure 66: Inverter 1 output voltage.....	56
Figure 67: Inverter 2 output current.....	56
Figure 68: Inverter 2 output voltage.....	56
Figure 69: Combined inverters output current.....	56
Figure 70: Combined inverters output voltage.....	56
Figure 71: Inverter 1 input voltage	57
Figure 72: Inverter 2 input voltage	57
Figure 73: Combined inverter input voltage.....	57
Figure 74: DC-Link Simulink implementation.....	58
Figure 75: LCI Simulink implementation	58
Figure 76: Rectifier input current.....	60
Figure 77: Inverter output current.....	60
Figure 78: DC-link current	60
Figure 79: Rectifier input current non ideal.....	60
Figure 80: Inverter output current non ideal.....	60
Figure 81: Interharmonics generated by the LCI model	61
Figure 82: GT model.....	62
Figure 83: Combined Cycle model	62
Figure 84: Combined Cycle Simulink Implementation.....	63
Figure 85: Total system Simulink implementation	64
Figure 86: Multi-Mass inertia Simulink implementation	64
Figure 87: Simplified total system Simulink implementation	66

Figure 88: Compressor Simulink implementation	67
Figure 89: Transformer model	68
Figure 90: LCI input transformer model.....	68
Figure 91: Cable Model	70
Figure 92: System network	71
Figure 93: Network with transformers shifted to the input	72
Figure 94: Simplified network	73
Figure 95: Network after applying two simplification steps.....	74
Figure 96: State Space Network.....	75
Figure 97: Controller Simulink implementation	80
Figure 98: Speed controller Simulink implementation	80
Figure 99: Current controller Simulink implementation.....	80
Figure 100: Field voltage controller Simulink implementation	81
Figure 101: LCI input spectrum with 5mH DC-link inductance	82
Figure 102: Generator input spectrum with 5mH DC-link inductance	82
Figure 103: LCI input spectrum with 10mH DC-link inductance	82
Figure 104: Generator input spectrum with 10mH DC-link inductance	82
Figure 105: Generator current spectrum all drives at 48.74Hz	84
Figure 106: Torque on coupling 2-3 all drives at 48.74Hz	84
Figure 107: Generator current spectrum all drives on 48.85Hz	85
Figure 108: Torque on coupling 2-3 all drives on 48.85Hz	85
Figure 109: Second test model	86
Figure 110: Constant excitation signal (14.973Hz)	87
Figure 111: Torque with constant excitation.....	87
Figure 112: Sloppy excitation signal (1,2Hz variation, 10s period).....	88
Figure 113: Torque with sloppy excitation	88
Figure 114: Constant excitation signal (15.4Hz)	88
Figure 115: Torque with constant excitation.....	88
Figure 116: Sloppy excitation signal (1,2Hz variation, 10s period).....	88
Figure 117: Torque with sloppy excitation	88
Figure 118: Excitation signal with triangular disturbance	89
Figure 119: Torque with triangular disturbance	89
Figure 120: Excitation signal with square wave disturbance (1,2Hz variation, 10s period)	89
Figure 121: Torque with square wave disturbance	89
Figure 122: Torque with square wave disturbance for various frequencies	90
Figure 123: Torques with sinusoidal disturbances with dynamic parameters	91
Figure 124: Sweep without mitigation measures	92
Figure 125: Sweep with torque feedback.....	92
Figure 126: LCI input current spectrum without mitigation.....	93
Figure 127: Torque on coupling 2-3 without mitigation.....	93
Figure 128: LCI input current spectrum with sinusoidal speed variation	94
Figure 129: Torque on coupling 2-3 with sinusoidal speed variation.....	94
Figure 130: LCI input current spectrum with square wave speed variation.....	94
Figure 131: Torque on coupling 2-3 with square wave speed variation	94
Figure 132: LCI input current spectrum with square wave inverter firing angle variation.....	95

Figure 133: Torque on coupling 2-3 with square wave inverter firing angle variation	95
Figure 134: Generator current spectrum all drives at 48.85Hz	96
Figure 135: Torque on coupling 2-3 all drives at 48.85Hz	96

Abbreviations

AC – Alternating Current
AFE – Active Front End
CHB – Cascaded H-Bridge
CSI – Current Source Inverter
DC – Direct Current
DOL – Direct On-Line
FSC – Floating Symmetrical Capacitor
GT – Gas Turbine
GTG – Gas Turbine Generator
IGBT – Isolated Gate Bipolar Transistor
IGCT – Integrated Gate Commutated Thyristor
ITMD – Integrated Torsional Mode Damping
LCI – Load Commutated Inverter
LNG – Liquefied Natural Gas
MTBF – Mean Time Between Failures
MTPA – Million Ton Per Annum
NPC – Neutral-Point Clamped
PWM – Pulse Width Modulated
SER – Slip Energy Recovery
SM – Synchronous Machine
THD – Total Harmonic Distortion
VSD – Variable Speed Drive
VSI – Voltage Source Inverter

1 Introduction

With rising energy prices, more and more work is done to produce fossil fuels as efficient as possible. By reducing the amount of energy used to get fossil fuels from the well to the customer, the amount of fuel that can be sold is increased.

Demand for natural gas is increasing as it is considered to be a clean burning fuel. To transport natural gas efficiently over long distances, it has to be turned into a liquid, creating Liquefied Natural Gas (LNG). In this process large compressors are used which are conventionally driven by Gas Turbines. When these compressors are instead driven by electrical motors on a variable speed drive, less energy is needed and on-stream time is increased as well thus increasing revenue.

The use of variable speed drives does come with a problem: interharmonics. Much research has already been done on this subject. However variable speed drives for LNG applications require special attention for several reasons. First of all, the power levels are very high, in the order of tens of megawatts. This is higher than power levels considered in most research.

Secondly, the system has to be very reliable. Outages are very expensive, not only due to the large amount of products that has to be flared, but also due to the loss of revenue before the whole plant is up and running again.

Finally, several aspects of an LNG setup aggravate the problem. In most cases the plant operates in Island mode without a large grid to damp interharmonics. Electric power is provided by Gas Turbine Generators which are very susceptible to resonance problems.

Goal of this research is to find mitigation measures for interharmonics in LNG setups. This is verified by simulation of a complete setup, including both motor and generator dynamics and interaction between different VSDs, which has not been done before.

This report will be built up as follows.

First some background research is presented, on the LNG process, harmonics and interharmonics, and converter technology used for variable speed drives. This is done in chapter 2.

After this several existing and new solutions for interharmonics are investigated and the most promising is selected in chapter 3.

To be able to verify whether the solution actually works an existing LNG setup is simulated in chapter 4.

After this the selected solutions from chapter 3 are tested on small scale and on the full system in chapter 5 to see whether the interharmonic problem is indeed sufficiently reduced.

In chapter 6 the conclusions are drawn and recommendations are given.

2 Background

To fully understand the different aspects in this thesis it is important to understand the background. The objective of this chapter is to give background information on several aspects. Section 2.1 describes the basics of LNG (Liquefied Natural Gas) and why electric drives are desirable for this application. Section 2.2 explains what interharmonics are and how they are created. Section 2.3 explains the effect of torsional resonance that is caused by interharmonics. Section 2.4 describes the basic operation of converters used for the power levels considered here as these are the source of interharmonics.

2.1 LNG

To be able to transport natural gas efficiently over long distances (more than 1000km offshore or more than 3500km onshore [1]) it is necessary to turn it into a liquid. For this purpose Liquefied Natural Gas (LNG) plants are built that cool gas down to -162°C [2]. At -162°C the gas will turn into a liquid reducing to $1/600^{\text{th}}$ [2] of its original volume. After liquefaction it can be shipped in special tankers to customers around the world. A large part of the natural gas available is found on locations far away from high consumption areas, large scale gas liquefaction is therefore necessary.

Figure 1 shows the basic operation of LNG production. Natural gas is fed into a number of heat exchangers to cool it step by step. The cooling in the heat exchangers is done by expanding refrigerant. This refrigerant is then compressed, cooled against ambient air and for the colder steps also against other refrigerants, and the fed back into the heat exchanger.

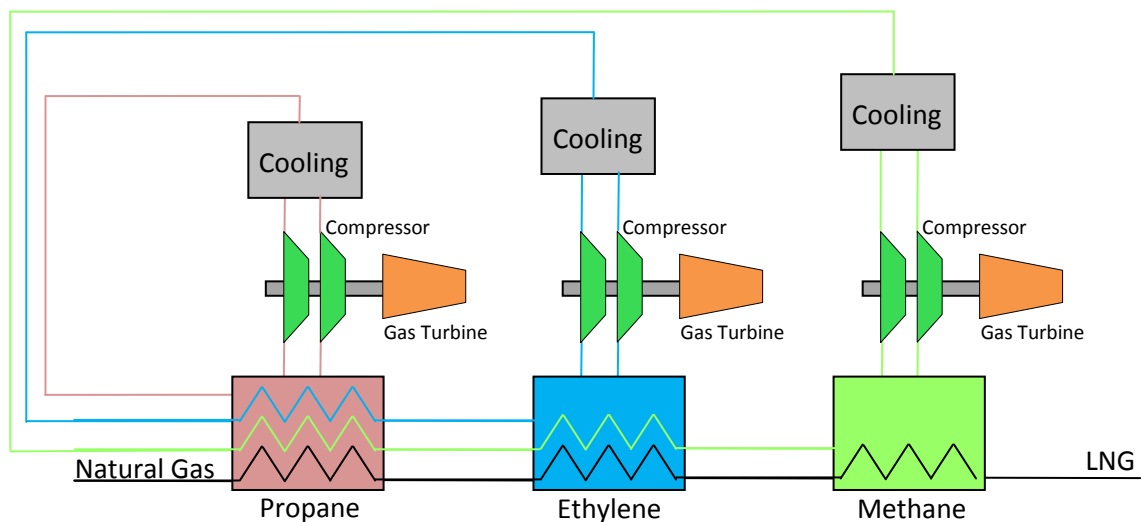


Figure 1: Simplified LNG production

The large scale of typical several million ton per annum (MTPA) and the low temperatures that need to be reached call for very large compressors. A traditional setup is shown in Figure 2, here the compressors are driven directly by gas turbines (GTs), in some cases assisted by an electric helper drive to assist the GT and start the system up.

There are however a number of disadvantages to using GTs. First off all with a MTBF of 4000 hours, a trip of the GT and thereby the whole process can be expected twice a year. Furthermore, 12 to 20

days of maintenance are necessary each year further limiting the on-stream-time. The efficiency is relatively low and has a narrow peak range resulting in an overall efficiency of around 25%[3]. Electric motors on the other hand have a MTBF of >25000 hours so a trip can be expected roughly only once every 3 years. With longer maintenance intervals and shorter maintenance duration, less than one day of on-stream-time per year will be lost [3].

As a result there is a growing interest in all electric setups as shown in Figure 3, where the compressor is fully driven by an electric motor, often connected to a variable speed drive (VSD).

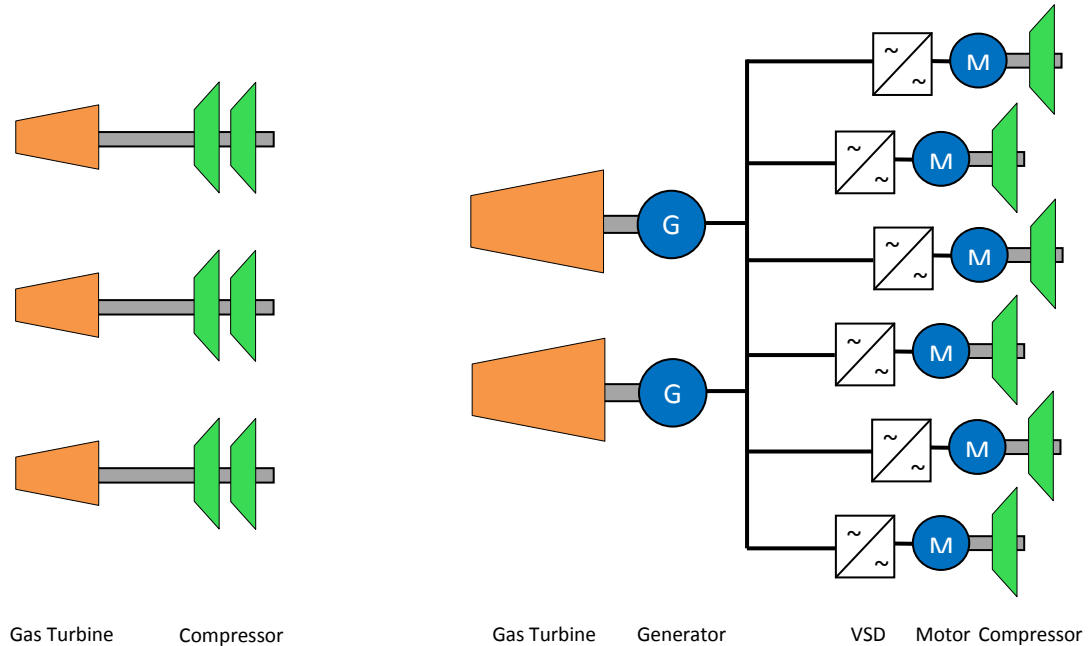


Figure 2: Traditional setup[3]

Figure 3: All electric setup[3]

When a VSD is not applied, the flow has to be regulated by throttling the compressor suction line. The amount of power versus flow of a compressor with throttling or a VSD is shown in Figure 4. Keeping in mind that the compressor considered here are tens of MWs, the potential energy savings are also large if a variable flow is desired.

Another more practical reason to use a VSD is that motors of these power ratings can't be simply started Direct On-Line (DOL). Applying a VSD can also lead to a more optimized compressor design, as a wide range of speeds is now available. Reliability is also an important reason to choose for a VSD. After a generator trip, when lower power is available, the plant can continue to operate although on a lower production level.

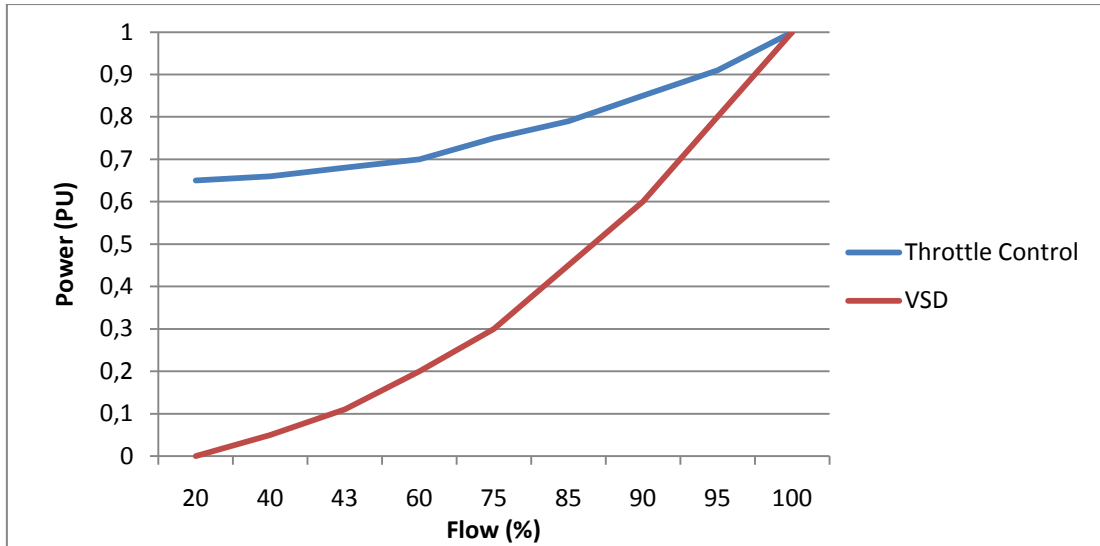


Figure 4: Power consumption of Throttle Control and VSD [4]

1 MTPA corresponds to roughly 38-40MW [1] of necessary drive power, so both motor and VSD will need to be rated at several tens of megawatts. One of the largest drives installed at this moment is the 65MW drive in the Snøhvit LNG project in Norway, but drives of 70-80MW are expected in the near future [1].

However as most LNG plants are located in remote areas where there usually is no existing electrical grid or the grid is not sufficiently strong, electric power usually has to be generated on site by GTs. A setup with redundant GTs is usually chosen to ensure a high on-stream-time.

2.2 Harmonics and Interharmonics

Harmonics are well known to most electrical engineers. They are the spectral components on the voltage or current that are an integer multiple of the fundamental frequency [5]. Interharmonics occur much less, but can be generated by VSDs. As the name suggests, these are spectral components on frequencies between the integer multiples of the fundamental frequency [5]. This means that interharmonics can have any frequency and are not limited to integer multiples of the fundamental frequency. Sub harmonics is a term that is often used for the frequency components that occur between DC and the fundamental frequency. Interharmonics are generated when two AC systems with different frequencies are connected, as happens in a VSD.

A more mathematical way to describe this is[6]:

Harmonics $f = k * f_1$ where k is an integer > 0

Interharmonics $f \neq k * f_1$ where k is an integer > 0

Sub-harmonics $f > 0$ Hz and $f < f_1$

DC $f = 0$ Hz ($f = k * f_1$ where $k = 0$)

Where f_1 is the fundamental frequency.

To get an understanding of how interharmonics are created in a VSD the ideal AC side current is shown in Figure 5 for a converter with constant current in the DC link. This square waveform will only produce harmonics, not interharmonics.

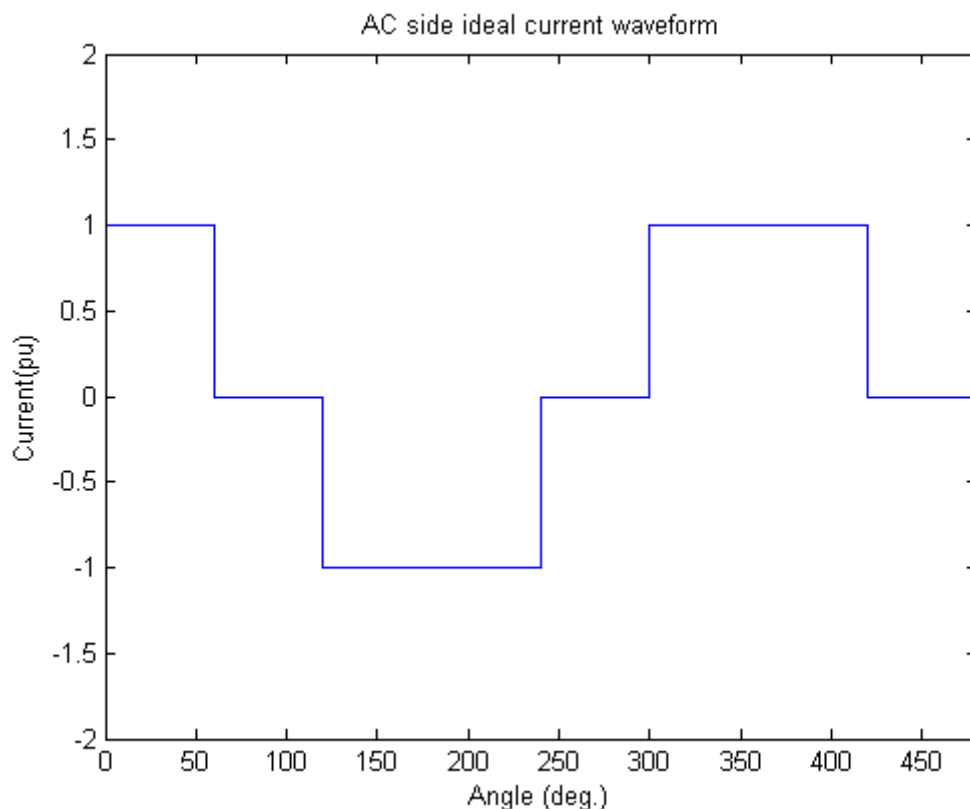


Figure 5: Ideal AC side current

However, the voltage on both sides of the DC-link inductor won't be perfectly smooth, due to the AC waveforms on the grid and motor side. As the DC-link inductance can't be made infinitely large in reality, the current in the DC link will not be perfectly smooth but will have a small ripple. As a result, this ripple will also be visible on the grid side as shown in Figure 6.

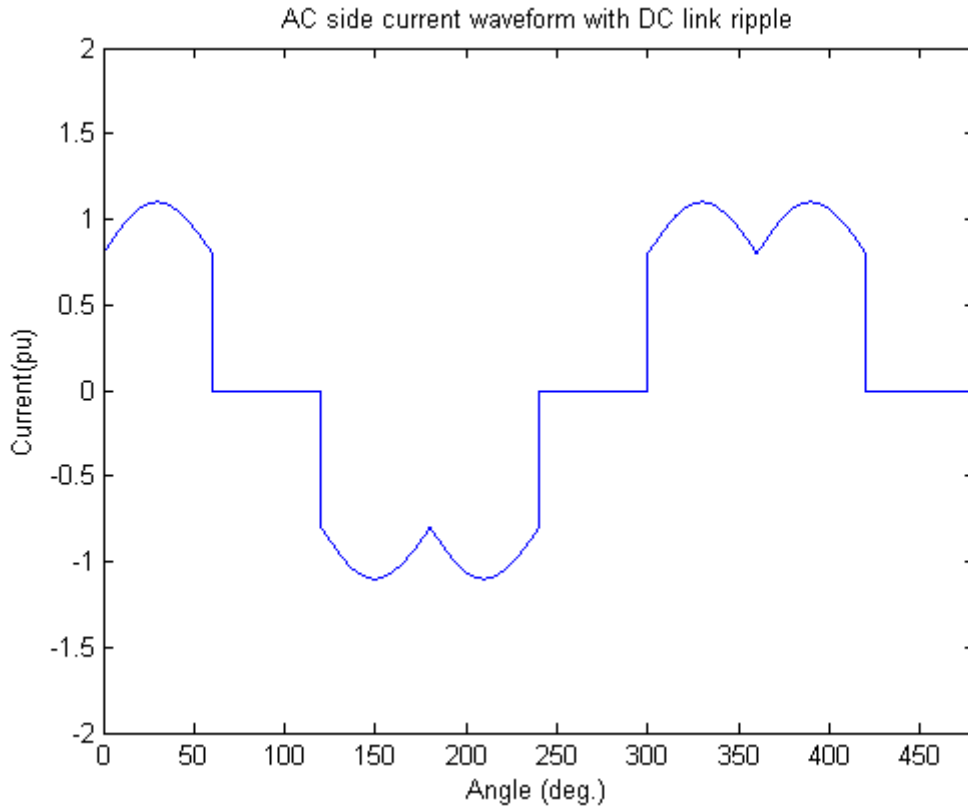


Figure 6: AC side current with DC ripple

The grid harmonics of the square wave, and the motor harmonics creating the DC ripple will combine into interharmonics. In most cases this is via the modulation effect, resulting in frequency components on the grid side of:

$$f = (n \cdot P + 1) \cdot f_{grid} \pm m \cdot P \cdot f_{motor} \quad [7] \quad (1)$$

Where we have motor frequency f_{motor} , grid frequency f_{grid} , switch frequency f_{switch} , converter pulse number (6, 12, 24 etc) P and integers (0, 1, 2, 3....) m and n .

It is important to notice that the created interharmonics depend on the motor frequency and therefore the motor speed. These interharmonics can be graphically presented in a so called Campbell diagram as demonstrated Figure 7. By plotting problematic frequencies as a horizontal line, it is easy to see at which drive frequencies problems may occur and which interharmonic causes it. The Campbell diagram of Figure 7 is deliberately kept very simple with a very limited amount of interharmonics to explain how it is built up. On the vertical axis the grid frequency and the fifth, seventh, eleventh and thirteenth harmonic can be seen as the motor speed is still zero here. When motor speed is increased, interharmonics are formed by addition and subtraction of motor frequency components. It is important to notice that only grid harmonics are present when motor and grid frequency are equal.

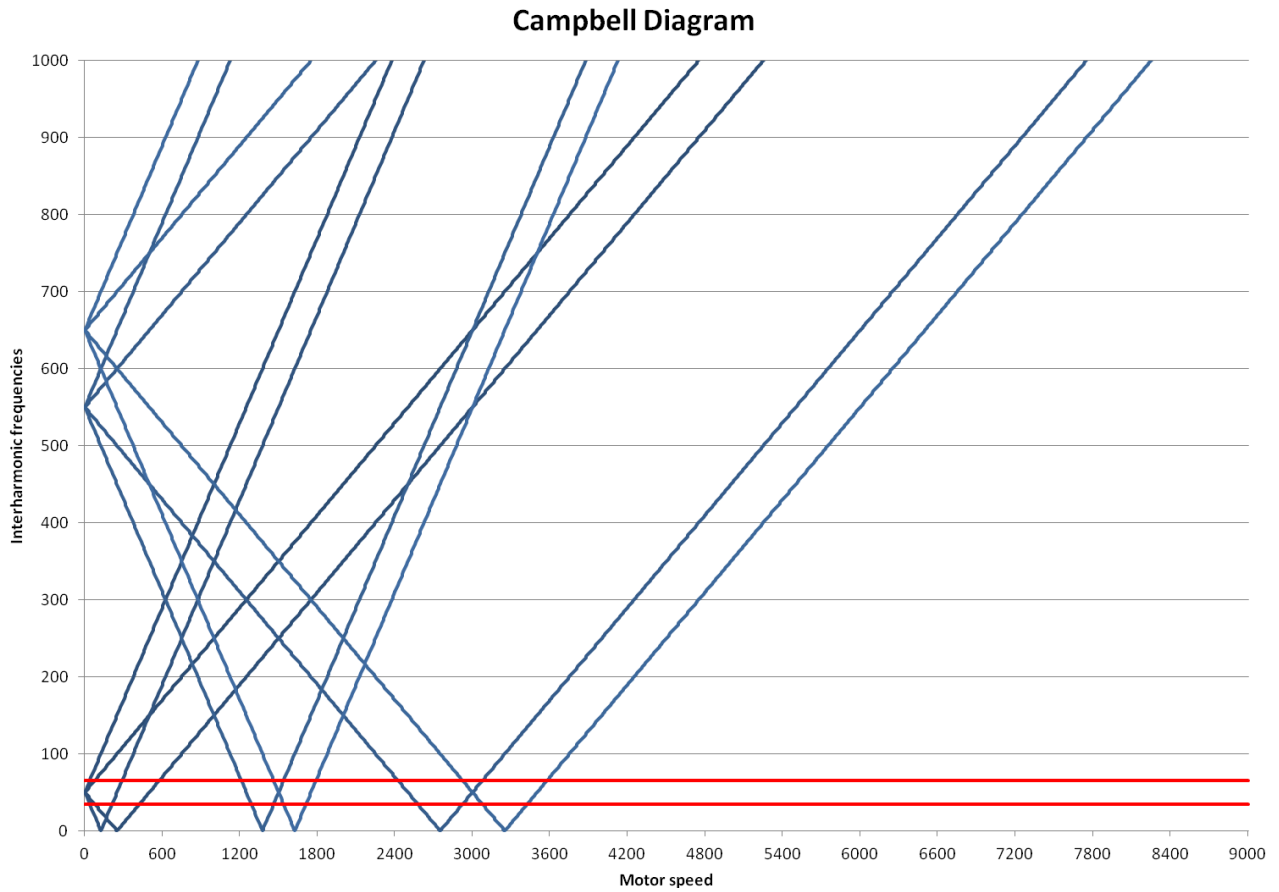


Figure 7: Simple Campbell diagram of a 6 pulse converter connected to a 2 pole machine

Of course the Campbell diagram of Figure 7 is too limited for most use. A more realistic Campbell diagram is given in Figure 8.

Campbell Diagram

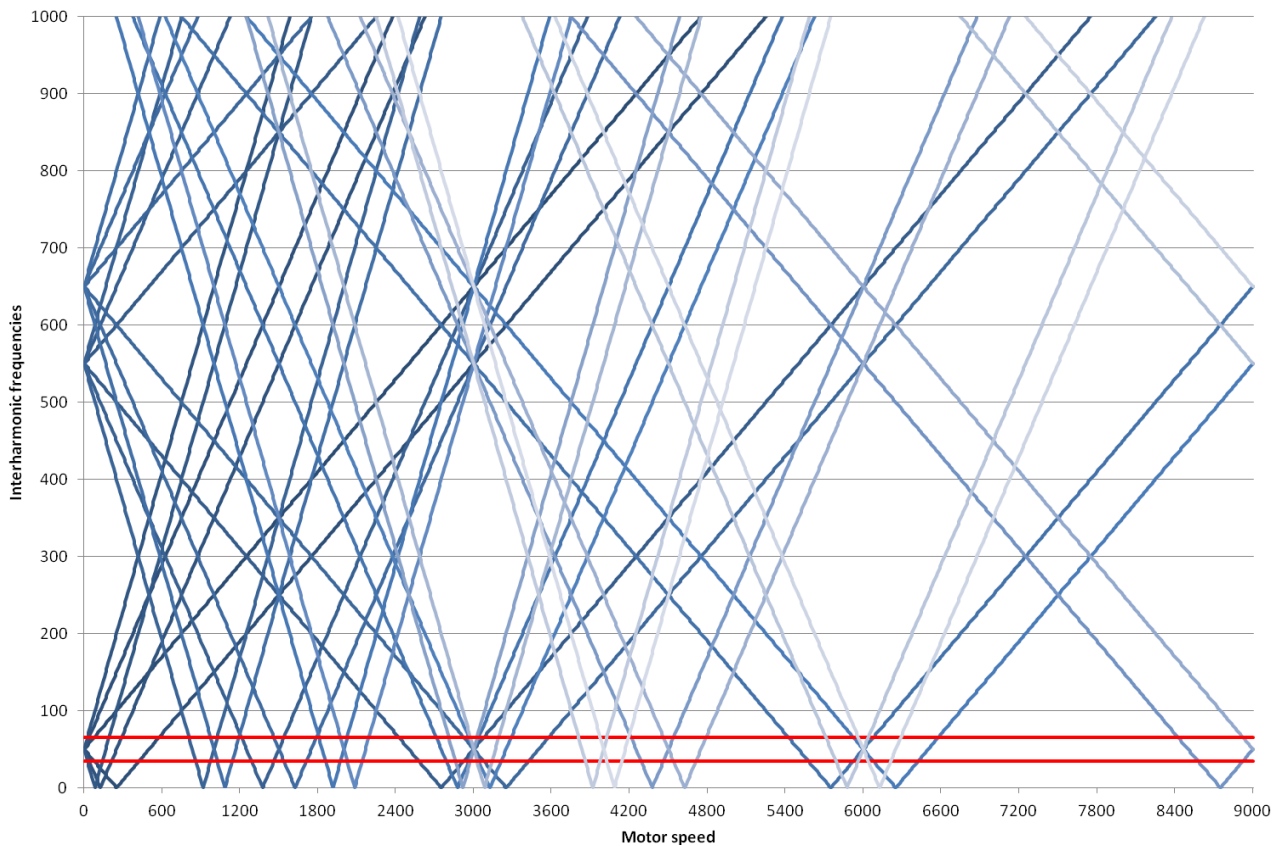


Figure 8: Elaborate Campbell diagram of a 6 pulse converter connected to a 2 pole machine

There are three important reasons to limit harmonics and interharmonics.

1. They can cause disturbances in other systems connected to the same bus, e.g. sensor or communication systems, or flicker [8]. Standards are prescribed for a maximum Total Harmonic Distortion (THD) in order to prevent disturbance of other systems.
2. Harmonics and interharmonics will generate heat due to increased losses which can cause machines to overheat.
3. As interharmonics can occur at every frequency they can also occur at a resonance frequency of the grid or a machine connected to it. If the interharmonics are large enough and damping is small, this can cause fatigue or even catastrophic failure of equipment [9].

This last reason is the most serious concern when applying VSD in LNG plants as they usually operate in island operation. Because of the absence of damping of a large grid, resonances can easily occur. The machines used for LNG applications are usually very large and large shafts are more susceptible to resonances. As a loss of production will have significant costs, motor or generator trips due to resonance, or even catastrophic failure of these machines is unacceptable.

2.3 Gas Turbine Generator Resonance

Interharmonics can cause torsional resonance. The reason to limit the amount of interharmonics is that this resonance can lead to fatigue or direct failure. The component most susceptible to resonance is the Gas Turbine Generator (GTG). Besides the coupling of the gas turbine to the generator, the complicated rotor of the gas turbine, as seen in Figure 9, will also contribute to the resonance problem. To understand the behavior of this resonance the shaft is modeled and several situations are simulated.



Figure 9: Alstom GT26 Gas turbine rotor

The generator shaft can be modeled by a multi-mass model, like the four-mass model in Figure 10. As the name suggests, there are four masses, with their corresponding inertia. These are coupled by both a damper and a spring. Besides the damping between two masses, there will also be an overall damping on each mass. However, this is so small that it can be neglected. It is easy to recognize the basic mass-spring system in the four-mass model, which create the oscillatory behavior.

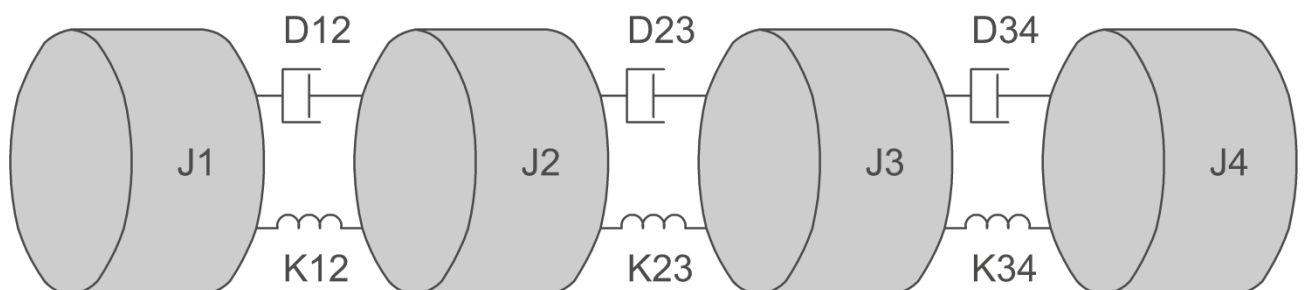


Figure 10: Four mass model

The torque on element J1 can be described by equation 2, where T_{J1} is the torque on J_1 , T_{in} is the externally applied torque, T_{D12} is the torque applied by the damper and T_{K12} is the torque applied by the spring.

$$T_{J1} = T_{in} - (T_{D12} + T_{K12}) \quad (2)$$

The torque applied by the damper is related to the speed difference as described in equation 3.

$$T_{D12} = D_1 \cdot (\omega_1 - \omega_2) \quad (3)$$

The torque applied by the spring is related to the difference in angle as described in equation 4.

$$T_{K12} = K_1 \cdot (\alpha_1 - \alpha_2) \quad (4)$$

The sum of these two torques will also be applied to J_2 with opposite sign.

The total torque on J_1 will affect the speed as described in equation 5. The well known relation between speed and angle is given in equation 6 for clarity.

$$\omega_1 = \frac{1}{J_1} \cdot \int T_{J1} dt \quad (5)$$

$$\alpha_1 = \int \omega_1 dt \quad (6)$$

The four mass model is implanted in Simulink to test the effect of different disturbances on the shaft. This is done by connecting four single-mass models together forming one four-mass model. The Simulink implementation of a single-mass unit is shown in Figure 11. The connection of the four models is shown in Figure 12. The last model is slightly different as this has no following block to take into account. Therefore, the effects of a following block can be omitted from the model. The parameters used for the four mass model are those of an Alstom GT13E2 gas turbine generator which are given in Table 1.

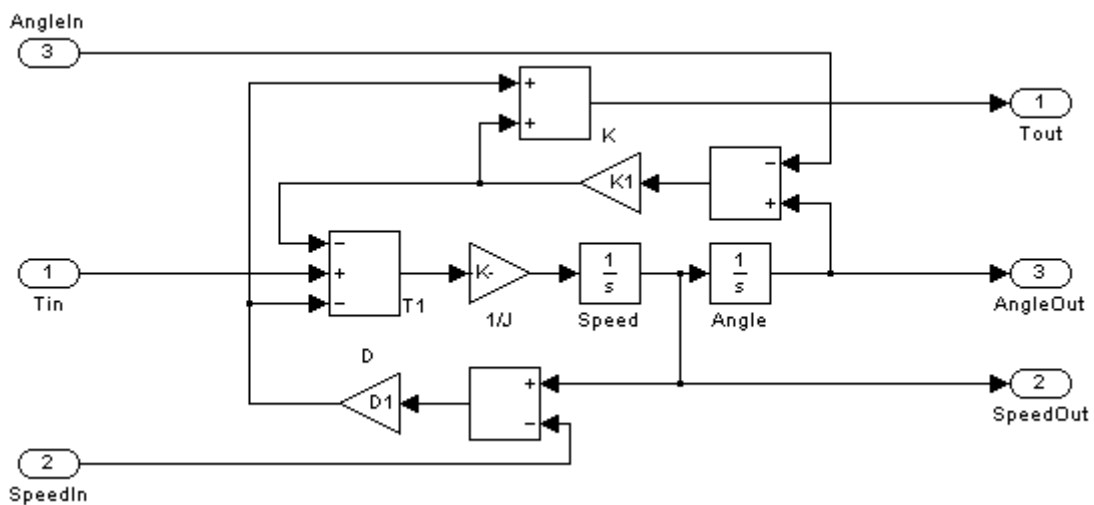


Figure 11: Multi-mass model element

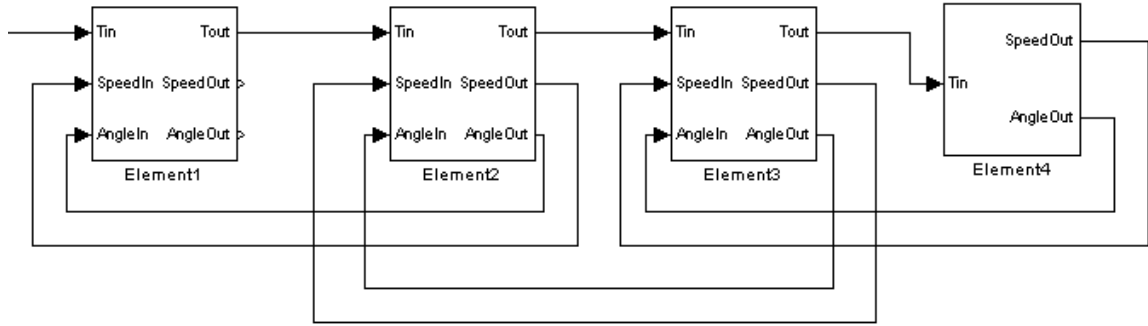


Figure 12: Multi-mass model

	Value	Represents
J_1	$2.234 \cdot 10^3 \text{ kgm}^2$	Generator
J_2	$2.893 \cdot 10^3 \text{ kgm}^2$	Generator
J_3	$1.512 \cdot 10^4 \text{ kgm}^2$	Compressor
J_4	$9.52 \cdot 10^3 \text{ kgm}^2$	Turbine
K_{12}	$9.400 \cdot 10^5 \text{ kNm/rad}$	
K_{23}	$3.793 \cdot 10^4 \text{ kNm/rad}$	
K_{34}	$2.660 \cdot 10^6 \text{ kNm/rad}$	
D_{12}	1743 Nms/rad	
D_{23}	647.0 Nms/rad	
D_{34}	6361 Nms/rad	

Table 1: Alstom GT13E2 GTG four-mass model parameters

Now a model is made, some test can be done to determine the behavior. First of all a pulse of 1pu is applied measuring both time response and frequency response. The result is a resonant behavior which slowly damps out. This is shown in Figure 13 and Figure 14 respectively. We can see that the peaks are exactly where they should be, on 15Hz, 107Hz and 138Hz.

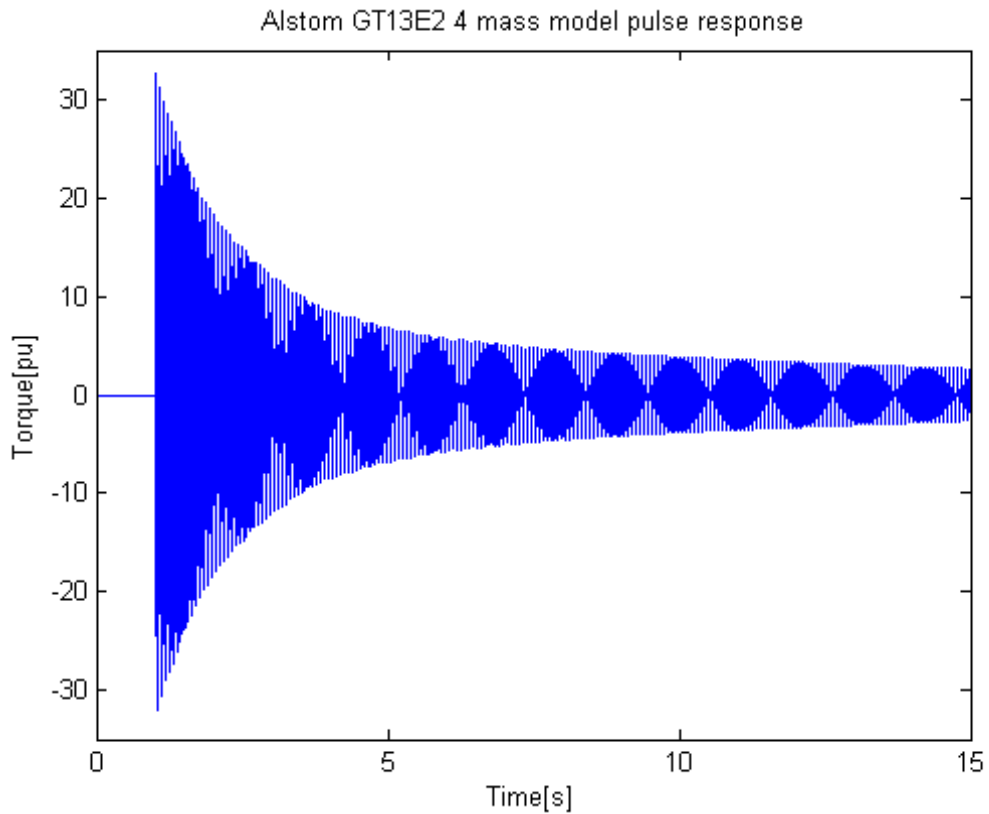


Figure 13: Multi-mass pulse time response

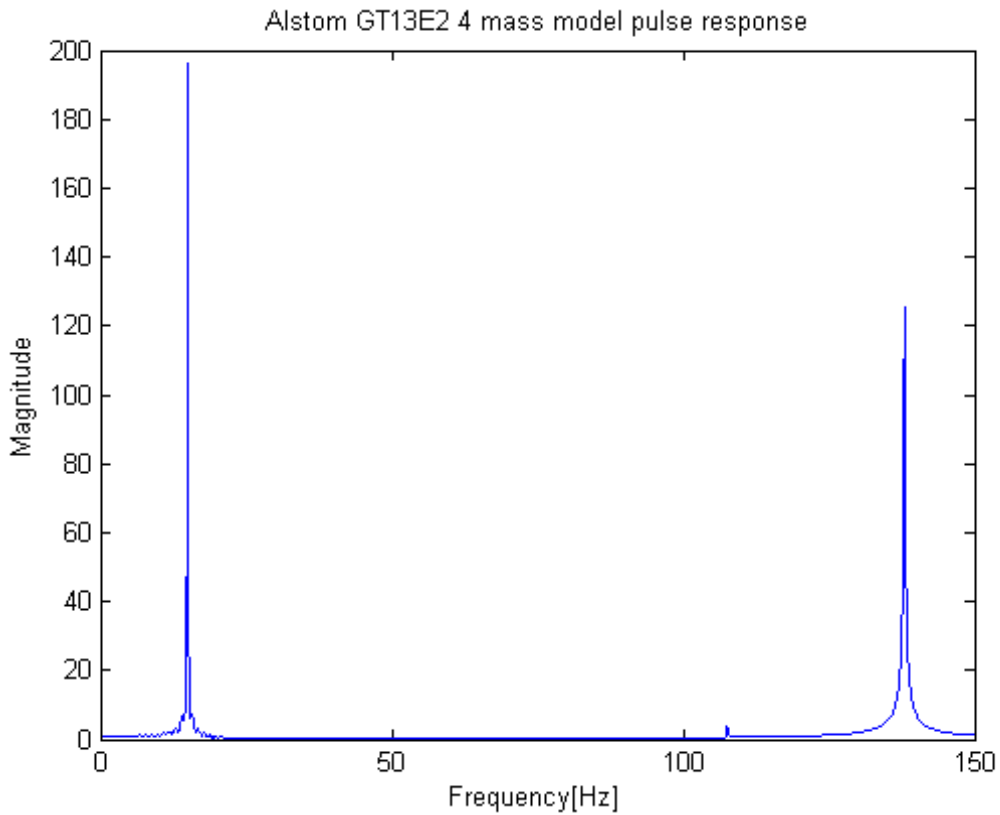


Figure 14: Multi-mass pulse frequency response

Next the behavior is evaluated if a constant excitation of 1pu on the torque on one of these resonance points is given. As shown in Figure 15 the torque will keep increasing up until the point where the damping and excitation match each other. As damping is often limited for these

resonances this can result in very high torques creating the fatigue or failure problems mentioned earlier. This is the reason that constant operation on a point that creates resonance should be avoided. If we move the excitation frequency by as little as 0.1Hz, the results are much less (five times less) dramatic, as we can see in Figure 16. Another important observation to make is that the resonance takes quite some time to build up. Figure 17 shows that the maximum torque will therefore indeed be lower if the frequency passes a resonance point, as the resonance does not get time to fully build up. As can be expected, a faster sweep will result in even less torque, as demonstrated in Figure 18.

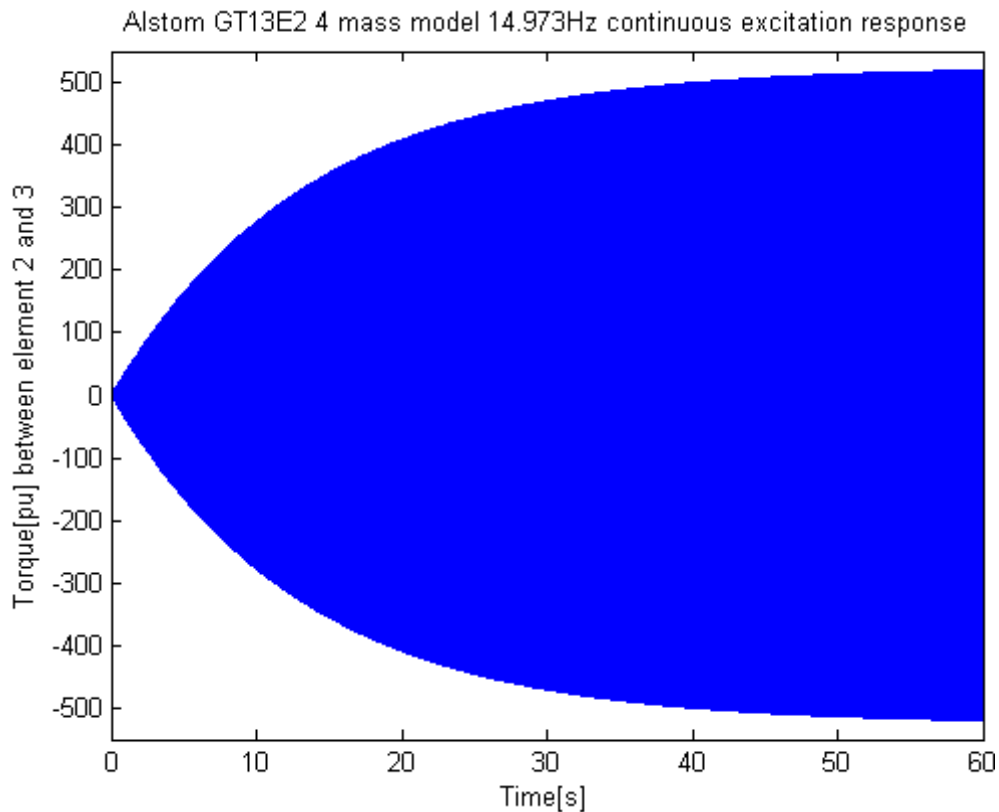


Figure 15: Continuous excitation on a resonance frequency

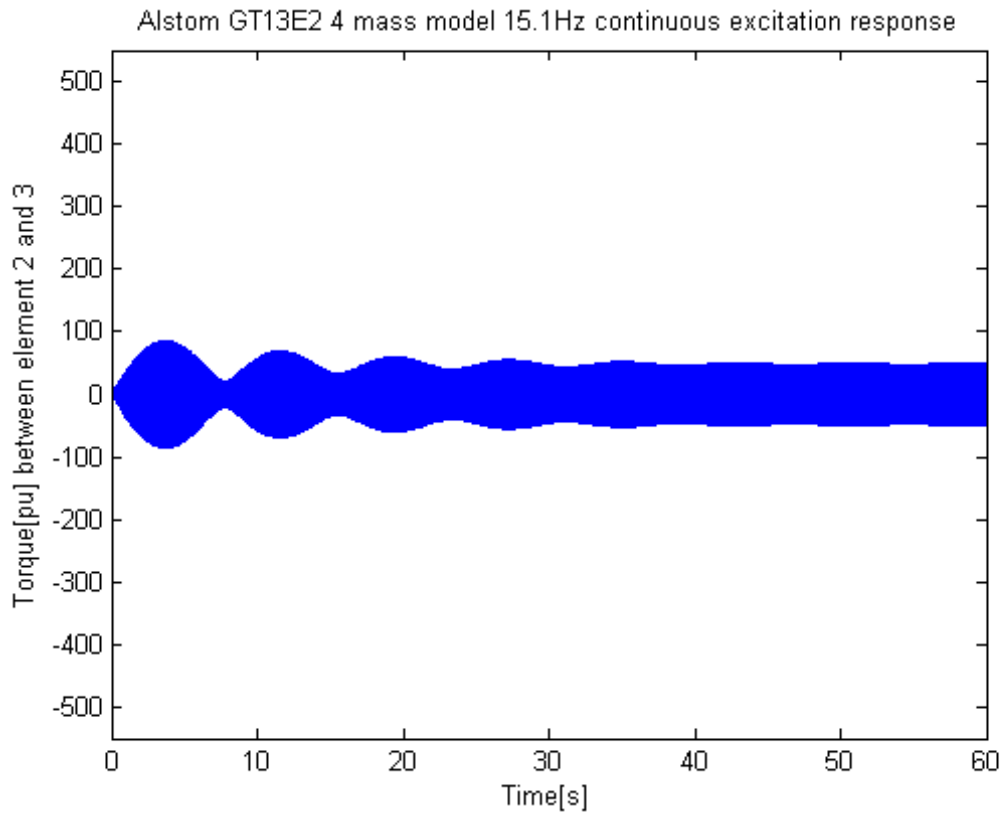


Figure 16: Continuous excitation near a resonance point

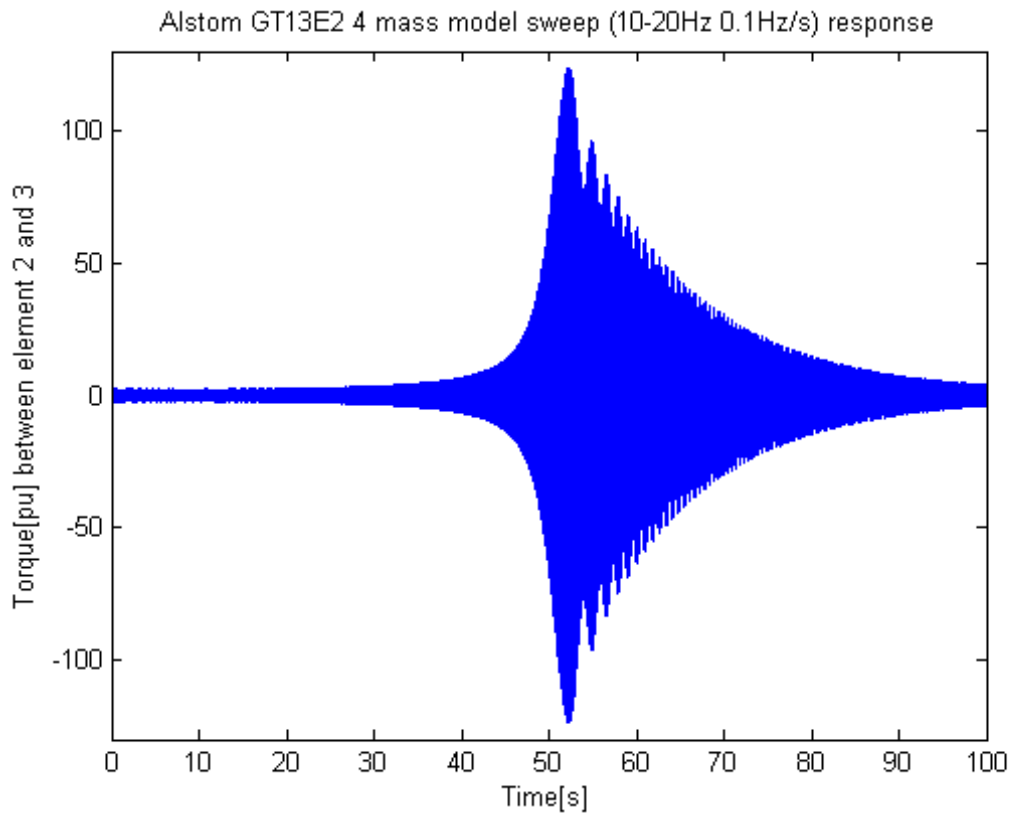


Figure 17: Slow Sweep passed a resonance point

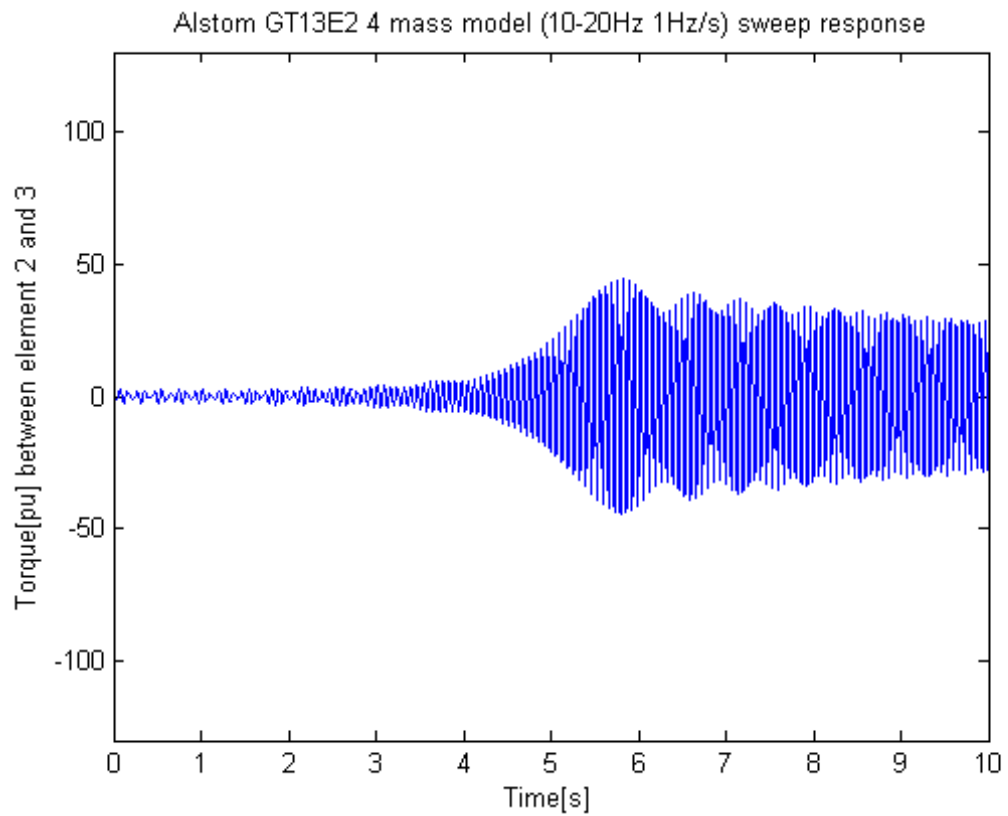


Figure 18: Fast Sweep passed a resonance point

2.4 Converters

As interharmonics are created by the VSD it is important to understand how it works. There are different topologies available for VSDs, which all create a different amount of interharmonics. The topologies used for LNG applications are LCI or VSI. Therefore these two topologies are investigated in more detail. Cycloconverters, Current Source Inverters and Slip Energy Recovery systems have also been investigated, but are not considered to be suitable for this application based on power, speed and reliability.

2.4.1 Voltage Source Inverters

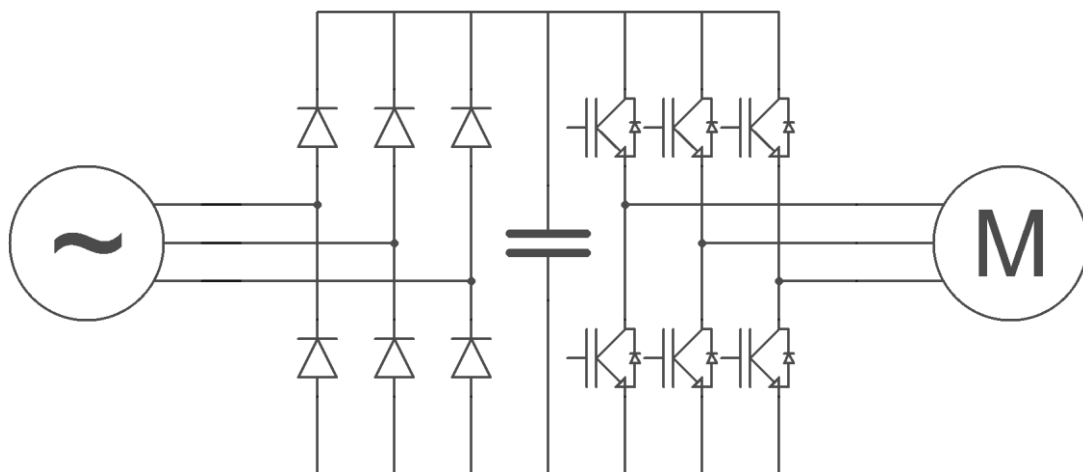


Figure 19: VSI setup (Diode rectifier, IGBT inverter)

The basic setup of a VSI drive is shown in Figure 19. A VSI drive is an AC to DC to AC converter, with a constant voltage, and therefore a capacitor, in the intermediate circuit.

This constant voltage is supplied by the rectifier. This can be controlled or uncontrolled, but in case the rectifier is of the uncontrolled type, only two quadrant operation is possible and the inverter has to be able to control the output power.

The inverter side of the VSI can be square wave or PWM. In both cases fully controllable switching elements are needed, thyristors can only be applied if an elaborate commutation circuit is added. As noted earlier, a square wave inverter only works when a controlled rectifier is used. Nowadays, with the availability of fast switching semiconductors, most VSI drives are PWM.

VSIs capable of delivering power up to 30MW [10] are available. In some cases even higher power ratings are reported, but this is realized by combining several separate VSIs.

The PWM operation can compensate for grid harmonics, but switching harmonics are added. The resulting pulsating torque frequencies on the motor shaft are:

$$f = n \cdot P \cdot f_{switch} \pm m \cdot P \cdot f_{motor} \quad [11] \quad (7)$$

The frequencies components that can be found in the grid current (not using a PWM rectifier) are:

$$f = (n \cdot P + 1) \cdot f_{grid} \pm m \cdot P \cdot f_{motor} \quad [12] \quad (8)$$

Here we have motor frequency f_{motor} , grid frequency f_{grid} , switch frequency f_{switch} , converter pulse number (6, 12, 24 etc) P and integers (0, 1, 2, 3....) m and n .

To reduce harmonics, it is possible to use the VSI in a so called multi-level setup. In this setup, the output can produce more than the standard two voltages levels. The higher the number of voltage levels possible, the lower the distortions will be. Added benefit is that with each level that is added, the maximum voltage of the output is increased [13].

The VSI drive is able to drive both induction- and synchronous machines. Combined with its low harmonics and interharmonics and the ease of application, it is the most popular converter for drives [14]. An important disadvantage however, is the lack of automatic limitation of short circuit current. Other protection circuits are therefore necessary [15]. Another disadvantage is the high dV/dt which can cause significant currents to flow through parasitic capacitances. Therefore special care has to be taken when designing a motor for a VSI drive.

2.4.2 Load Commutated Inverters

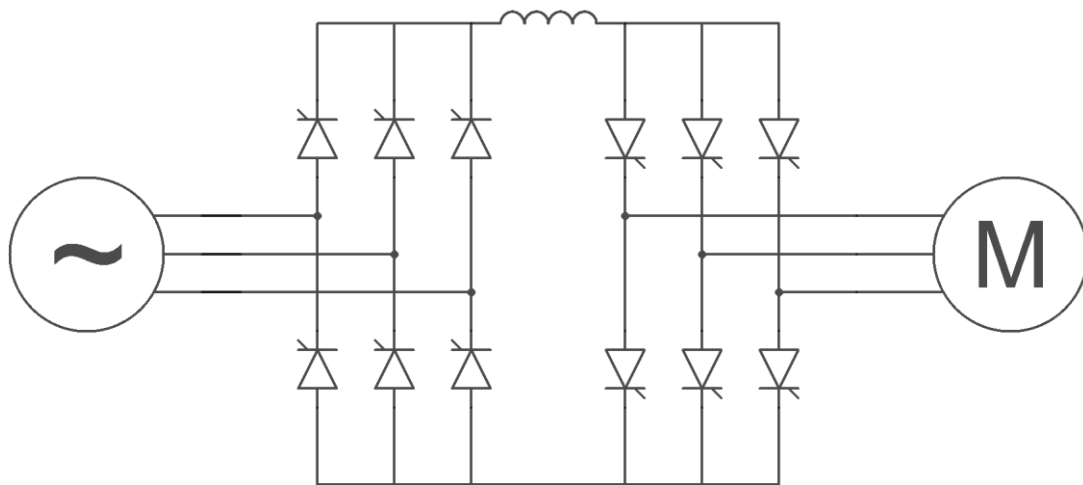


Figure 20: LCI setup

As part of the Current Source Inverter group, the LCI has a constant current, and therefore an inductor, in the intermediate circuit as depicted in Figure 20. Again the converter is an AC to DC to AC converter.

For an LCI the rectifier has to be controlled as the inverter is not able to control the output power. Therefore, an LCI is inherently able to operate in all four quadrants.

The LCI uses a square wave inverter. Its distinct advantage is that there is no need for fully controllable switches as the load can commutate the switches. This means that thyristors can be used without an extra commutation circuit. Therefore, LCI drives are available up to 120MW [10,16].

In an LCI setup the following pulsating torque frequencies can be found on the motor side:

$$f = n \cdot P \cdot f_{grid} \pm m \cdot P \cdot f_{motor} \quad [17] \quad (9)$$

On the grid side, the frequency components that can be found in the current are:

$$f = (n \cdot P + 1) \cdot f_{grid} \pm m \cdot P \cdot f_{motor} \quad [7] \quad (10)$$

With grid frequency f_{grid} , motor frequency f_{motor} , number of pulses of the converter P (6, 12, 24 etc) and integers m and n (0, 1, 2, 3...).

Similar to the CSI, the DC link inductor determines the amount of interharmonics. The higher the inductance, the lower the interharmonics will be, but the converter will respond slower to changes.

As the load has to commutate the inverter, an LCI can only be used to drive an overexcited synchronous machine. As a result of this inflexibility, combined with the relative complexity of the system, the LCI is only used for very high power drives, where VSI drives are not suitable.

2.4.3 Pulse number

As the voltage levels of the supply, VSD and motor are usually not the same; a transformer is used between each component. This also creates the opportunity to use a multi-pulse converter, thus reducing harmonics and interharmonics [18].

A standard three phase rectifier as depicted in Figure 21 is a six pulse system. This can be understood when looking at the waveform that is created at the DC side by the rectifier, which shows 6 “pulses” as seen in Figure 23, the frequency spectrum in Figure 25 shows typical harmonics.

Besides a change in voltage levels, transformers can also introduce a phase shift. This effect is exploited in a multi-pulse converter. By using different combinations of star, delta or zigzag connections, a three phase input can be converted in a multiphase (6, 9, 12, etc.) output and vice versa. As the pulse number of a system is two times the number of phases a multi-pulse (12, 18, 24, etc.) system can thus be created. A commonly used system is the 12 pulse system depicted in Figure 22. There are different options for the transformer windings, but star-delta combinations are the most common. As one transformer will have no phase shift, while the other has 30° phase shift [18] the resulting waveform at the DC side, created by the rectifier will have 12 “pulses” as seen in Figure 24. The frequency spectrum in Figure 26 shows that the number of harmonics is reduced.

The 6 pulse spectrum in Figure 25 shows all $n \cdot 6^{\text{th}}$ harmonics (6^{th} , 12^{th} , 18^{th} , etc.). The 12 pulse system will only produce $n \cdot 12^{\text{th}}$ harmonics (12^{th} , 24^{th} , 36^{th} , etc.) as the spectrum in Figure 26 shows. The same applies to other pulse numbers, so the 18 pulse system will produce $n \cdot 18^{\text{th}}$ harmonics, the 24 pulse system will produce $n \cdot 24^{\text{th}}$ harmonics, and so on.

Switching to a higher pulse number will therefore eliminate the lowest harmonic. As this is also the highest in amplitude, the total harmonic reduction will be quite significant.

In the case of an LCI, the way the rectifier, inverter and DC-link are coupled is very important when determining the interharmonic content.

- In Figure 27 the simplest setup is shown, where basically two separate 6 pulse converters with a phase angle between them are used. As a result there are two separate dc-links which don't influence each other. At the grid side the multiples of the 6^{th} , 18^{th} , 30^{th} etc. motor harmonic will be cancelled out, but interharmonics created by it are not.
- In Figure 28 a series connection is shown so only one dc-link channel exists. As a result the 6^{th} , 18^{th} , 30^{th} , etc. motor harmonic are cancelled in the dc-link and as a result the corresponding interharmonics will be eliminated too. However the 12^{th} , 24^{th} , 36^{th} , etc. harmonics will increase. The order in which the rectifiers and inverters are connected in series will not influence the operation. It will however influence the voltage levels, which is probably why the setup shown in Figure 28 is usually found in practice.
- The third setup in Figure 29 is between the first two setups. It has two separate circuits, but the magnetic coupling between the DC-links will provide attenuation of the 6^{th} , 18^{th} , 30^{th} , etc. harmonics, but will again increase the 12^{th} , 24^{th} , 30^{th} , etc. harmonics.

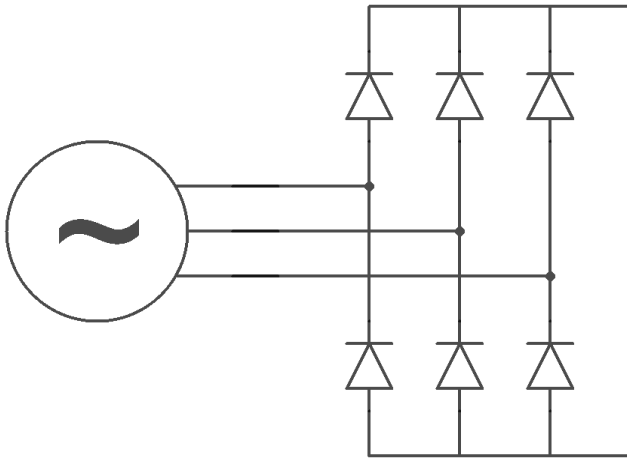


Figure 21: 6-pulse rectifier

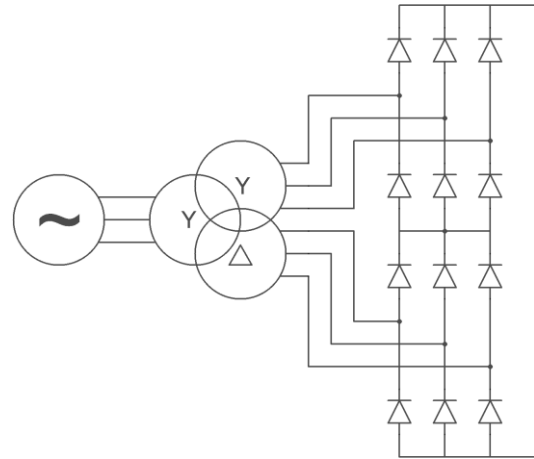


Figure 22: 12-pulse rectifier

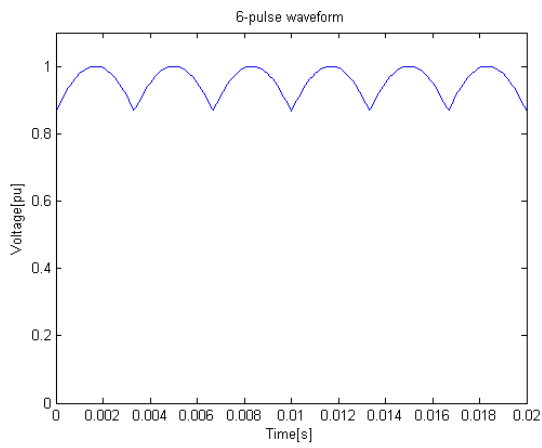


Figure 23: 6-pulse rectifier waveform

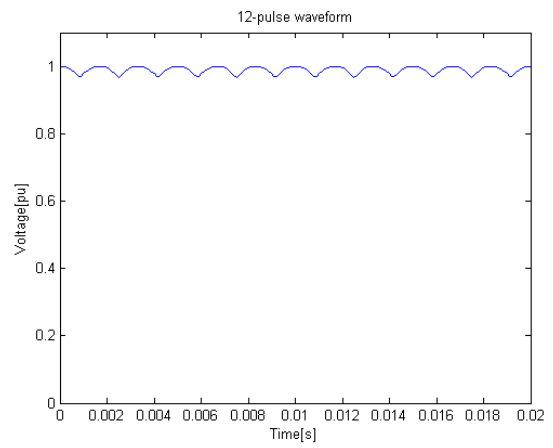


Figure 24: 12-pulse rectifier waveform

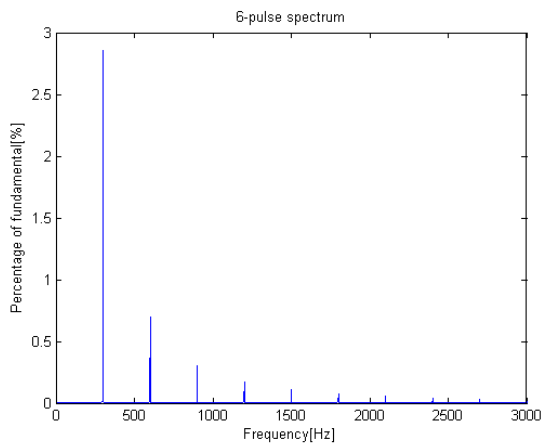


Figure 25: 6-pulse rectifier spectrum

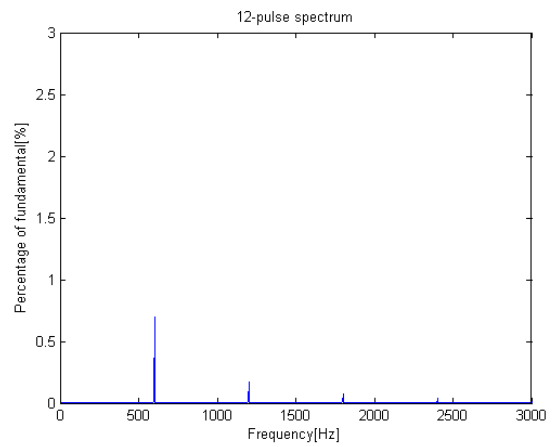


Figure 26: 12-pulse rectifier spectrum

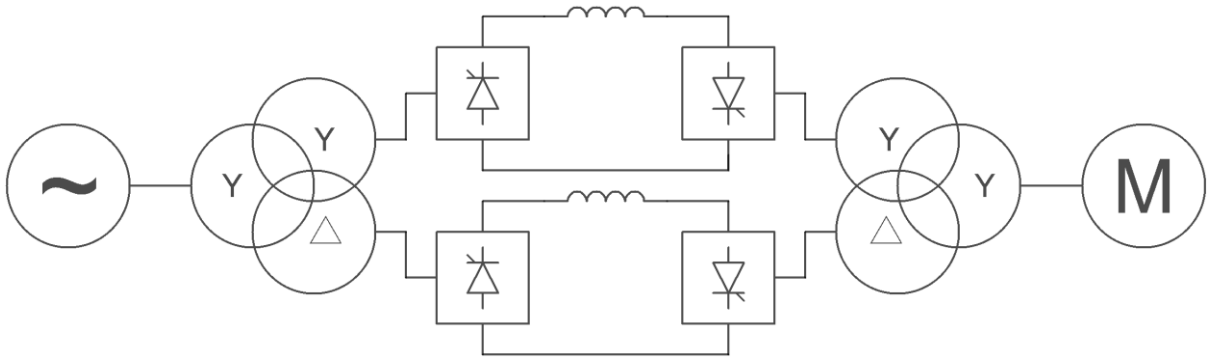


Figure 27: 12-pulse LCI with two independent DC links

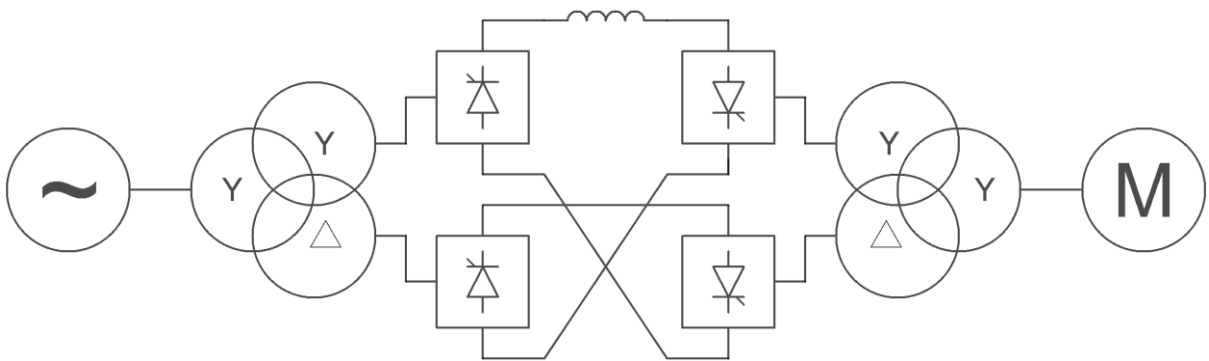


Figure 28: 12-pulse LCI with single DC Link

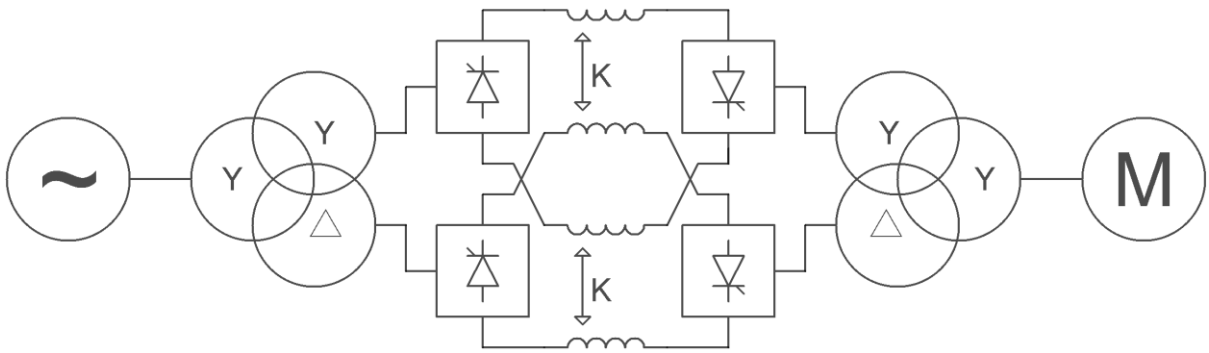


Figure 29: 12-pulse LCI with two mutually coupled DC links

3 Possible Solutions

In the preceding chapters it was explained what interharmonics are, how they are created and why they are a problem. Solutions are needed that either prevent interharmonics from being generated, prevent interharmonics from reaching sensitive equipment or increase the tolerance level for interharmonics.

Solutions can be applied to several parts of the system. We will first look into solutions that apply to the bus that supplies the VSD. Next we will look into solutions that apply to the drive itself. After that we turn to solutions that can apply to the machine, both generator and motor. And finally we will see what solutions can apply to the system controller.

3.1 Passive Filters

A hitherto common practice to mitigate harmonic and interharmonic problems is the application of a passive filter. These filters are used to compensate the power factor, harmonics and interharmonics.

When problems are expected with harmonic or interharmonic spectral components, the first step is to do an elaborate study of the total system to find the resonance frequencies in both the mechanical and electrical system.

Next, a filter design has to be made that compensates these frequencies. These filters are usually made up of C-type filters and second order high pass filters shown in Figure 30 and Figure 31 respectively [19]. However, first or third order high pass filters can also be used [20]. Series tuned filters are not very often used in practice as they consume reactive power rather than supplying it.

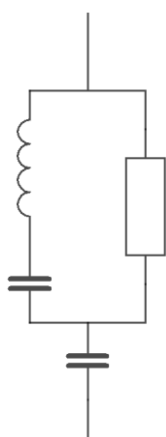


Figure 30: C-type filter

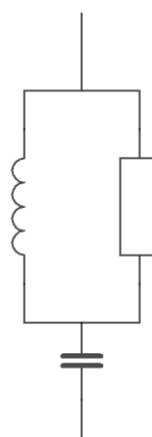


Figure 31: Second order High Pass filter

The filter is usually connected directly to the bus feeding the VSD or to an extra winding on the VSD input transformer. As harmonics and interharmonics are usually in the range of a few percent and VSDs are tens of MW the filter need to have high ratings. The result is a very bulky filter arrangement which not only results in high material costs, but also requires a lot of space to install.

When the filter design is made, it has to be simulated together with the system to see if the spectral component levels are all at a safe level.

Advantages of using passive filters are that they are simple circuits which have proven themselves in the past. Disadvantages are that they have to be custom made for each system, requiring a lot of work to be done [21]. Together with the high material costs this makes it quite an expensive solution. Another disadvantage is that they don't work very well for low frequencies, while these are the frequencies that cause problems with mechanical resonances [19]. Furthermore they need to be specially tuned for the system, while expansion of the system or removal of part of the system (for instance for maintenance), can detune the system enough to render it useless.

3.2 Active Filters

To overcome the problem of passive filters, active and hybrid filters have been proposed. The basic idea is to provide similar interharmonics with opposite phase to cancel out the interharmonics. A relatively small inverter is therefore an important part of an active or hybrid filter. Hybrid filters combine active and passive filters to keep the power level of this inverter low.

When considering active or hybrid filters, it is important to realize that an active or hybrid filter will never perform better than its detection system. Special care should therefore be taken to ensure that the required frequency components can be accurately detected.

When it comes to active filters there are basically two types.

1. The parallel, or shunt, active filter is depicted in Figure 32. Here current source I_c compensates harmonics. As this is a current source, it is specifically suited to compensate harmonic currents, which it does very well and independent of the source impedance. When used to compensate voltage harmonics, compensation is reduced and source impedance plays a very important role. Impedance parallel to the active filter should be kept high. It is possible to use passive filters in parallel but care should be taken that they don't compensate the same frequency components as resonance can then occur [22].
2. The series active filter is depicted in Figure 33. Here voltage source V_c compensates harmonics, and therefore this setup is very well suited to compensate harmonic voltages. Harmonic current sources can only be compensated in a hybrid setup with a series active filter. A large disadvantage is that the filter has to be capable of carrying the full current [22].

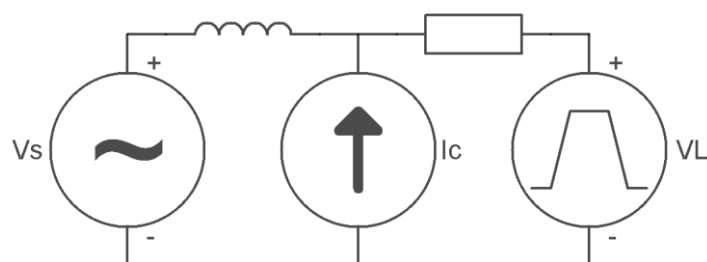


Figure 32: Shunt Active Filter

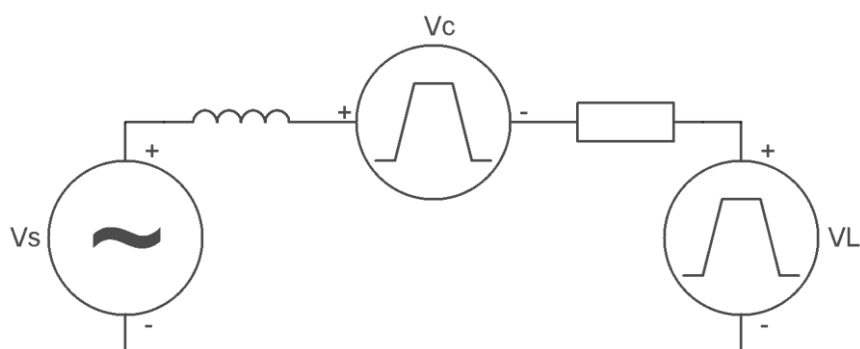


Figure 33: Series Active Filter

There are basically two locations to connect an active filter, on the DC-link or on the supply side. On the DC-link side, the goal is to suppress the motor harmonics as far as possible, so the modulation effect is limited. As the number of motor harmonics is smaller than the number of interharmonics this has advantages. Another advantage is that only a single phase inverter is required [23]. On the

supply side all harmonics and interharmonics can be compensated, but special attention can be paid to the harmful frequencies.

A shunt active filter is well suited to compensate harmonic current sources. As a result they are well suited to compensate harmonics on the grid side of an LCI as these appear as currents.

A series active filter would be better suited to compensate harmonic voltage sources. It is therefore a suitable compensation for the LCI DC side voltage harmonics. VSIs will produce voltage harmonics on the grid side which can also be compensated using a series active filter.

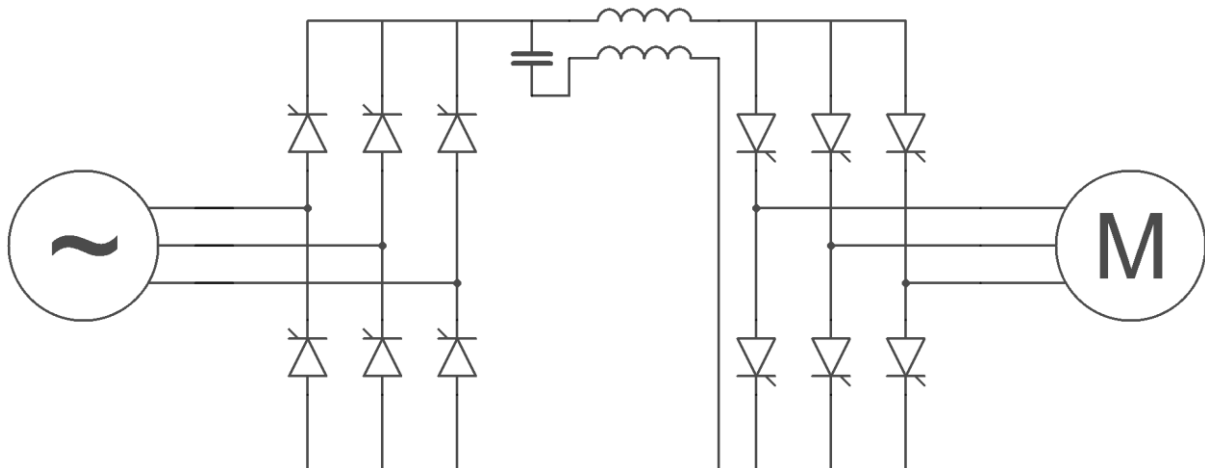


Figure 34: LCI with DC ripple reinjection

Another filter technique related to active filtering is ripple reinjection. The basic setup is depicted in Figure 34. Here too, the harmonics are also compensated by injecting a current with opposite phase. This is however done without active elements. The ripple on the rectifier output voltage will pass through the capacitor onto the primary side of the transformer. The secondary side of the transformer will inject this with opposite phase to cancel the ripple out. As this secondary coil will have to carry the full current without saturating, it will have to be quite large. Sometimes it can be combined with the smoothing reactance by adding a closely coupled primary winding to it. A large advantage is the lack of a complicated signal processing unit to capture, compare and process the harmonic signal [24].

Although these techniques appear to be very promising, no large scale filters are used till date. Smaller scale filters, simulation and laboratory test all suggest that this could be an efficient way of compensating interharmonics and harmonics.

3.3 Active Front End

The output stage of a VSI can be used both as rectifier and as inverter. In an AFE setup, this same fully controllable rectifier/inverter is used on the input side as well. The basic setup of a VSI with AFE is shown in Figure 35.

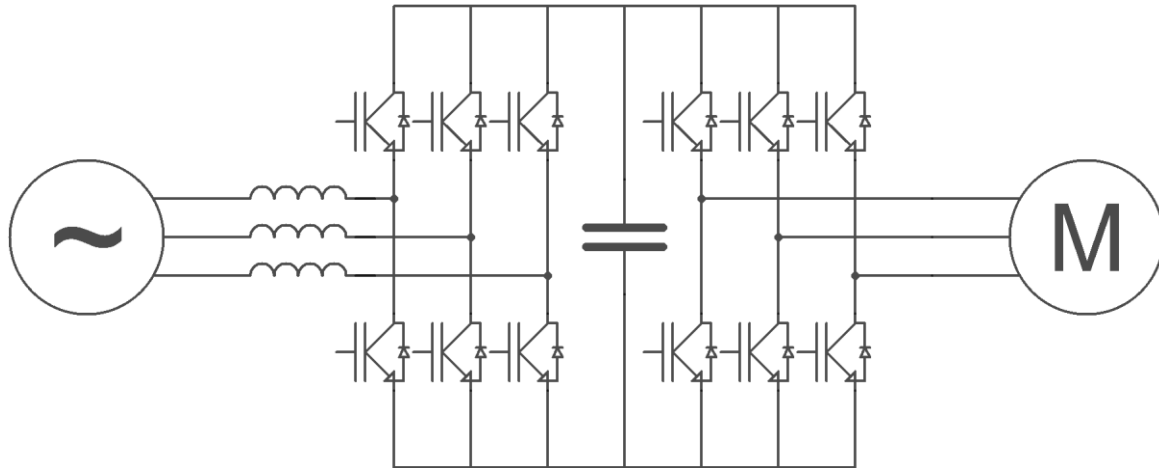


Figure 35: VSI with Active Front End

In rectifier mode the switches will work together with the grid side inductances as a boost converter. To make sure that the output voltage is controllable, it has to stay above $\sqrt{2} V_{LL}$, otherwise the diodes will start to act as a standard rectifier[25].

The main advantage of the AFE lies in the fact that it has full control over the current that is drawn from the grid, regardless of the grid phase. This means that the input current can be made close to sinusoidal. As a result there will ideally be no harmonics or interharmonics created by the rectifier, and any harmonics that are already present on the DC link voltage will not be fed back into the grid. The PWM operation however will add switching harmonics[25].

The full control of the current not only has a positive effect on the harmonics, it also allows full control over the power factor. As the current is no longer dependant on the phase of the grid, any phase angle between input voltage and current can be chosen. This means that the drive can operate at unity power factor or even at a leading power factor to supply reactive power to other (lagging) loads.

Besides its advantages in rectifier mode, the AFE also allows four quadrant operation [25]. When regenerative braking is applied to the motor, and the DC link voltage rises as a result, the AFE can act as inverter to feed the power back into the grid, instead of dissipating it in a braking resistor. As is already known from the operation of a VSI, full control of the waveform is also possible in inverter mode.

Application of an AFE will increase the cost of the VSI, as the input stage is more complicated. Its good harmonics properties will however allow reducing size and cost of filters[25]. Another advantage is the use of the same devices in both input and output stage, which will reduce the amount of spares that have to be kept.

3.4 Multi-level VSI

As the name already suggests, the difference between a conventional two-level converter and a multi-level converter lies in the number of voltage levels that can be produced on the output. Increasing the number of voltage levels has several advantages. First of all, switching between two adjacent levels will result in a lower dV/dt , as the voltage difference is smaller. This will reduce stress on the motor and reduce switching losses. As a level closer to the desired level can be chosen, harmonics will also be reduced, both in square wave modulation as in PWM modulation. The main disadvantage is the higher number of components which increases cost and reduces reliability. For voltage levels that require series connection of switches this is less of a problem as the extra switches are already present[26].

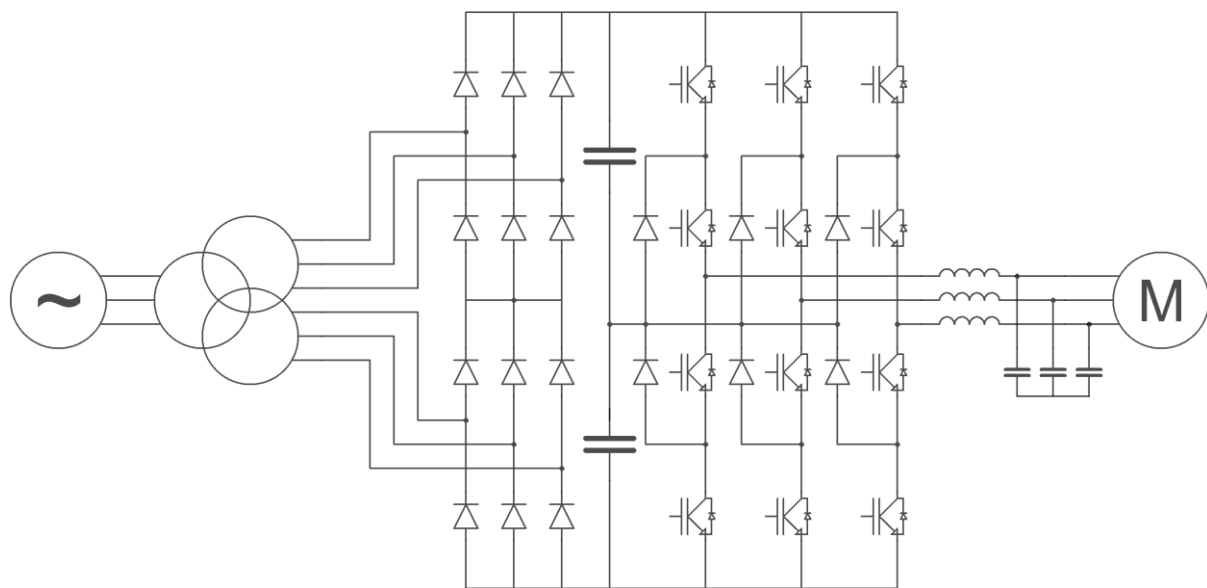


Figure 36: Neutral Point Clamped VSI

There are different topologies for the multi-level VSI, all with their own advantages and disadvantages. The first topology is the Neutral-Point Clamped converter as depicted in Figure 36 as a three level converter. The extra voltage level is created by splitting the DC Link capacitor into two capacitors. This creates an extra voltage level between the two existing voltage levels. This can be connected to the output via the switches and the clamping diodes. These switches are usually IGBTs or IGCTs. When IGCTs are used snubber networks have to be added. Special care has to be taken that the voltage over the capacitors stays balanced. This can be done by an open- or closed-loop control system, or by additional hardware such as DC-choppers or simple resistors. Advantages are that capacitors can be pre-charged as a group, a multilevel AFE can be added without increasing the number of capacitors, a relative small number of capacitors is needed and the footprint can be small. Disadvantages are that not all switches are loaded for the same amount of time which causes differences in de-rating. Furthermore the number of clamping diodes will dramatically increase with an increase in the number of voltage levels [26].

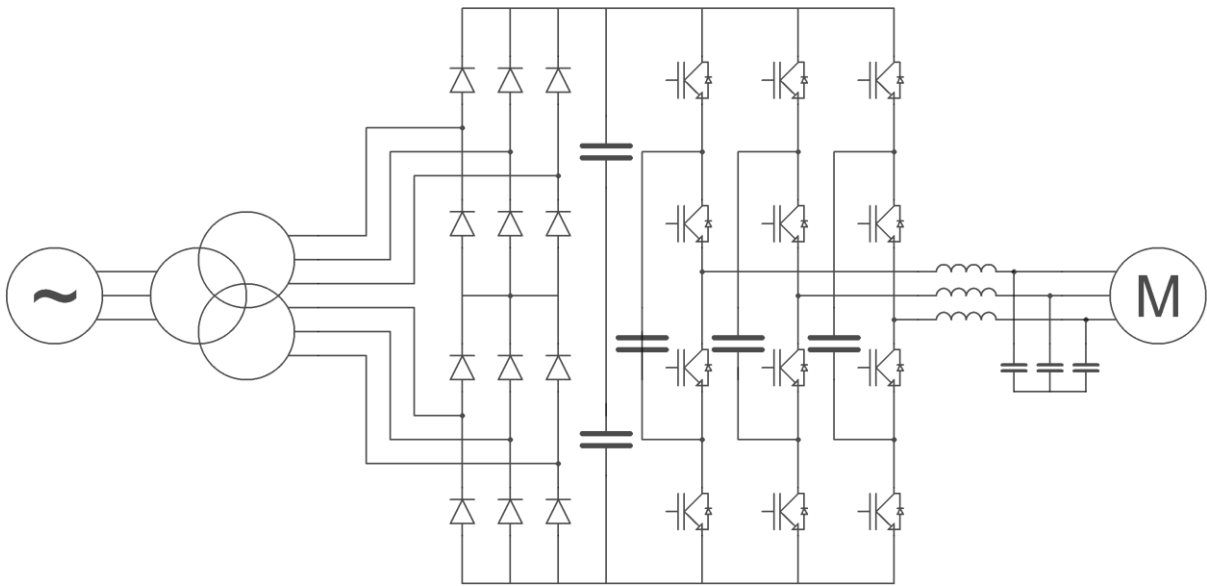


Figure 37: Floating Symmetrical Capacitor VSI

The second topology is the Floating Symmetrical Capacitor depicted in Figure 37 as a four-level converter. Instead of adding clamping diodes to add levels, clamping capacitors are added in a FSC converter. By switching the floating capacitor between the DC link and the load, an intermediate output voltage level is created and the capacitor is charged or discharged. As turn-on snubbers cannot be used it is only possible to apply IGBTs and not thyristor based switching devices such as IGCTs. Advantages of the FSC are that the voltage balancing problem is easier to solve partly due to the fact that multiple switching combinations can result in a certain output voltage. Furthermore the large amount of capacitances ensures good fault ride-through capability. Disadvantages however include the large amount of capacitors needed, resulting in a large footprint, especially when a multilevel AFE is used as the capacitors can't be shared. Furthermore the capacitors cannot be pre-charged as a group which makes start-up more complicated, the converter rating is limited by the current through the capacitors and capacitor voltages are redistributed after a supply voltage surge [26].

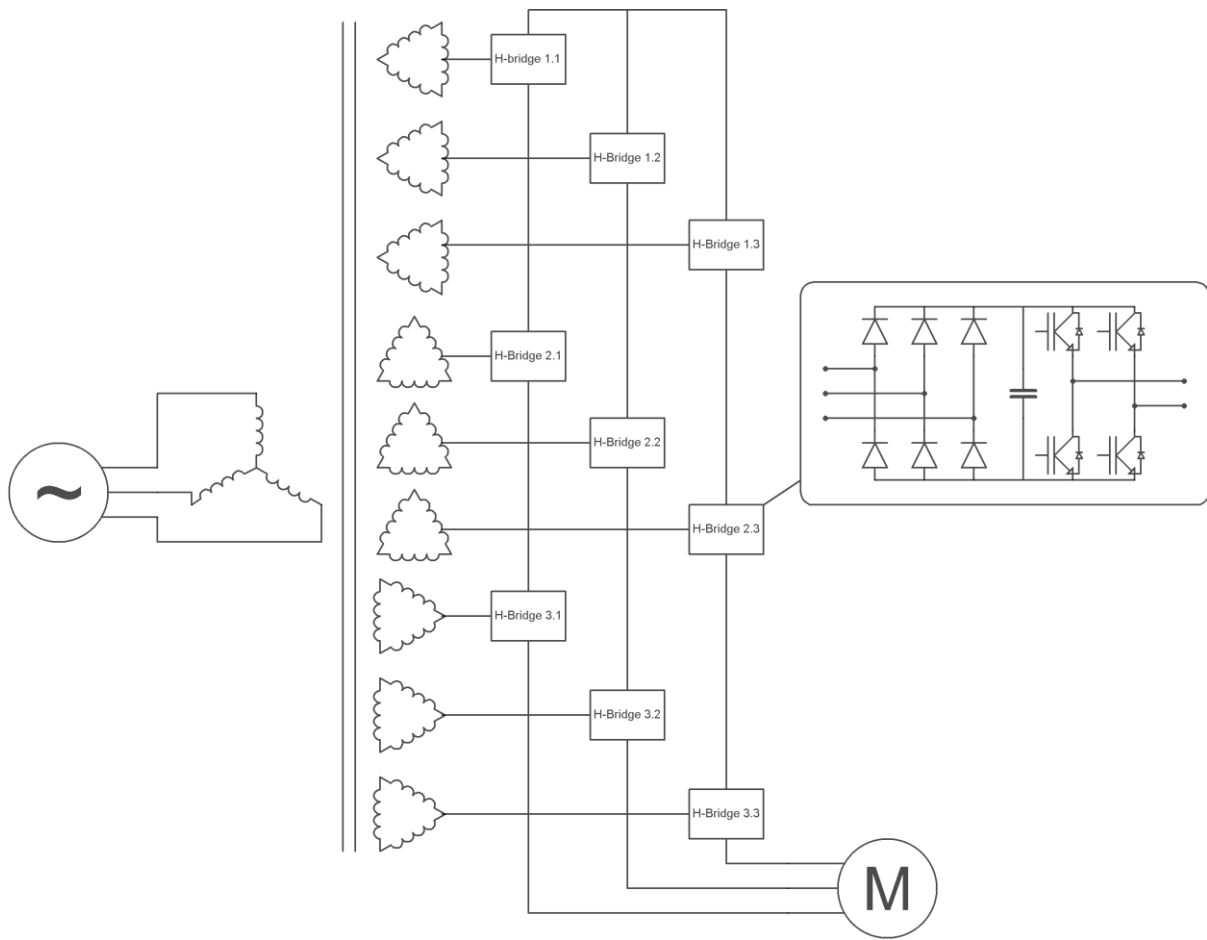


Figure 38: Cascaded H-Bridge VSI

The third topology is the Cascaded H-Bridge depicted in Figure 38 as a seven level converter. In a CHB converter several smaller single phase converters are cascaded to create the desired multilevel output. By connecting them in series, the maximum output voltage and number of voltage levels increase. By connecting units in parallel the current capability can be increased. Each of these converters needs its own secondary winding on the transformer. By using secondary windings with a phase shift relative to each other, harmonics can be cancelled. Advantages of this topology are that the modular design results in easy production and maintenance and flexibility for expansion of the number of levels. Furthermore there are very little low order harmonics, motor losses are low, lower voltage insulation can be used and voltage balancing of the capacitors is not required. Disadvantages however are the separate DC sources for each unit, which all need pre-charging of the capacitors and a by-pass arrangement to ensure availability. Furthermore the high number of components reduces reliability, regenerative braking makes the system very complicated and is therefore hardly used and the transformer has to be purpose built and is large and expensive. Added redundancy will require conservative voltage rating and can't prevent all failures, especially when the unit gets mechanically damaged and the bypass command can no longer be processed [26].

In each topology extra components have to be added to create extra voltage levels, which decrease reliability. Therefore, redundancy is often added to compensate this. However, care should be taken when considering this as the extra components might have a detrimental effect on reliability when it turns out they are not able to clear the fault [26].

3.5 Multi-phase

Electrical power is generated, transmitted and distributed using three phases all over the world. Commercially available machines are therefore practically always three phase motors. When an inverter is used between the grid and the motor, there is no need to stick to a three phase motor. Lower torque pulsations, lower stator losses and higher fault tolerance are reasons to consider a higher number of phases. In the high power range, where motors are often custom made, the use of more phases is an interesting option.

A multi-phase motor is a motor that has more than three phases. As the total power is divided over all the phases it is easier to match inverter power levels to phase power levels in a multi-phase setup, without needing parallel or series connection of inverters. This also means that a lower current per phase can be achieved without increasing the voltage levels [27]. As more harmonics will cancel out in a multi-phase motor, stator copper losses can be reduced. This reduction can be up to 8.81% with a theoretical infinite number of phases, but with 6 phases, reduction is already 6.70% when compared to the same machine with a three phase winding with similar pitch and the same amount of copper in the stator windings [28].

As there are more phases, the supply side will see more pulses per rotation. The behavior from a supply side of view is therefore similar to a multi-pulse setup. Like in a multi-pulse setup a number of harmonics, and therefore interharmonics, can be cancelled [28]. As harmonics get lower in amplitude with higher frequencies, the harmonic content will be lower.

Fault tolerance is another important advantage of a multi-phase machine. When a standard three-phase motor without neutral connection loses a phase, current through the two remaining phases can no longer be controlled independent of each other. As a result it is not possible to continue to run the machine, let alone start it. A multi-phase machine can continue to run and be started smoothly, even with up to $n - 3$ faults, in which n is the number of phases. It is however necessary to use a special current control strategy after a fault, and to operate the machine at a lower level than rated [29].

3.6 Multi-pole

The Campbell diagram in part 2.2 shows that the order of interharmonics in the sub harmonic region will increase when the drive output frequency is increased. A way to increase drive output frequency without increasing the motor speed is the use of a multi-pole machine. This is a machine that has more than one pole pair on its rotor. An example of the rotor of a 2-pole machine and a 4-pole machine is given in Figure 39 and Figure 40 respectively.

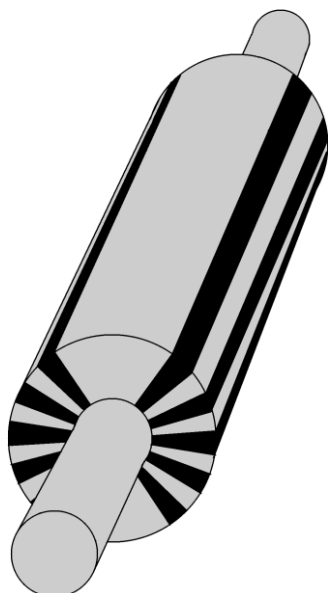


Figure 39: 2 Pole rotor

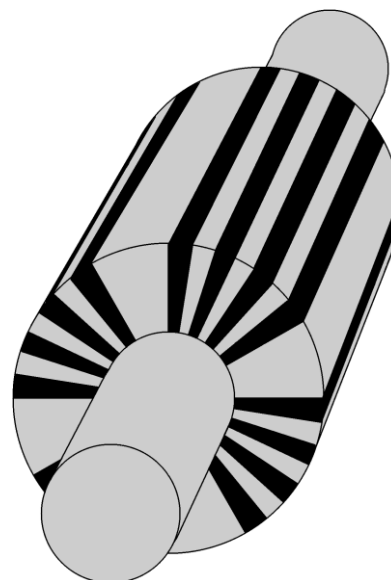


Figure 40: 4 Pole rotor

As a result of the higher number of poles, the machine will have a gearing action. When machines with equal power but different number of poles are driven by the same frequency the speed will decrease and the torque will increase with increasing number of poles[30]. Decreasing the number of poles will have the opposite effect. As a result a higher drive frequency can be obtained, without increasing the motor speed. However, this also has limitations and drawbacks. First of all the converter needs to be able to supply these higher frequencies, this can prove to be challenging, especially for an LCI drive [31]. Furthermore, core losses will increase due to the higher frequencies as magnetic losses are:

$$P_{magnetic} = k_H \cdot B^\alpha \cdot f + k_E \cdot B^2 \cdot f^2 \quad (\text{W/kg}) \quad [31] \quad (11)$$

Where K_H is the hysteresis related coefficient, K_E is the eddy current related coefficient, α is a constant depending on the hysteresis loop, B is the flux and f is the frequency.

Another advantage of using extra poles in an induction motor is the reduction of the double line frequency vibration. As increasing the number of poles decreases the angle between two nodes, the resulting system will be stiffer to movement [32].

In Figure 41 the speed bands of a 2-pole, 4-pole and 6-pole machines are shown. Areas that should be avoided are in red, problem free areas are in green. The red areas can be caused by interharmonics or, by the limit on the output frequency of the converter.

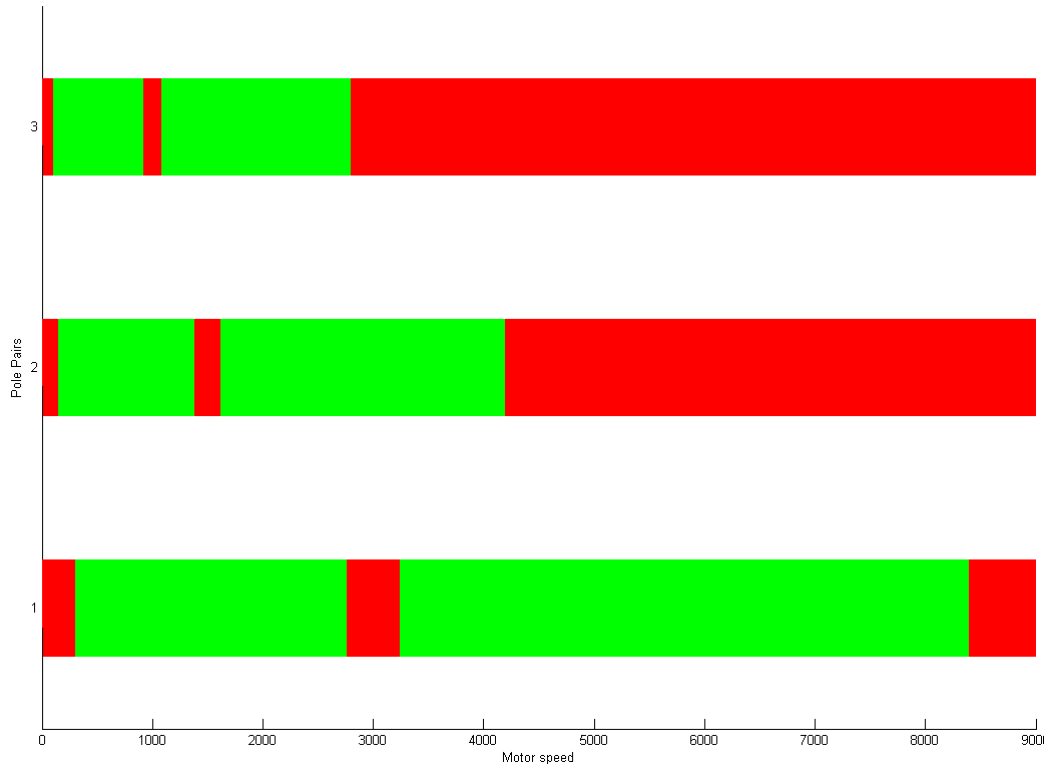


Figure 41: Allowed and forbidden speed bands

Problems can be avoided by choosing a motor design which has no problems over the operating range. Problems can however still occur during the speeding up of the system, or when a wide range of operating speeds is necessary.

An interesting option would therefore be to have a machine that can switch between a 2-pole and 4-pole design during operation so a problem free area can always be used. Machines that could change their number of poles during operation were applied early twentieth century as relatively simple means of changing motor speed. With the rise of VSDs, the use of pole changing machines decreased, but renewed interest is shown for electric vehicle applications.

Most pole-changing motors are induction motors. The reason for this is that their rotor can inherently be used for different pole numbers. The simplest way to create the pole changing stator is to give it both sets of windings. However, this will result in high cost and poor performance. Therefore other winding schemes, like the Dahlander winding, were more popular where the windings are separated in several coils which can be reconnected to change the pole number [33]. A more modern approach is to use separate coils that are each independently driven by an inverter [34], a disadvantage of this system is the space harmonics that are inherently produced.

To change the pole number of a synchronous machine, modification of the rotor is also necessary. Such pole-changing motors have been built [35], but their complexity and therefore high cost along with the increased availability of other means of speed control has resulted in limited application.

The high cost and lower efficiency of these motors, combined with the short intervals where pole changing is necessary makes this solution not practically viable.

3.7 Increased motor speed

As seen in section 3.6, increasing drive output frequency will reduce the interharmonics in the subharmonic region. Increasing drive frequency will also increase the motor speed if no other changes are made to the system. Increasing motor speed will affect the other parts in the mechanical system.

To manage the speed difference between the motor and compressor a gearbox can be added between the motor and the compressor. Due to the high maintenance and relatively low reliability associated with a gearbox, this is not a desirable solution. In some cases, a gearbox is already present to increase speed between the motor and the compressor. There it would be an interesting option to reduce or even eliminate the gearbox from the setup.

From a compressor point of view, higher speeds are desirable as the compressor can be made smaller. There are however limits on this, especially in terms of the speed of gas through the compressor. As a result, it is possible to increase the speed up to 10% when power is 80MW or less, but higher speeds are only viable for lower power ratings.

A point that cannot be overlooked is the ability of the electric drive itself to rotate at higher speeds. The limiting factor in this is the speed at the circumference of the rotor. To increase the motor operating speed it would therefore be necessary to decrease the rotor diameter. As a result the machine would have to be longer for the same power rating. Besides the obvious increase in footprint, this would also increase the chance of resonance problems in the motor shaft.

Increasing motor speed is therefore an interesting and relatively simple option. But the limitations on rotating speed have to be kept in mind.

3.8 Damper

During resonance, very high torques can be reached due to the limited damping of this oscillation. A logical step would therefore be to add mechanical damping in the form of elastomeric dampers. As the torque will increase to the point where excitation and damping match, the torque will decrease linearly with increased damping. It is important to install this damper as close to the problematic node as possible to ensure maximum damping.

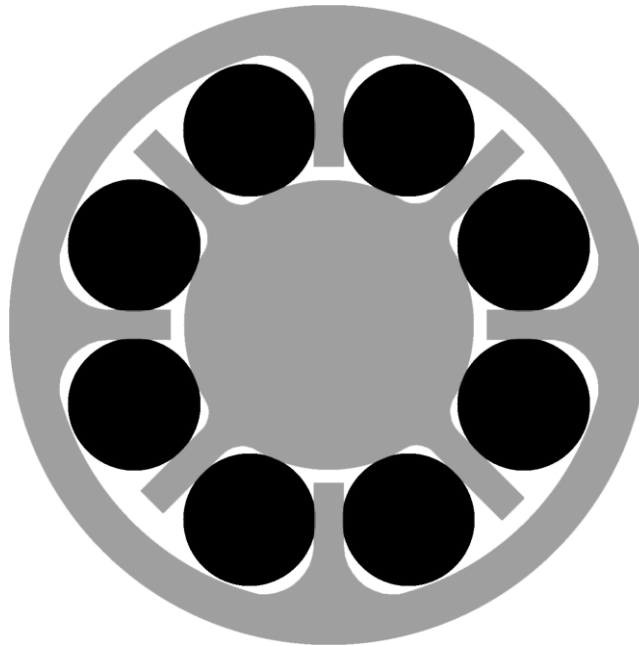


Figure 42: Mechanical damper

The basic setup of an elastomeric damper is shown in Figure 42. Both the input and output elements are typically made of steel (grey). Between them, elastomeric elements (black) are installed, which will absorb the vibrations by compressed deformation. During this deforming, energy is dissipated in the elastomeric elements. This will heat up the elements, which, combined with environmental factors, will lead to degrading of the elements. As a result, regular maintenance is needed to ensure reliable operation.

Due to the added damping, the system can operate safely on resonance frequencies. Care however has to be taken when operating on a resonance point continuously. The magnitude of torsional resonance can be quite high, so the elastomeric elements can be overloaded when operating on a resonance point for a longer period of time.

As a result of the high maintenance and the risk of overloading, dampers are only used as a last resort when a design turns out to have resonances that can't be solved in other ways.

3.9 Speed through

As seen in the Campbell diagram in section 2.2, the frequency of the created interharmonics depends on the drive output frequency. By avoiding certain drive frequencies, resonance can be avoided.

When the resonance points are known and the motor speeds which cause corresponding interharmonics are calculated, forbidden speed bands can be derived. The frequency bands that cause resonance are very narrow, only a few tenths of a Hertz. However, variation in material parameters, due to aging, temperature or other causes will require the band to be wider. Variations in grid frequency can make the forbidden band even wider.

Avoiding operation in these frequency bands is possible, but will limit the flexibility of operation. It is however not possible to avoid these frequency bands altogether as they will have to be passed when speeding up the drive or when going from one operating point to the other. In most cases this can be done without resulting in problems as is already illustrated in Figure 17 and Figure 18. As was concluded earlier, the faster the forbidden bands can be speeded through, the lower the torque will stay. To decrease the time that is needed to speed through a forbidden band, compressor load could be reduced or motor torque can be increased. Increasing motor torque will also increase the amount of interharmonics created, so caution should be taken when increasing motor torque for the speed through. Reducing compressor load is not always possible, but only when the process allows a temporary reduction of compression.

3.10 Mechanical torques insertion

The interharmonic problem is a combined electrical and mechanical problem. As the largest problems arise on the mechanical side, it makes sense to look for solutions on the mechanical side too. The damper system described in section 3.8 is one of the solutions where the resonance is limited by increasing the damping. A setup that actively compensates torques, like the active filter does on the electrical side, would be an interesting option.

It seems that research in this area is very limited. An important reason for this is that mechanical systems on this scale do not respond well to varying torques. If a countering torque pulsation was created by blow-off valve in the gas turbine, the blades of the turbines would take a lot of stress. The risk of damage to the mechanical systems that have to transport the inserted torques makes this system undesirable.

There is however some research done on using noise cancelling techniques to cancel mechanical vibrations in systems. By placing actuators on the machine and driving them in response to measured displacements, impressive damping of vibrations and noise levels can be achieved [36]. If this could be applied to torsional vibrations it would be an interesting way of adding damping to the generator-turbine shaft. The amount of force that can be counteracted with such a system is of course very limited, but a small damping can be enough to avoid resonance building up.

Unfortunately this kind of system is still in an experimental stage, but it could be an effective solution in the future.

3.11 Firing pulse

Interharmonics are created by the switching action of the inverter. Changes in the firing pulse of the switches can therefore have a significant effect. Both LCI drives and VSI drives can profit from a different firing pulse although the limited switch control in LCIs can make it challenging.

As seen in section 3.2, active filters can be used to insert damping torques into the grid. These are essentially small inverters that provide the desired waveforms. As an inverter is already present in a VSD, it would be an interesting option if it can provide this extra task as well. This is exactly what is done with Integrated Torsional Mode Damping. To do this the torque has to be measured on different points, which is complicated to do in practice. This can be both on the generator or on the motor side, depending on the place where pulsating torques have to be suppressed. Alternatively it can also be deduced from the machine voltage and current by using an observer. This is then used to adjust the firing angle. To suppress torque pulsations on the motor side the inverter pulses are adjusted. To suppress torque pulsations on the generator side the rectifier pulses are adjusted, which means that a controllable rectifier is needed to apply this technique. To ensure that adjustments to the rectifier firing angle don't influence the motor, the inverter firing angle should also be adjusted [37].

A much simpler approach is a 'sloppy' speed control. Here the speed control deliberately gets a small disturbance. As a result, the system will never operate constantly at any frequency. As the resonances are very sharply tuned, only small deviations are necessary to greatly reduce the torque. The speed with which this frequency is changed is also important: too fast and the system won't be able to respond to it, too slow and torques will still get too high. As a reference, the torque for a system constantly excited by a 1pu torque is repeated in Figure 43.

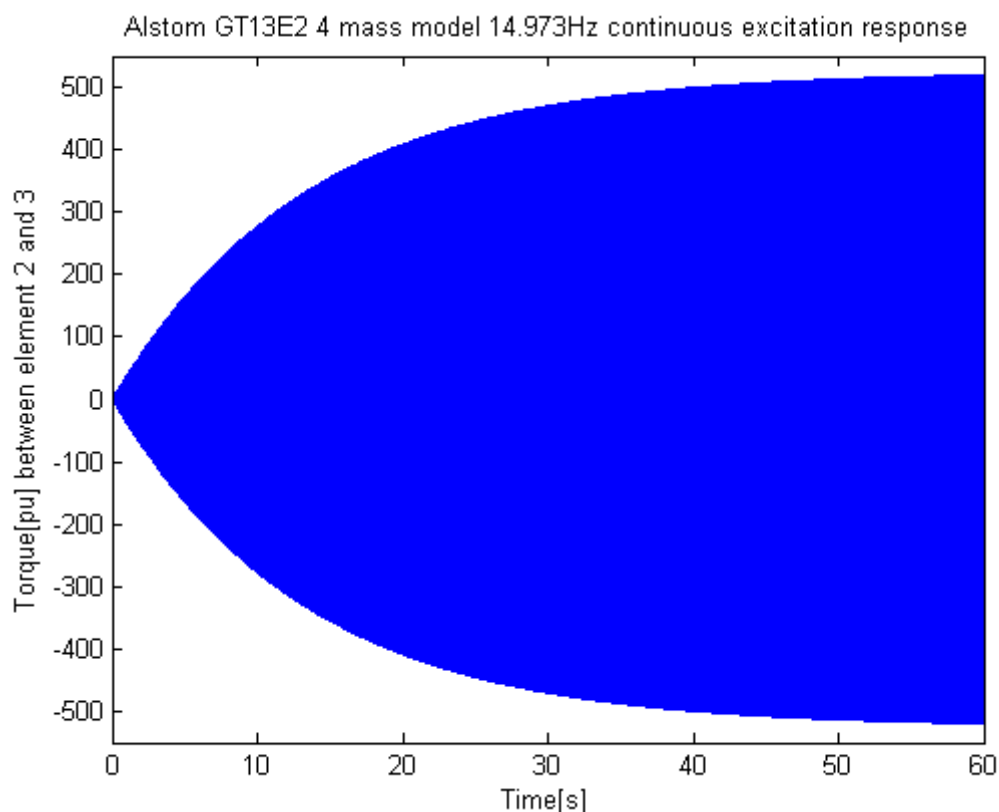


Figure 43: Continuous excitation

In Figure 44 the same system is excited with the same frequency, but now with a sinusoidal disturbance of 1.2Hz with a 10 second period. With a 12-pulse converter this would mean a 0.1Hz deviation in output speed as the largest interharmonics are $11 \cdot F_{\text{grid}} - 12 \cdot F_{\text{motor}}$ and $13 \cdot F_{\text{grid}} - 12 \cdot F_{\text{motor}}$. The torque is strongly dependent on both the amplitude and frequency of the disturbance. In this case, torque stays more than ten times lower than it would with normal excitation.

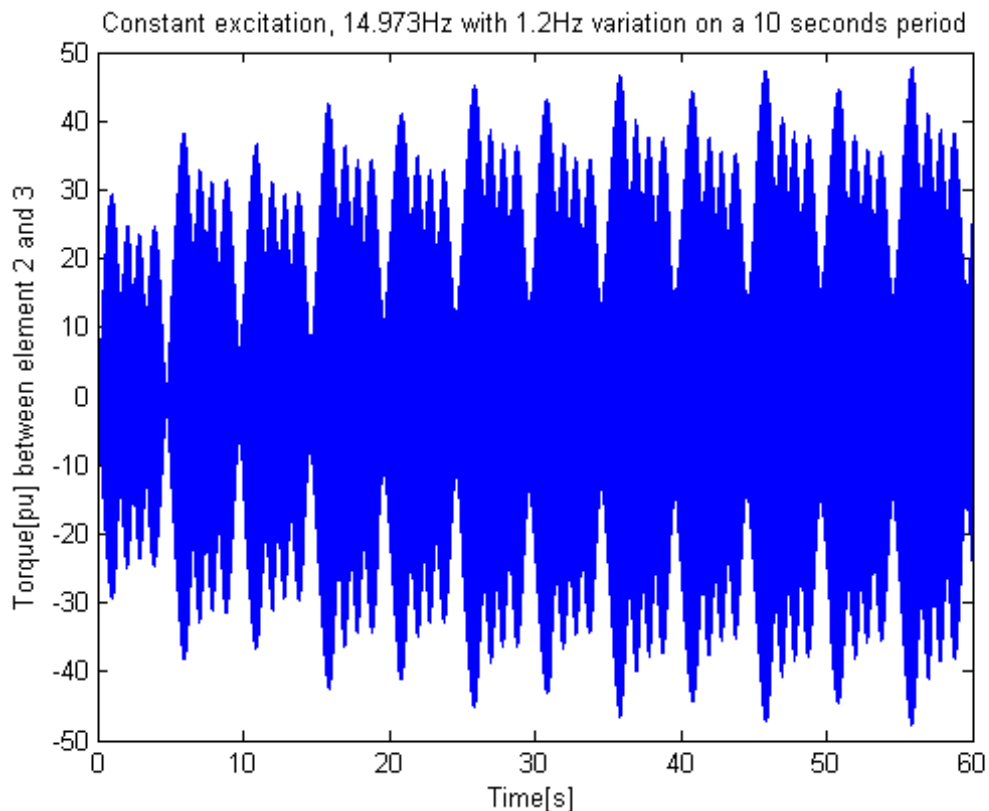


Figure 44: Constant excitation with 1.2Hz disturbance with a 10 second period

The higher level of control over the output with a PWM VSI also results in more options to compensate pulsating torques. As the switching action creates the pulsating torques, and the switch is fully controllable there are several options available. The first option is to invert the PWM carrier, which will also invert the created disturbance so the pulsating torque reduces. Figure 43 to Figure 46 show the effect of inverting the carrier. In Figure 43 the carrier is not inverted, resulting in large torques. In Figure 45 the carrier is inverted every five seconds, thereby limiting the torque that is built up. In Figure 46 the carrier is inverted every second further reducing torques. As can be see, the shorter the interval of inverting, the lower the pulsating torques will stay [37]. The inversion itself will however produce extra distortions and, when combined with certain frequencies, can even excite resonance. It is therefore wise to only use inversion when resonance is either expected or measured, as can be seen when comparing Figure 47 and Figure 48.

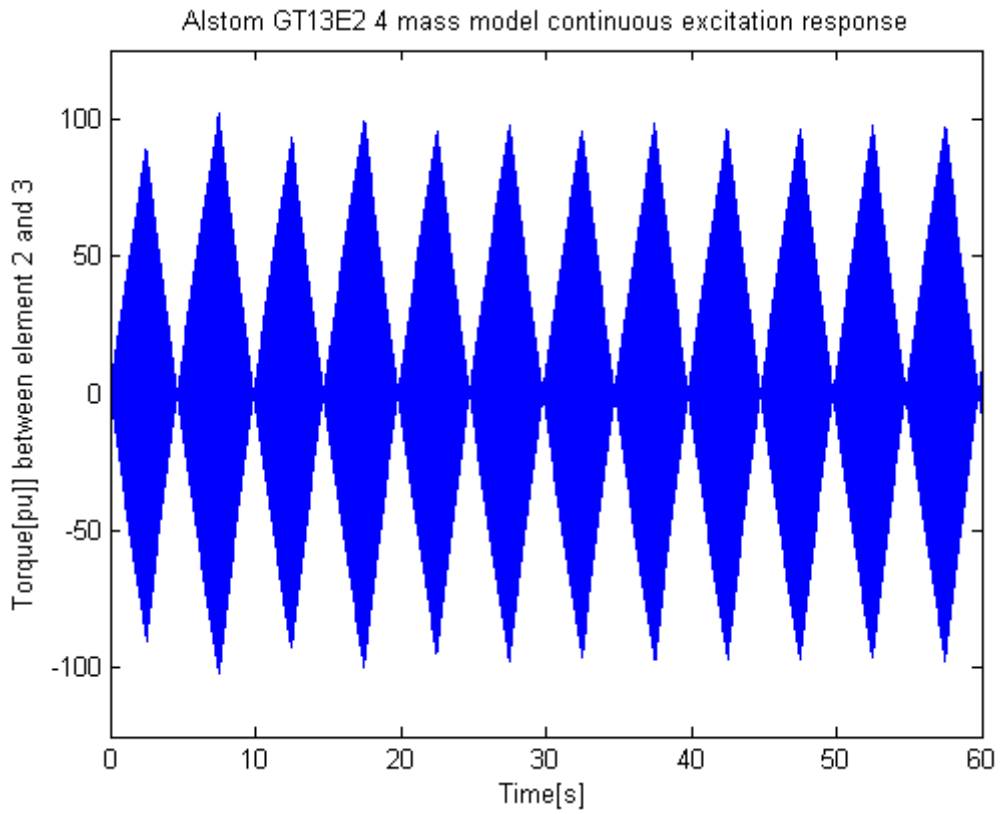


Figure 45: Continuous excitation with carrier inversion every five seconds

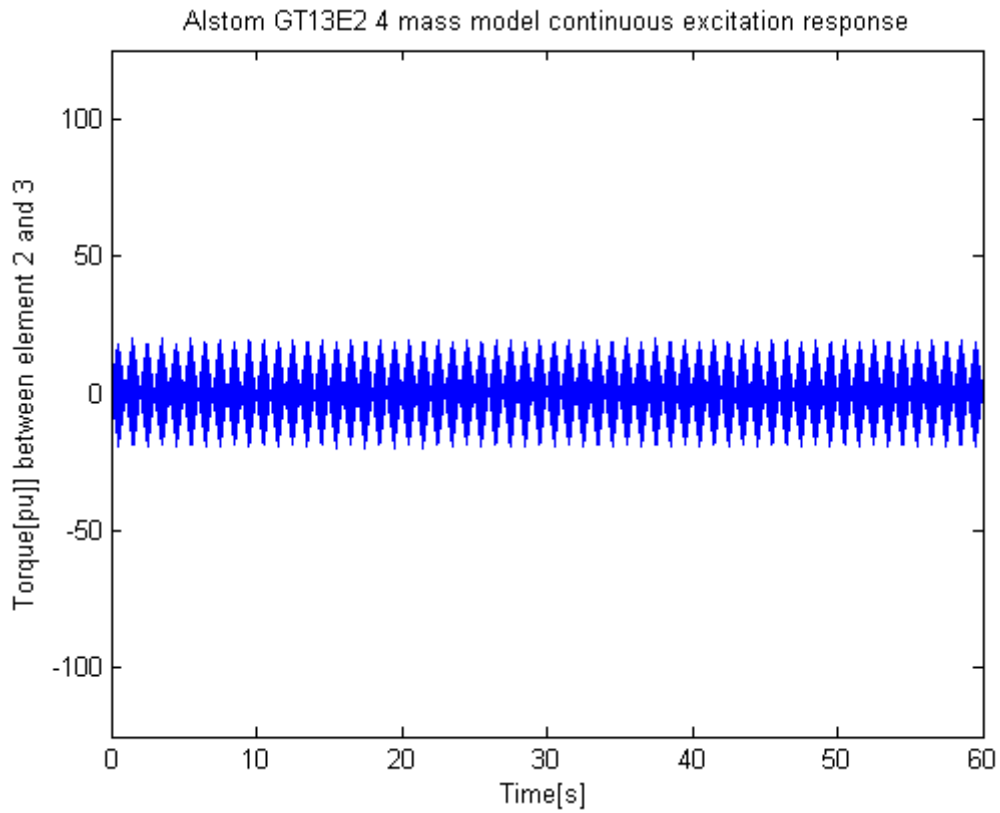


Figure 46: Continuous excitation with carrier inversion every second

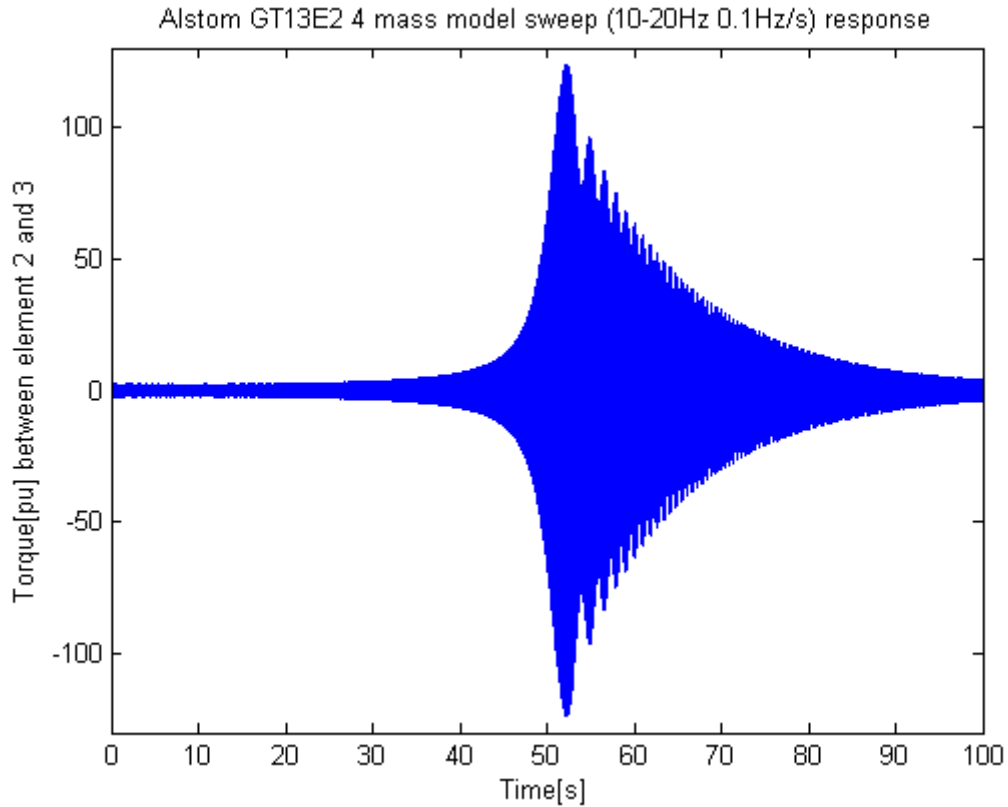


Figure 47: 10-20Hz 0.1Hz sweep without carrier inversion

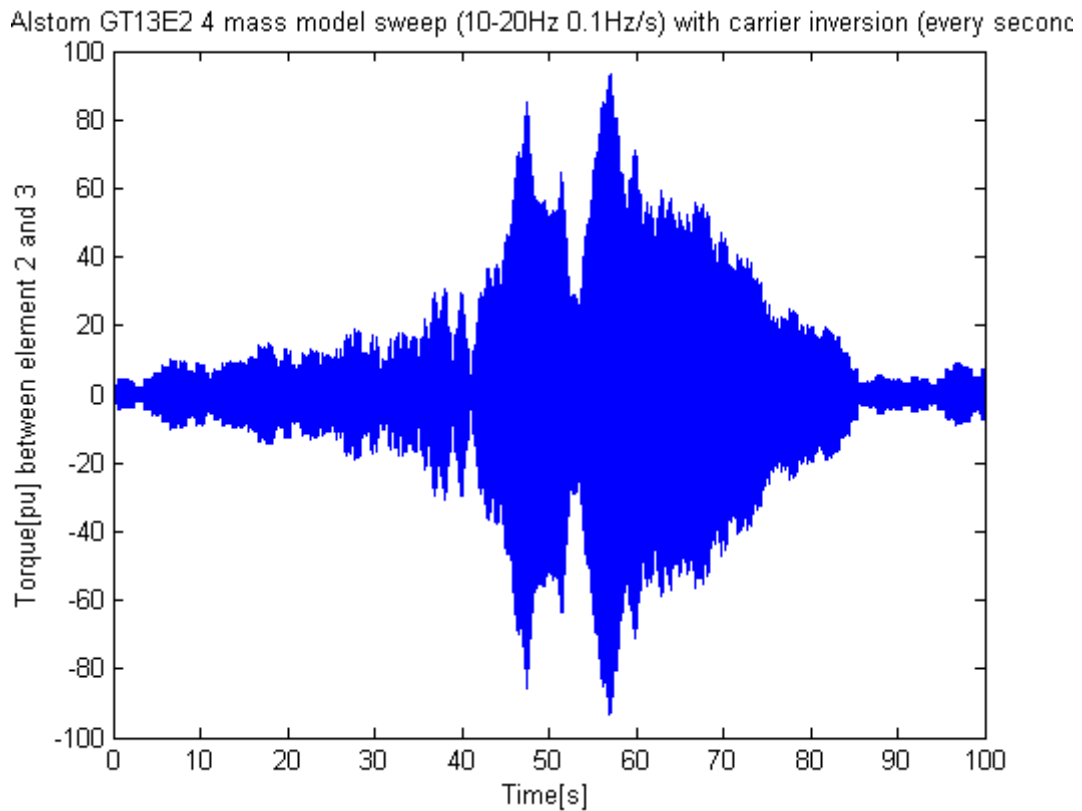


Figure 48: 10-20Hz 0.1Hz sweep with carrier inversion every second

As the carrier frequency of the PWM operation influences the created frequency components, critical frequencies can be avoided by changing the carrier frequency as a function of the drive

speed. The Campbell diagram will also change when changing the switching frequency, as illustrated in Figure 49. This diagram shows that by being able to use even a limited number of switching frequencies, natural frequencies can be avoided [11]. This does however rely on knowledge of the natural frequencies, which increases the work that has to be done to apply this technique.

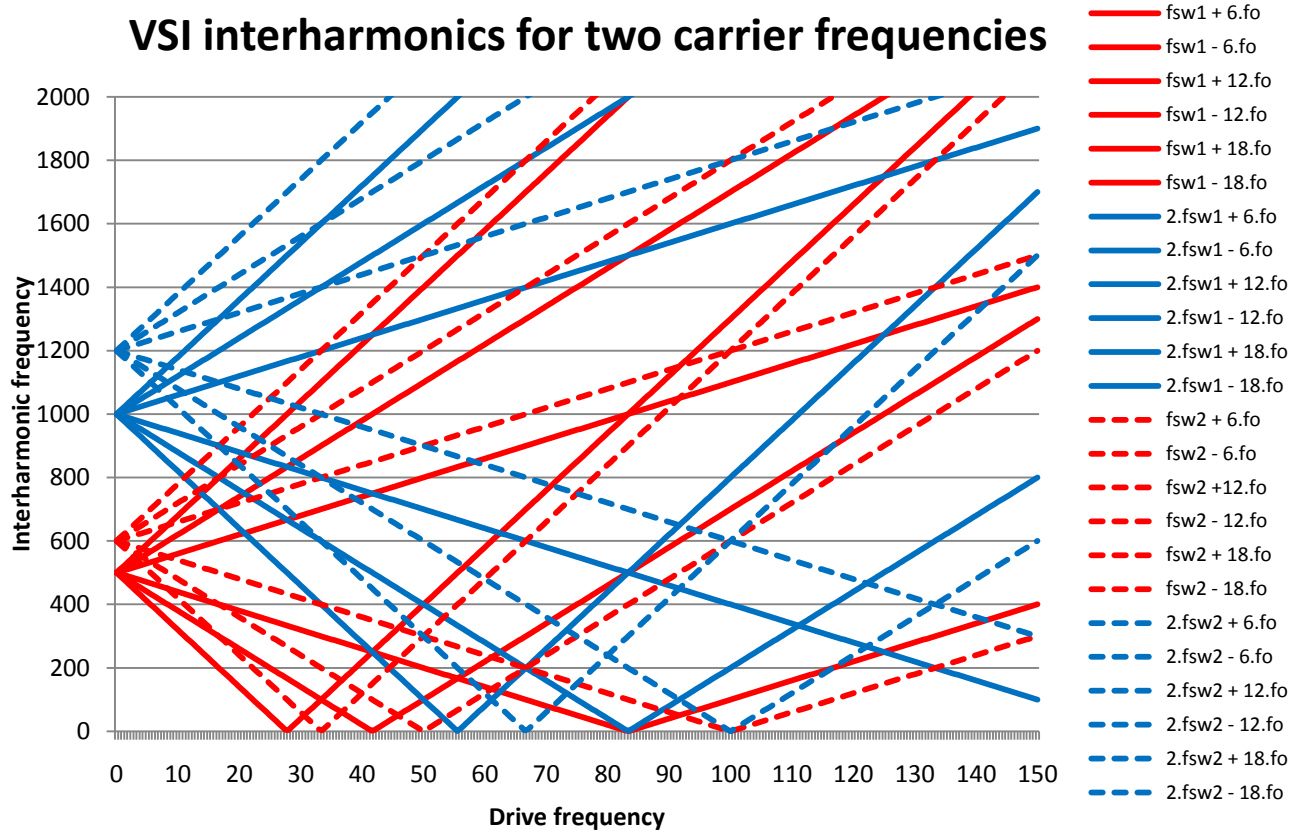


Figure 49: Campbell diagram for a PWM VSI with 500Hz (fsw1) or 600Hz (fsw2) PWM carrier

3.12 Summary of solutions

When comparing different solutions to interharmonics an important difference is whether the solution attenuates the interharmonics, like filters do for instance, or change the frequency of interharmonics, like for instance varying the number of poles.

The reason for this lies in the fact that were the resonance point of a turbine-generator shaft is usually well known, the damping factors are much less known, and can vary by up to a factor 100. Therefore very strong attenuation of the interharmonics is necessary to assure problem free operation.

It is therefore wiser to look at solutions that avoid the problematic frequencies altogether. The simplest way to do this is to choose an operation speed band where no problematic interharmonics are produced. This requires thorough coordination between the choice for the turbine, VSD and compressor.

When it is not possible to stay outside the problematic areas during operation, a changing firing pulse should be considered. This requires a relative small modification to the VSD, can be easily altered when new equipment is installed and shows promising results.

For the lower power ranges, VSIs can be used which already lower the amount of interharmonics created. This can be extended with an AFE and a Multi-level setup to further reduce the amount of interharmonics.

To verify whether changing the firing pulse will reduce interharmonics, various ways of changing the firing pulse of an LCI will be simulated in a typical setup. Slight changes in frequency both with and without feedback of a torque sensor will be tested.

4 System Simulation

4.1 Overview

To evaluate and compare different solutions to interharmonics, they should be tested in a realistic LNG setup. The setup in Figure 50 is chosen as this is a setup that has already been simulated in the past, so results can be compared for validation.

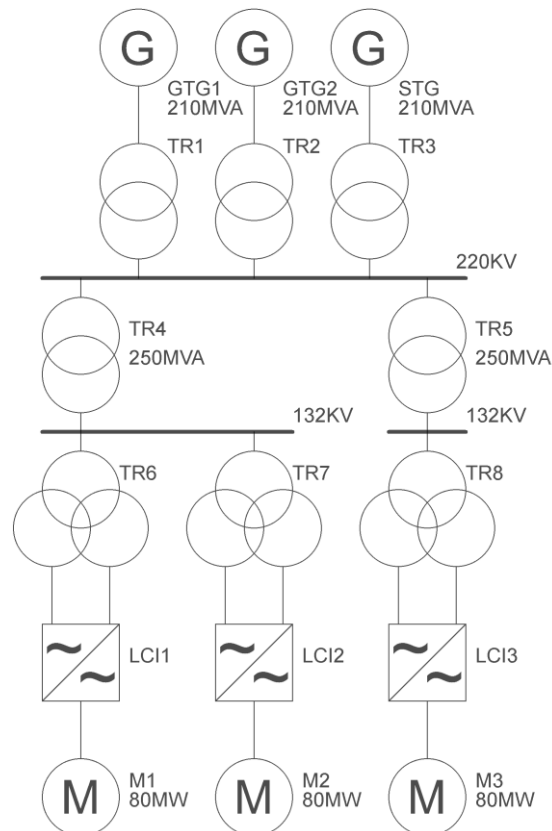


Figure 50: Simulated system overview

The setup consists of two GTs, one ST, three LCIs and three 80MW motors. The transformers and cables connecting all the separate components are also included in the model. Before looking to the results, the models of the separate systems are given.

4.2 Motor model

To be able to simulate transient situations, it is important to have an elaborate motor model, where mechanical behavior and damper action is also taken into account.

The motor is modeled using the dq-system depicted in Figure 51 and Figure 52 [38]. Equations 12 to 26 are the corresponding equations. Subscripts d and q indicated the d or q axis, subscript σ indicates the leakage inductance, subscript m indicates the main inductance, subscript 1 indicates a damper, the prime indicates reference to the stator, capitals indicate that quantities are referred to the stator.

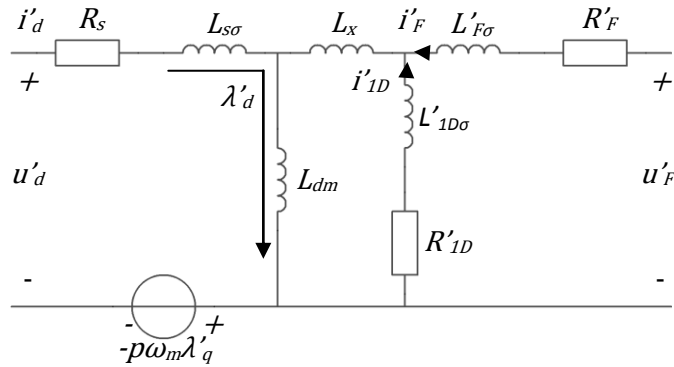


Figure 51: dq system equivalent d circuit

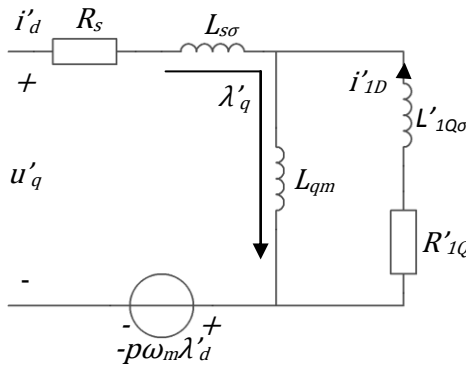


Figure 52: dq system equivalent q circuit

The motor voltages are defined by equations 12 to 16, where the damper voltages are zero as the damper windings are short circuited.

$$u'_d = R_s \cdot i'_d - p \cdot \omega_m \cdot \lambda'_q + \frac{d\lambda'_d}{dt} \quad (12)$$

$$u'_q = R_s \cdot i'_q + p \cdot \omega_m \cdot \lambda'_d + \frac{d\lambda'_q}{dt} \quad (13)$$

$$u'_F = R'_F \cdot i'_F + \frac{d\lambda'_F}{dt} \quad (14)$$

$$0 = R'_{1D} \cdot i'_{1D} + \frac{d\lambda'_{1D}}{dt} \quad (15)$$

$$0 = R'_{1Q} \cdot i'_{1Q} + \frac{d\lambda'_{1Q}}{dt} \quad (16)$$

The referred inductances used in Figure 51 and Figure 52 can be calculated by using equation 17 to 20.

$$L_x = L_{dm} \cdot \frac{M_{f1d}}{\sqrt{L_{fm} \cdot L_{1dm}}} - L_{dm} \quad (17)$$

$$L'_{F\sigma} = \frac{L_{dm}}{L_{fm}} \cdot L_{f\sigma} - L_x \quad (18)$$

$$L'_{1D\sigma} = \frac{L_{dm}}{L_{1dm}} \cdot L_{1d\sigma} - L_x \quad (19)$$

$$L'_{1Q\sigma} = \frac{L_{dm}}{L_{1qm}} \cdot L_{1q\sigma} - L_x \quad (20)$$

Now the fluxes can be calculated by using equations 21 to 26.

$$\lambda'_d = L_{s\sigma} \cdot i'_d + L_{dm}(i'_d + i'_F + i'_{1D}) \quad (21)$$

$$\lambda'_q = L_{s\sigma} \cdot i'_q + L_{qm}(i'_q + i'_{1Q}) \quad (22)$$

$$\lambda'_F = L'_{F\sigma} \cdot i'_F + L_x(i'_F + i'_{1D}) + L_{dm}(i'_d + i'_F + i'_{1D}) \quad (23)$$

$$\lambda'_{1D'} = L'_{1D\sigma} \cdot i'_{1D} + L_x(i'_F + i'_{1D}) + L_{dm}(i'_d + i'_F + i'_{1D}) \quad (24)$$

$$\lambda'_{1Q'} = L'_{1Q\sigma} \cdot i'_{1Q} + L_{qm}(i'_q + i'_{1Q}) \quad (25)$$

Finally the produced torque is calculated using equation 26.

$$T_e = p \cdot (-i'_d \cdot \lambda'_q + i'_q \cdot \lambda'_d) \quad (26)$$

As the motor will be driven by an LCI, ideally it should take current as an input. However, when the equations are rewritten to have current as an input, a derivative term will be present resulting in an unstable system. Therefore the motor is modeled with a voltage input, together with speed, angle and field voltage inputs. The outputs consist of current and torque. Equations 12 to 16 can now be rewritten into equations 27 to 31.

$$\frac{d\lambda'_d}{dt} = u'_d - R_s \cdot i'_d + p \cdot \omega_m \cdot \lambda'_q \quad (27)$$

$$\frac{d\lambda'_q}{dt} = u'_q - R_s \cdot i'_q - p \cdot \omega_m \cdot \lambda'_d \quad (28)$$

$$\frac{d\lambda'_F}{dt} = u'_F - R'_F \cdot i'_F \quad (29)$$

$$0 = R'_{1D} \cdot i'_{1D} + \frac{d\lambda'_{1D}}{dt} \quad (30)$$

$$0 = R'_{1Q} \cdot i'_{1Q} + \frac{d\lambda'_{1Q}}{dt} \quad (31)$$

Combining this all into a matrix form, we reach equations 32 and 33, with L_{mat} , P_{mat} and R_{mat} defined as in equations 34 to 36.

$$\lambda = \int U_{in} - R_{mat} \cdot I - P_{mat} \cdot \omega_m \cdot \lambda dt \quad (32)$$

$$I = L_{mat}^{-1} \cdot \lambda \quad (33)$$

$$R_{mat} = \begin{bmatrix} R_s & 0 & 0 & 0 & 0 \\ 0 & R_s & 0 & 0 & 0 \\ 0 & 0 & R_f & 0 & 0 \\ 0 & 0 & 0 & R'_{1D} & 0 \\ 0 & 0 & 0 & 0 & R'_{1D} \end{bmatrix} \quad (34)$$

$$P_{mat} = \begin{bmatrix} 0 & -p & 0 & 0 & 0 \\ p & 0 & 0 & 0 & 0 \\ 0 & 0 & 0 & 0 & 0 \\ 0 & 0 & 0 & 0 & 0 \\ 0 & 0 & 0 & 0 & 0 \end{bmatrix} \quad (35)$$

$$L_{mat} = \begin{bmatrix} L_{s\sigma} + L_{dm} & 0 & L_{dm} & L_{dm} & 0 \\ 0 & L_{s\sigma} + L_{qm} & 0 & 0 & L_{qm} \\ L_{dm} & 0 & L'_{F\sigma} + L_x + L_{dm} & L_{dm} + L_x & 0 \\ L_{dm} & 0 & L_{dm} + L_x & L_{dm} + L_x + L'_{1D\sigma} & 0 \\ 0 & L_{qm} & 0 & 0 & L_{qm} + L'_{1Q\sigma} \end{bmatrix} \quad (36)$$

The implementation of this model in Simulink is shown in Figure 53.

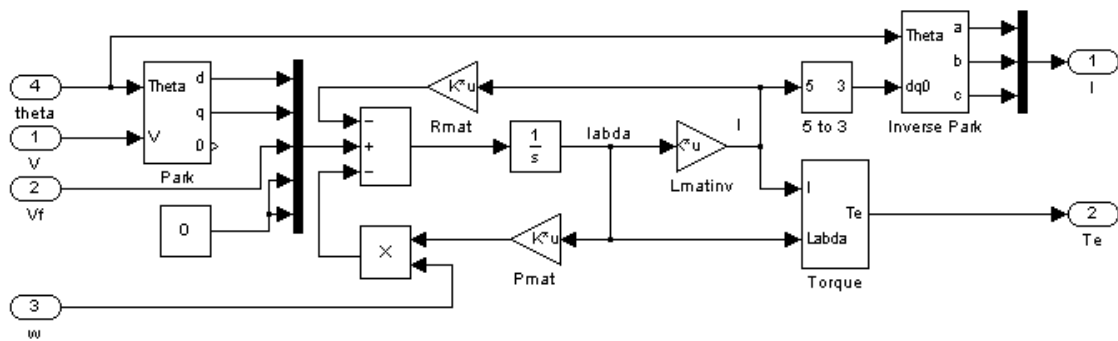


Figure 53: Motor model

To be able to use this model we need to know the parameters R_s , R'_F , R'_{1D} , R'_{1Q} , L_{dm} , L_{qm} , $L_{s\sigma}$, L_x , $L'_{F\sigma}$, $L'_{1D\sigma}$ and $L'_{1Q\sigma}$. The parameters given in Table 2 are from a motor of similar size also used for LNG compression and driven by a VSD, that is built and in operation.

R_s	10.6mΩ
R'_F	1.29mΩ
R'_{1D}	24.8mΩ

R'_{1Q}	24.8m Ω
L_{dm}	7.80mH
L_{qm}	6.86mH
$L_{s\sigma}$	567 μ H
L_x	0H
$L'_{F\sigma}$	48.5 μ H
$L'_{1D\sigma}$	430 μ H
$L'_{1Q\sigma}$	430 μ H

Table 2: Motor parameters

$$L_d = L_{ad} + L_l \quad (37)$$

$$L_q = L_{aq} + L_l \quad (38)$$

$$L'_d = L_l + \frac{L_{ad} \cdot (L_{fd} + L_{pl})}{L_{ad} + L_{fd} + L_{pl}} \quad (39)$$

$$L''_d = L_l + \frac{L_{ad} \cdot L_{fd} \cdot L_{1d} + L_{ad} \cdot L_{pl} \cdot L_{1d} + L_{ad} \cdot L_{fd} \cdot L_{pl}}{L_{ad} \cdot L_{fd} + L_{ad} \cdot L_{1d} + L_{1d} \cdot L_{fd} + L_{1d} \cdot L_{pl} + L_{pl} \cdot L_{fd}} \quad (40)$$

$$L''_q = L_l + \frac{L_{aq} \cdot L_{1q}}{L_{aq} \cdot L_{1q}} \quad (41)$$

$$T'_{d0} = \frac{L_{ad} + L_{fd} + L_{pl}}{R_{fd}} \quad (42)$$

$$T''_{d0} = \frac{1}{R_{1d}} \left(L_{1d} + \frac{L_{ad} \cdot (L_{fd} + L_{pl})}{L_{ad} + L_{fd} + L_{pl}} \right) \quad (43)$$

$$T''_{q0} = \frac{L_{aq} + L_{1q}}{R_{1q}} \quad (44)$$

Model	Equations	Value
R_s	R_a	2.36m Ω
R'_F	R_{fd}	7.5m Ω
R'_{1D}	R_{1d}	99.9m Ω
R'_{1Q}	R_{1q}	328m Ω
L_{dm}	L_{ad}	7.10mH
L_{qm}	L_{aq}	6.82mH
$L_{s\sigma}$	L_l	539 μ H
L_x	L_{pl}	0
$L'_{F\sigma}$	L_{fd}	258 μ H
$L'_{1D\sigma}$	L_{1d}	80.8 μ H
$L'_{1Q\sigma}$	L_{1q}	75.8 μ H

Table 4: Generator parameters (fundamental definition)

The field voltage is assumed to be constant for the short simulation periods considered here, therefore no voltage regulator is applied here.

4.4 LCI model

As we are looking at interharmonics, the LCI is the most important model. Here, the motor and grid voltages and currents meet, resulting in interharmonics. A 12-pulse LCI is chosen which is also the most common setup used.

All the different states due to switching actions make the LCI model a very complicated model. To keep things clear, the model is split into several parts: the rectifier, inverter and DC link. A 12-pulse setup with single dc-link is chosen as this has the lowest distortion and is commonly used. Both inverter and rectifier block are modeled as a Matlab function which can be called upon in Simulink. A schematic representation of the model is shown in Figure 55 to clarify the location of the different components.

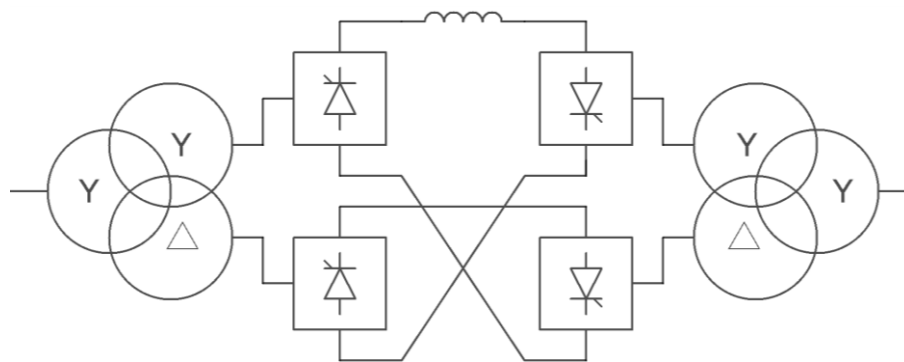


Figure 55: LCI setup

4.4.1 Rectifier

The rectifier model is a 6-pulse unit. Two of these units are combined to create a 12-pulse unit.

The rectifier determines the current on input and the voltage on the output based on the state of the thyristors and the output current and input voltage. As long as only one pair of thyristors per 6-pulse unit is conducting, the voltage and current on input and output are equal.

The tricky part is the commutation. When the current is commutated from one thyristor to another, the two input currents should total the output current, and the output voltage and both input voltages are equal. This voltage should be such that the current in the AC side inductances is reduced in one phase and increased in the other. Based on knowledge of the order of magnitude of the AC side inductances and the difference between the two connected input voltages, the derivative of the current can easily be determined.

The MATLAB function will be explained based on the positive half of the inverter. The negative half operates similar, but of course with a different sign.

First the function compares the motor angle with the firing angle to determine the switch mode. When a thyristor should be fired it is changed to the on state. All thyristors that were on last iteration are considered to be still on. Now the state of the thyristors is known, the function can determine whether it is in a steady mode, or in commutation.

In steady mode the input current of the connected phase should equal the output current. The difference between the two currents is therefore divided by the time step to obtain the necessary

di/dt to make them equal within one time step. This is important as input and output current should always be equal.

In commutation mode, the voltages of both connected phases would be equal in practice. Due to limitations in the model, the voltages will remain slightly different. The phase with the highest open circuit voltage will have a slightly higher voltage. This way it can be determined in which phase current increases and in which phase current decreases. The output voltage is chosen to be equal to the highest voltage of these two.

When the current in the phase with the lowest voltage is still above zero, commutation will still occur. The difference in voltage in the model mentioned earlier is caused by an offset in the input currents. The difference in voltage between the two phases is therefore a measure of how much the currents are off. By dividing this voltage difference by the system inductance a di/dt can be deduced. This system inductance should be derived from the network model and generator model, which can prove to be difficult. However, as the actual voltage and current levels are not affected by this value, only the speed at which offsets are compensated, an approximation of this value can be used. The voltages on the input will automatically vary with the current drawn. After output voltage and derivatives of the input current are derived, both phases are checked for positive current and the thyristors states are set accordingly.

The MATLAB function for the rectifier is given in Appendix 2. The Simulink implementation is given in Figure 56. The positive and negative values for the DC-link voltage are combined to one signal. The derivative of the current is fed to an integrator and fed back to the input for feedback. The states of the thyristors are also fed back to the input after being delayed less than one time step. This time step is used to prevent an algebraic loop.

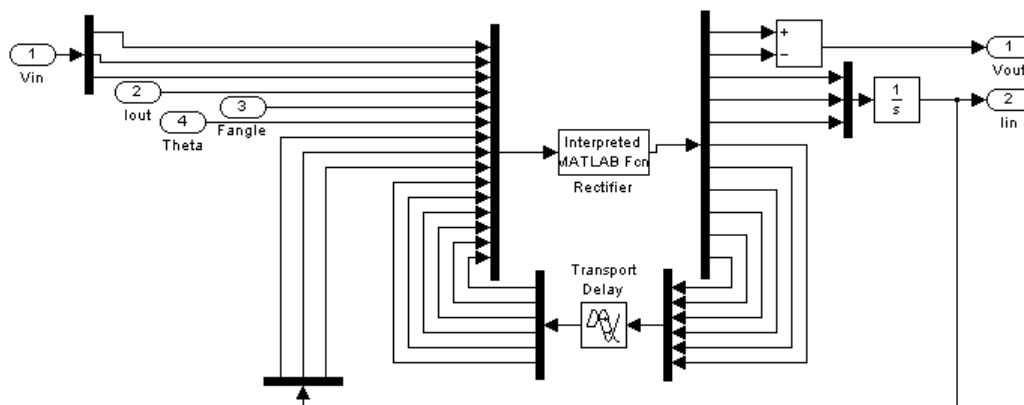


Figure 56: Rectifier Simulink implementation

To create the 12-pulse model, two rectifier models are combined with added phase shifts to represent the twelve pulse transformer operation. A constant DC current and firing angle are assumed along with the input signal of Figure 57. The output signals of rectifier 1, rectifier 2 and the combined signal, along with the current that drawn from the grid is shown in Figure 58 to Figure 63. These waveforms correspond very well to those that are shown in literature [14].

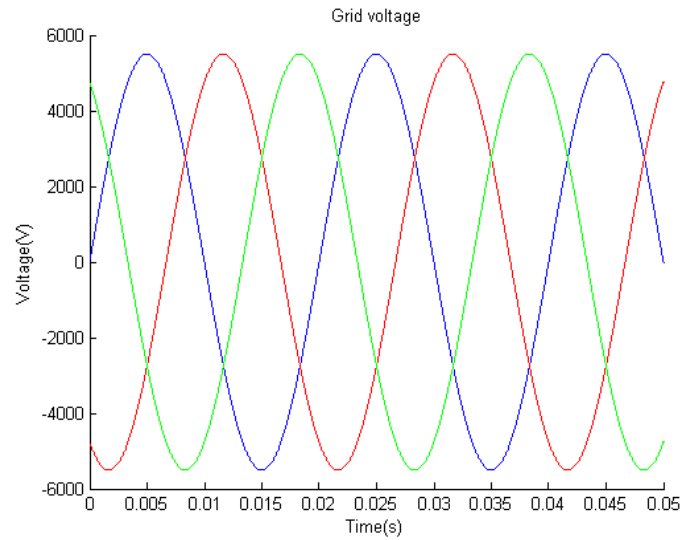


Figure 57: Grid voltage

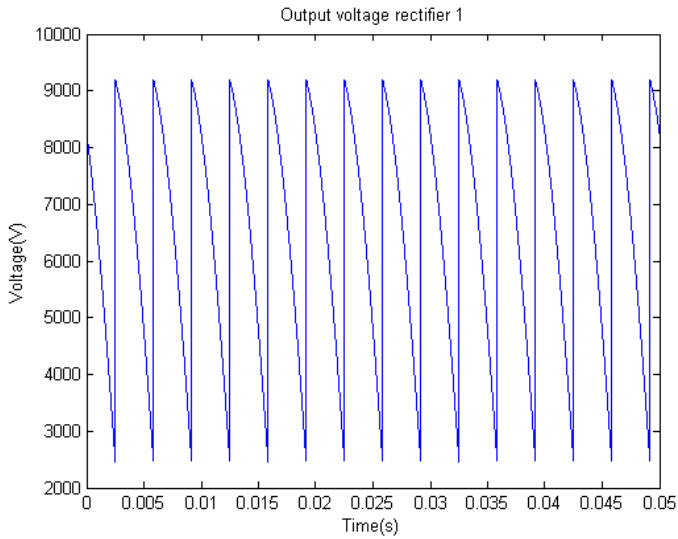


Figure 58: Rectifier 1 output voltage

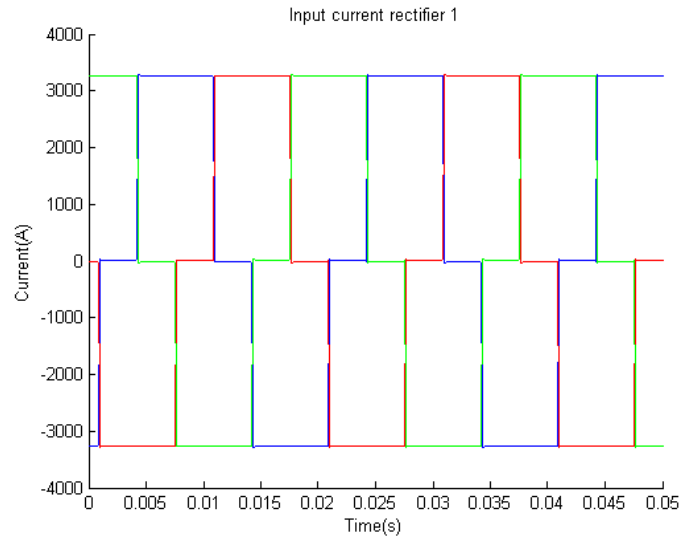


Figure 59: Rectifier 1 input current

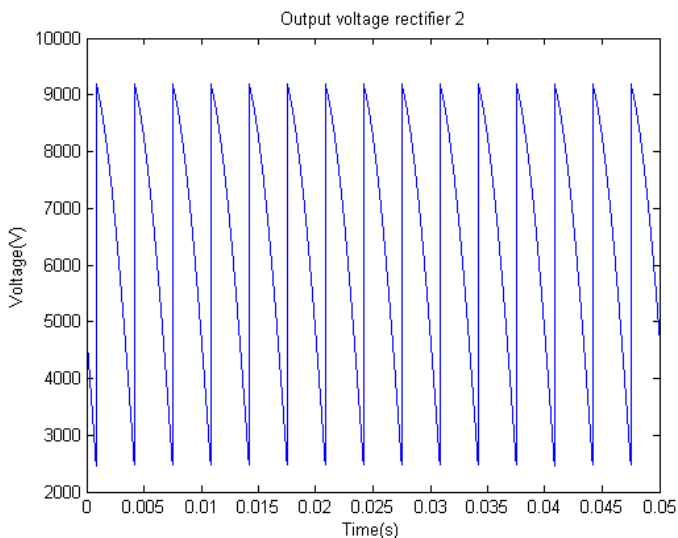


Figure 60: Rectifier 2 output voltage

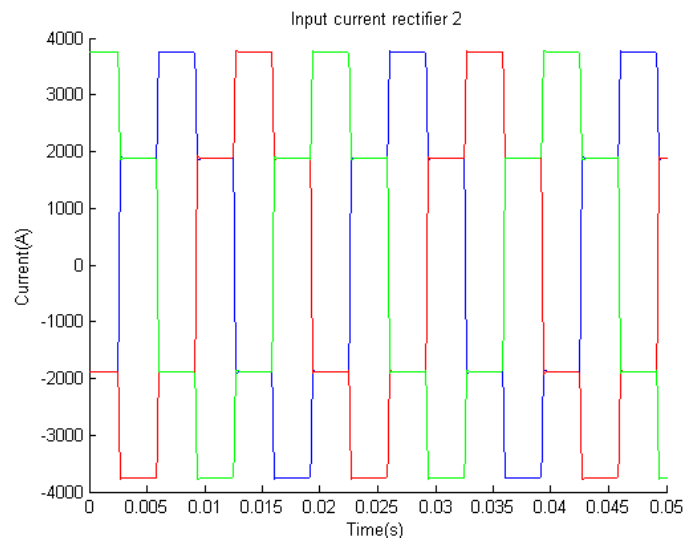


Figure 61: Rectifier 2 input current

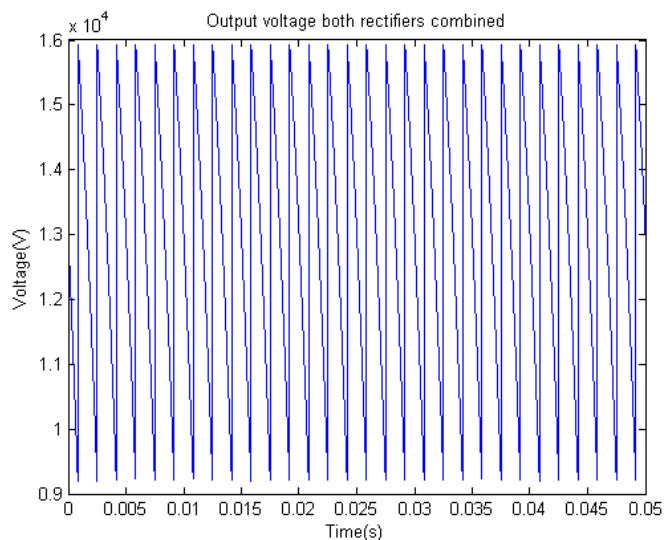


Figure 62: Combined rectifier output voltage

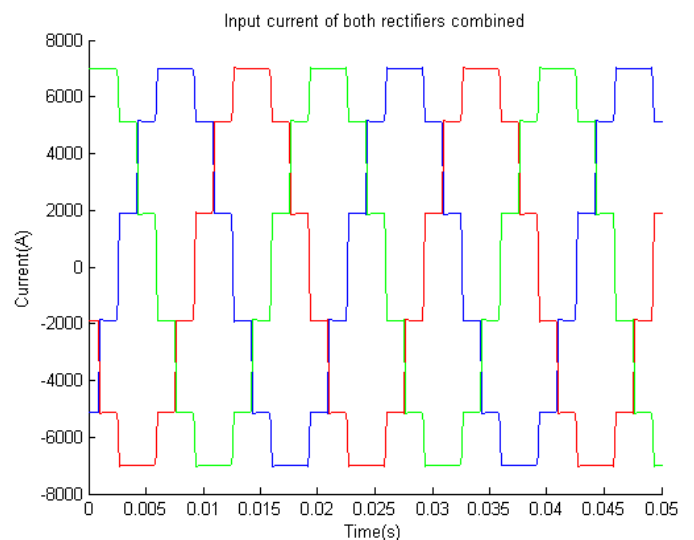


Figure 63: Combined input current

4.4.2 Inverter

The inverter model is directly built up as a 12-pulse unit. This is done because both units influence each other's operation.

The inverter determines the output and input voltage based on the input and output current. As mentioned before, it would be better to have a current output as this is closer to reality. However, as it isn't possible to feed the motor model in this way, an LCI model with voltage output is constructed. Again, as long as only one pair of thyristors per 6-pulse unit is conducting, the behavior is relatively simple, although slightly more complicated than the rectifier. The voltage on the output is altered, with knowledge of the order of magnitude of motor inductances, in order to ensure that the sum of currents entering the motor equals the DC-link current. The input voltage is equal to the output voltage of the connected phase.

During commutation the current should go from one phase to the other, where the sum of the currents should keep equal to the DC-link current. This is again done by applying the same voltage to both phases with the voltage chosen such that the correct currents flow. When the current in one of the phases reaches zero, the corresponding thyristor is turned off.

Again the MATLAB function will be explained for the positive side of a 6-pulse inverter. The other parts are similar in function.

Here too, the first thing that is done is compare the motor angle with the firing angle to determine if any thyristors need to be fired and change them to on state in that case. All thyristors that were on after the last iteration are considered to still be on. Now the state of all thyristors is known, the function can determine whether it is in steady mode or in commutation.

In steady mode the connected phase output current should equal the dc-link current. The voltage fed back to the DC-link is equal to the phase voltage of that is fed back by the connected output.

In commutation the new output current is equal to the DC-link current minus the output current in the other connected phase, as the two phases should add up to the DC-link current. However, due to the 12-pulse behavior, the other inverter will also contribute to the output current. Simply subtracting the output current in one phase from the DC-link current would result in a too low value for the current in the other phase. To compensate the output current supplied by the other inverter the DC-link current is first multiplied by $1 + \sqrt{1/3}$.

The two connected phases have equal voltage and the voltage fed back to the DC-link is also equal to this voltage. Again, the thyristors are checked for positive current and the thyristor states are set accordingly.

When this is done for all thyristor sets, the current of 6-pulse inverter set is added with the rotated current of the other 6-pulse inverter. The actual current fed back from the motor is subtracted from this, and the output voltage is derived by dividing this difference by the time step and multiplying it with an approximation of the connected machine inductance.

The MATLAB function for the inverter is given in Appendix 3. The Simulink implementation is given in Figure 64. Here too the positive and negative DC-link voltages are combined in one signal. The calculated output voltage is fed to an output and with a delay smaller than the time step back as

feedback signal. The thyristor states are also fed back to the input after passing a delay smaller than the time step. These delays are applied to avoid an algebraic loop.

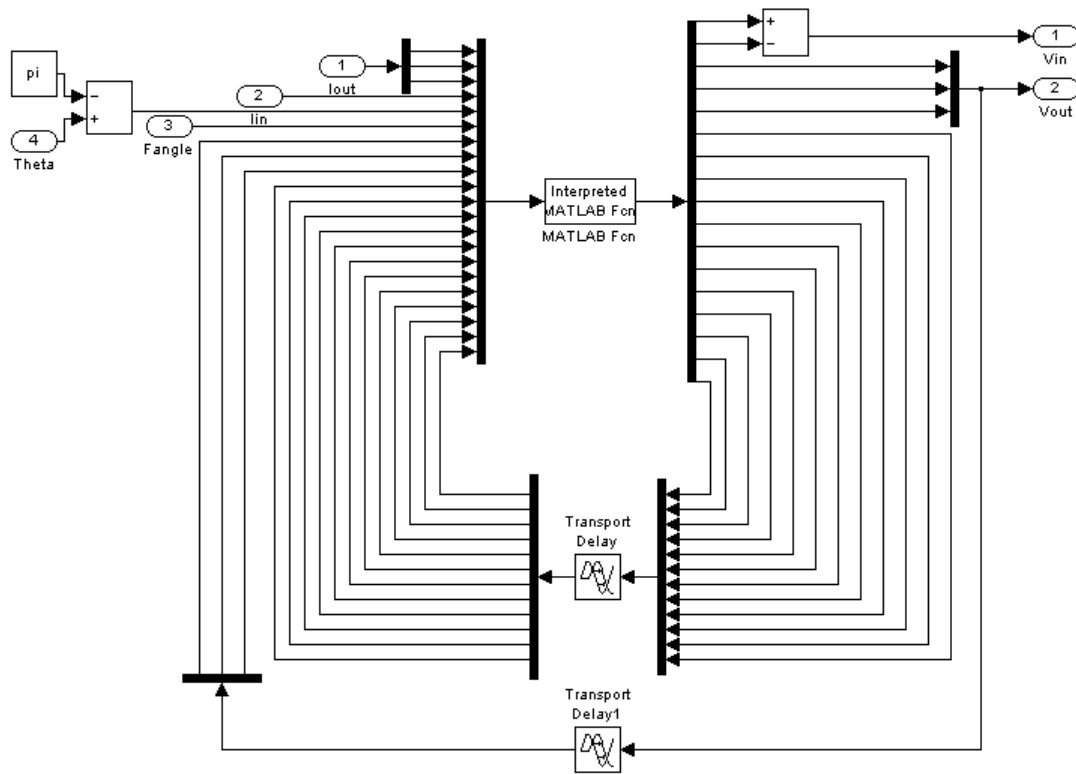


Figure 64: Inverter Simulink implementation

By making small alterations to the Matlab code, the waveforms of the separate 6-pulse units can be shown. Again a constant DC-link current is assumed, and the output is connected to a voltage source with an inductor in series, which is a simple model of a motor in steady state. The voltage and current waveforms of the separate inverters and the combined inverters, along with the voltage fed back to the DC-Link are shown in Figure 65 to Figure 73, these too correspond with the waveforms found in literature [14].

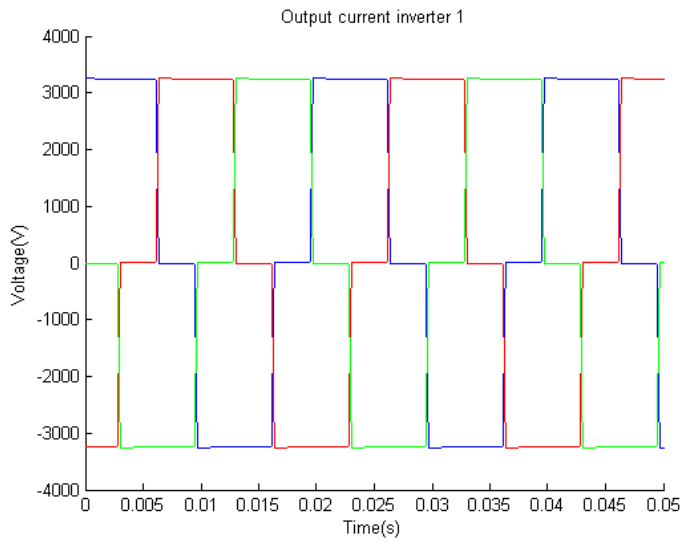


Figure 65: Inverter 1 output current

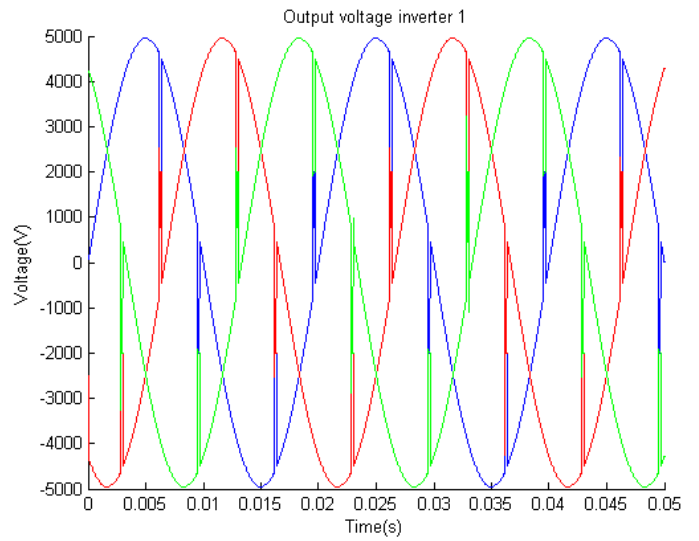


Figure 66: Inverter 1 output voltage

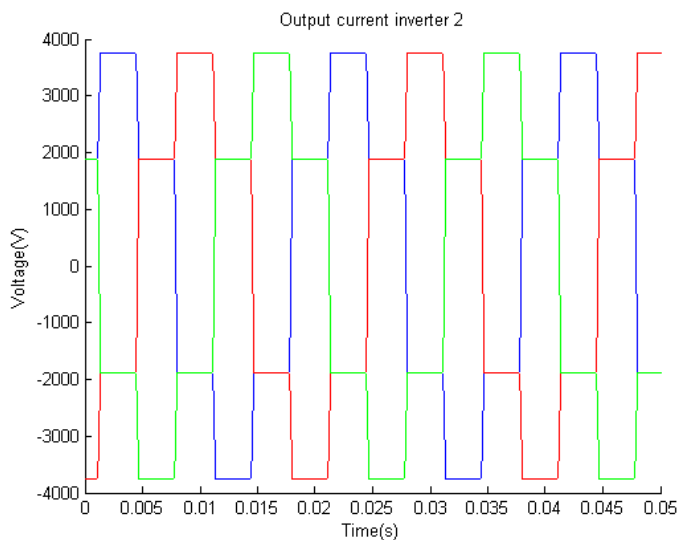


Figure 67: Inverter 2 output current

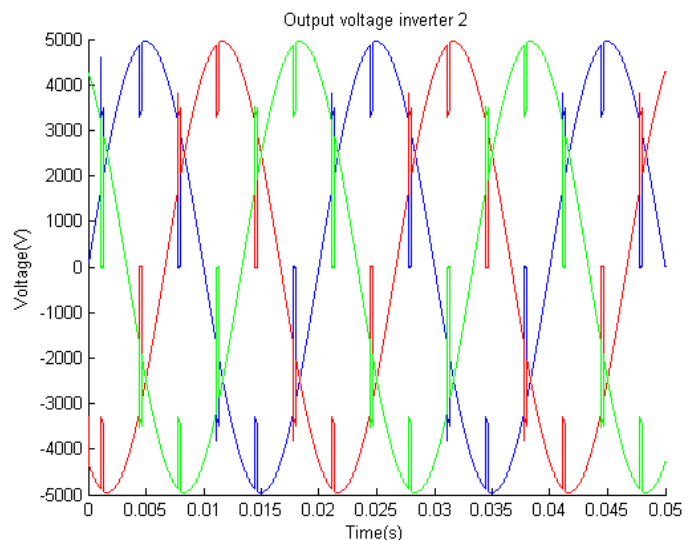


Figure 68: Inverter 2 output voltage

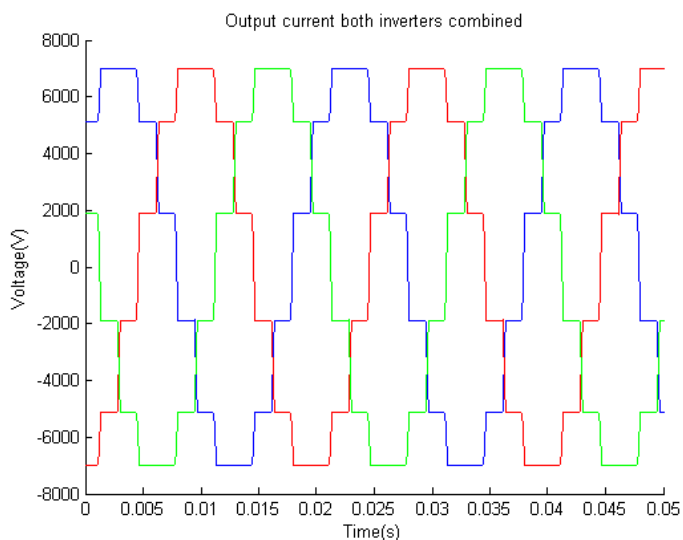


Figure 69: Combined inverters output current

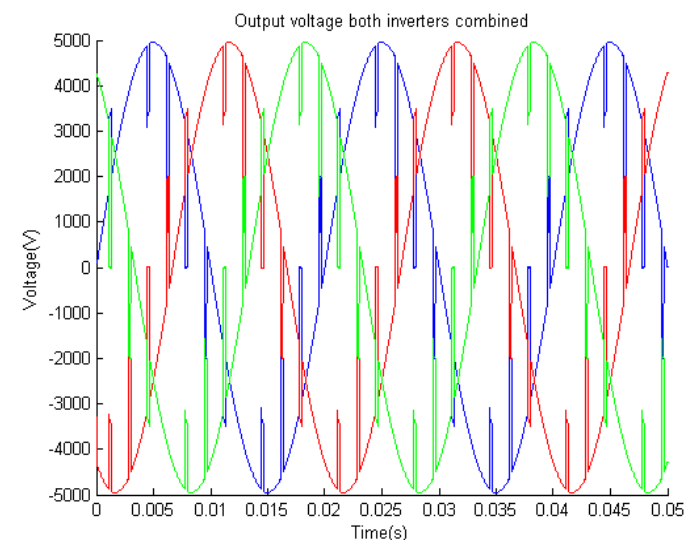


Figure 70: Combined inverters output voltage

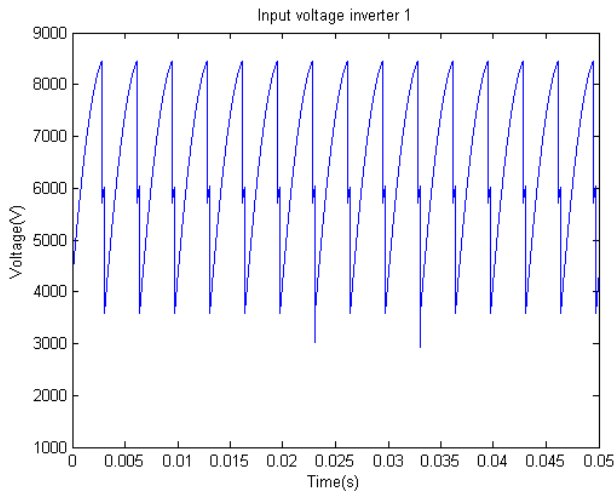


Figure 71: Inverter 1 input voltage

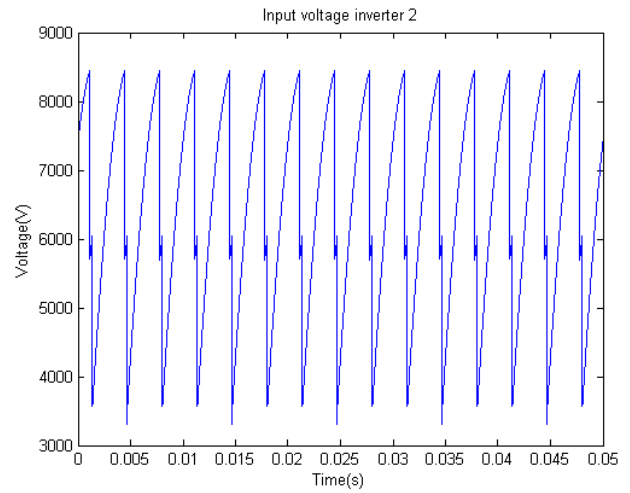


Figure 72: Inverter 2 input voltage

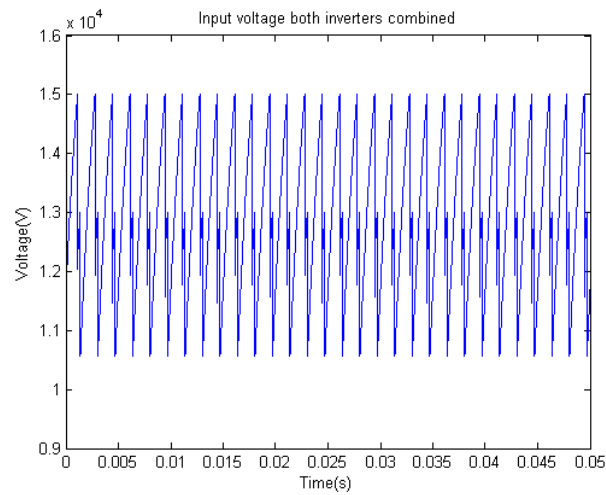


Figure 73: Combined inverter input voltage

4.4.3 DC-Link

The DC link is simply an inductor and can therefore easily be modeled. From the rectifier and inverter blocks, the voltage on both sides of the inductor can be derived. For an inductor the current is defined by:

$$I = \frac{1}{L} \cdot \int V_L \quad (45)$$

So the voltage difference is divided by the dc-link inductance and fed into an integrator to obtain the current. The Simulink implementation is shown in Figure 74.

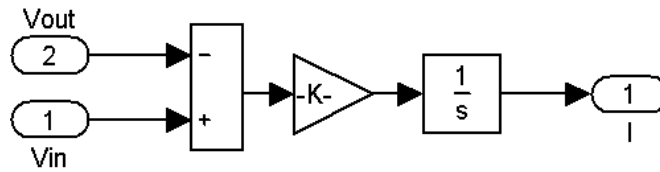


Figure 74: DC-Link Simulink implementation

4.4.4 Total system

The Simulink implementation of the total system is given in Figure 75. The rotation blocks connected to Rectifier 2 are part of the 12-pulse transformer and therefore discussed in section 4.7.

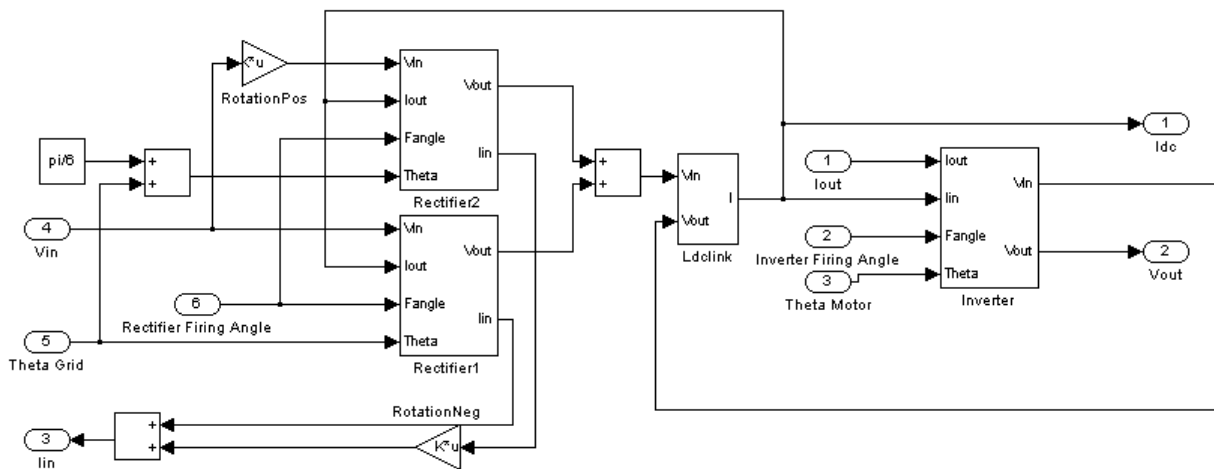


Figure 75: LCI Simulink implementation

A model is always a simplified version of reality, and as mentioned before, the LCI model used here also has its shortcomings. The necessity of a voltage output to feed the motor model is the major cause for this. However, as long as the limits of the model are kept in mind, there is no problem in using it.

The first limitation is that the input and output voltages are not completely accurate, nor are the currents derived from that. Due to these deviations, currents in a thyristor can shoot across the zero current point. To avoid problems with small currents still flowing, a function to actively pull this current to zero is built into both the rectifier and inverter model. However, step size should be kept small, as larger step size will result in greater over- and undershoot and give spikes on the signals.

The second limitation is that when current in the DC-link would get negative the thyristor should switch off. When this is done, the inductances will try to continue the current resulting in large voltage spikes. The current in the DC-link is not supposed to be negative as this isn't possible in reality. However, due to the previously mentioned small deviations, it is possible for the signal to go negative for a very short time when the current is already close to zero. If the thyristors would be switched off for these cases, large voltages and unstable behavior would occur. Therefore, in this model the thyristors will not turn off. It therefore important to assure that the DC-link current stays positive as negative DC-link current is not possible in reality.

The figures presented earlier show the waveforms we would theoretically expect and can also find in textbooks. However, in practice non-ideal effects such as commutation and DC-link current ripple will also play a role. Therefore the inverter output current, rectifier input current and dc-link current are given in Figure 76, Figure 77 and Figure 78 for a more realistic case with finite DC-link inductance. Figure 79 and Figure 80 are a zoomed in version of Figure 76 and Figure 77 respectively in which the commutation process can be seen.

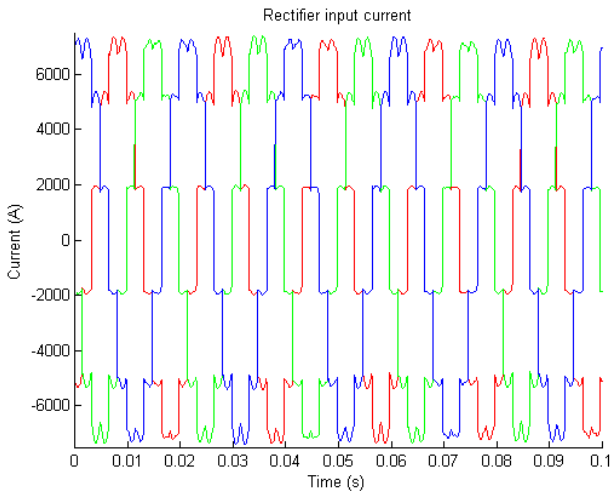


Figure 76: Rectifier input current

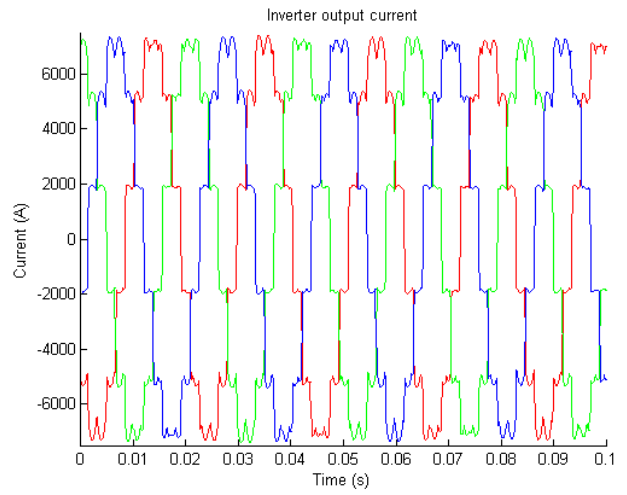


Figure 77: Inverter output current

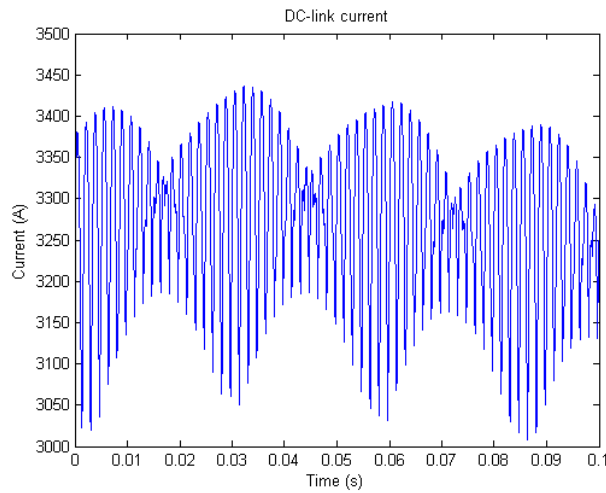


Figure 78: DC-link current

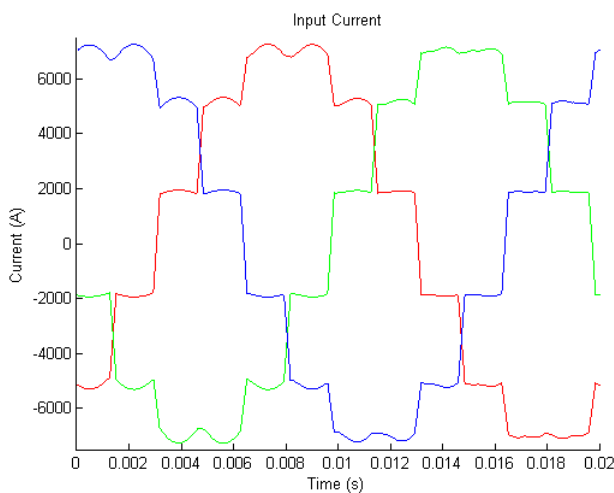


Figure 79: Rectifier input current non ideal

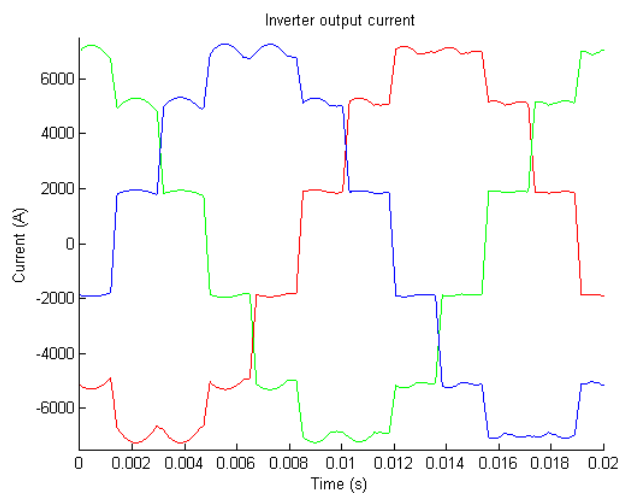


Figure 80: Inverter output current non ideal

For this research, the most important function of the LCI is to create interharmonics. By comparing Figure 6 and Figure 76 we know we can expect interharmonics. The frequency response in Figure 81

of a simple test clearly shows interharmonics being created. For this test a motor frequency of 47Hz is used and a grid frequency of 50Hz. In Table 5 the harmonic and interharmonic frequencies are given along with their relation to the motor and grid frequency, which corresponds to equation 1.

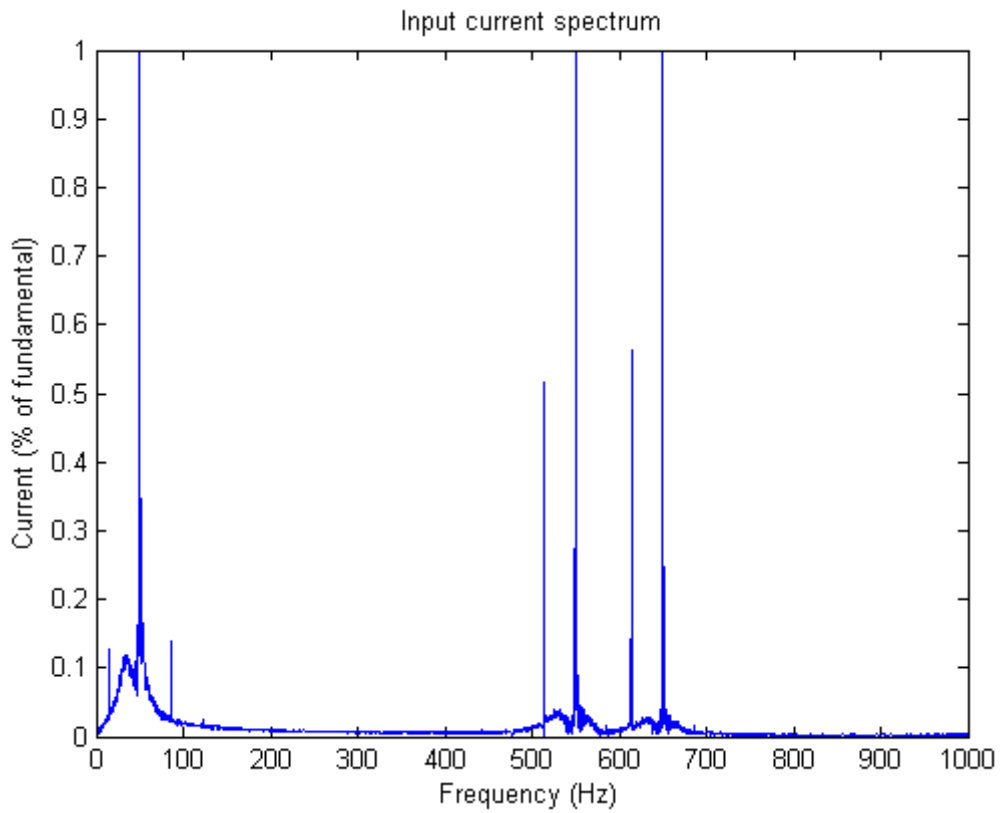


Figure 81: Interharmonics generated by the LCI model

Frequency	Relation to F_{grid} and F_{motor}
14Hz	$ 11 * F_{grid} - 12 * F_{motor} $
50 Hz	$ F_{grid} $
86 Hz	$ 13 * F_{grid} - 12 * F_{motor} $
514 Hz	$ F_{grid} - 12 * F_{motor} $
550 Hz	$ 11 * F_{grid} $
614 Hz	$ F_{grid} + 12 * F_{motor} $
650 Hz	$ 13 * F_{grid} $

Table 5: Interharmonic frequencies

4.5 Gas and Steam turbine model

Power is generated on site by two gas turbines and a steam turbine in a combined cycle setup. This way, the heat of the exhaust gasses of the gas turbines is used to drive a steam turbine, increasing the system efficiency.

The industry standard GT model shown in Figure 82 is used here which was originally developed by GE [40]. The ST model is based on the steam part of the combined cycle model shown in Figure 83 which is proposed in [41] and is connected to the two corresponding parts of the GT models.

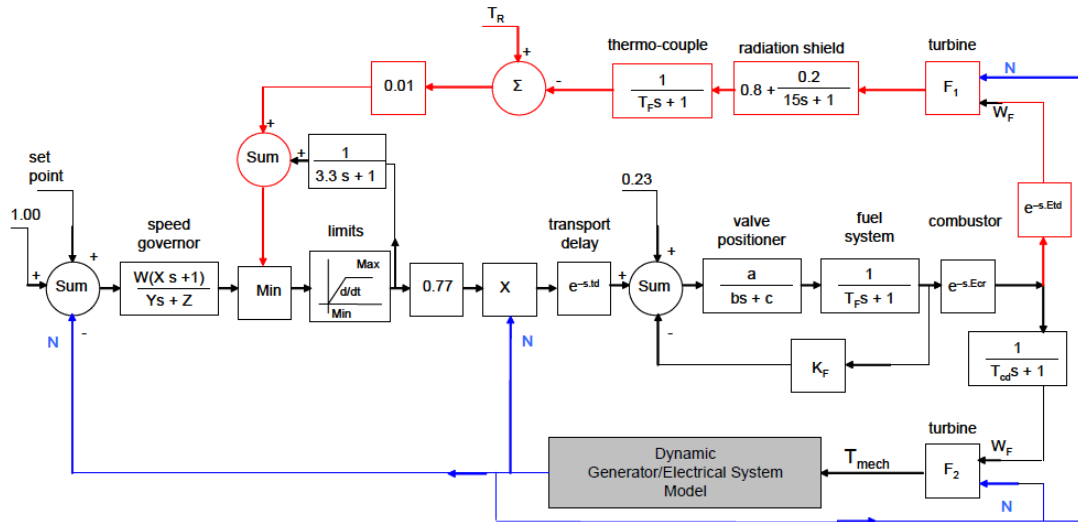


Figure 82: GT model

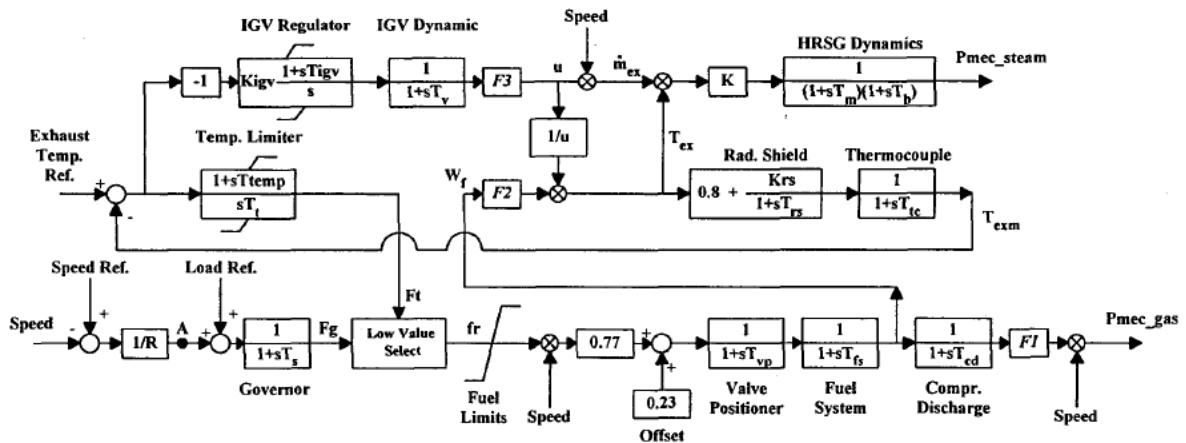


Figure 83: Combined Cycle model

The resulting Simulink implementation of the combined cycle system is shown in Figure 84. This basically is one GT and one ST connected. As we need two GTs and one ST for our model, two of these models are used; where the torque of the STs is added and fed to one inertia system. The GTs also have a controller included which ensures a constant output speed, and therefore a constant system frequency. As the ST is driven by waste heat from the GTs, it should always produce as much power as possible, and no controller is included. However, all models are electrically connected via

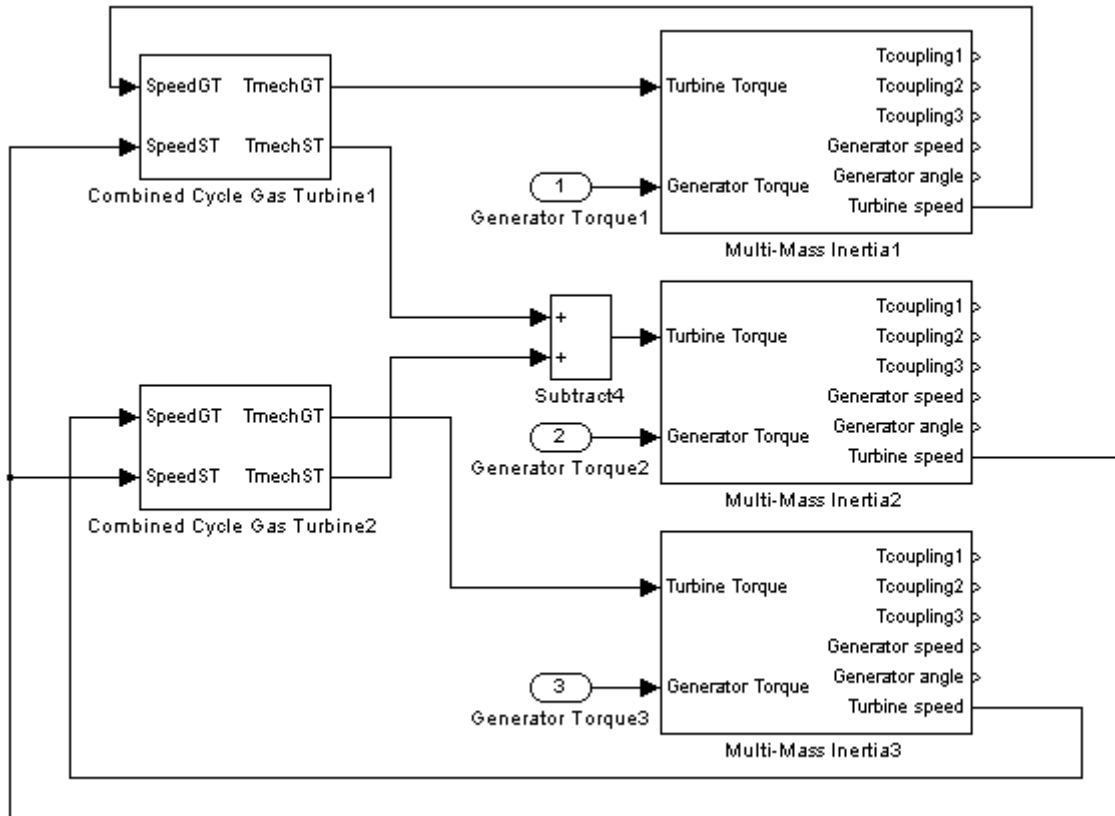


Figure 85: Total system Simulink implementation

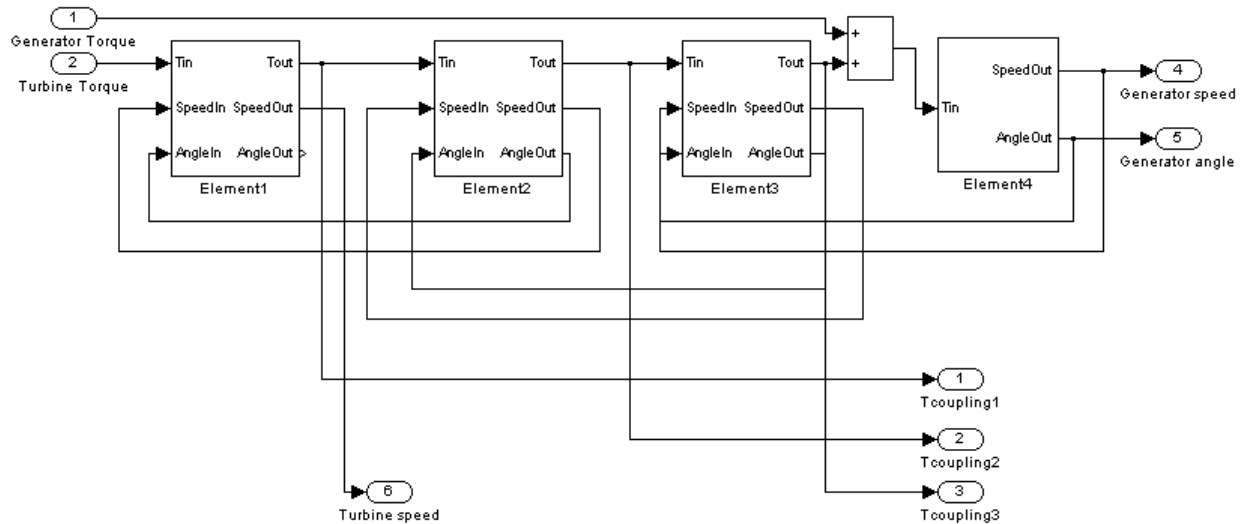


Figure 86: Multi-Mass inertia Simulink implementation

The parameters used for the model are given in Table 6.

GTJ1	9520		GTTnom	$6.685 \cdot 10^5$
GTJ2	15120		STTnom	$6.685 \cdot 10^5$
GTJ3	2893		Droop	15.6%
GTJ4	2234		W	6.41
GTK1	$2.660 \cdot 10^9$		X	0

GTK2	$3.793 \cdot 10^7$		Y	0.05
GTK3	$9.400 \cdot 10^8$		Z	1.00
GTD1	6360		td	0.25
GTD2	647.0		a	1
GTD3	1743		b	0.05
STJ1	1653		c	1
STJ2	2469		Tf	0.04
STJ3	263.3		Kf	0
STJ4	697.4		Ecr	0.01
STJ5	2360		Etd	0.02
STK1	$6.2910 \cdot 10^8$		Tcd	0.01
STK2	$8.157 \cdot 10^7$		Tr	508
STK3	$1.984 \cdot 10^8$		dPdt	$7.62 \cdot 10^{-5}$
STK4	$7.466 \cdot 10^8$		Kgs	0.001
STD1	3303		Kigv	27
STD2	660.6		Tigv	4
STD3	660.6		Tv	3
STD4	1982		Tm	5
GTPnom	$210 \cdot 10^6$		Tb	20
STPnom	$210 \cdot 10^6$			

Table 6: Turbine parameters

Unfortunately this model does not start in a steady state, and no initial conditions can be applied to the Simulink transfer function blocks. Therefore the model should be run for some time prior to measurements to obtain a steady speed. Real life turbines of these power levels take considerable time to reach a steady operating point. The model can reach a steady state relatively fast compared to real life turbines, but still will take around 100 seconds.

When full scale tests were run it turned out that running the complete model for more than 100 seconds is simply unacceptable in terms of computational time. The solution to this was to drop the turbines dynamics model and only keep the multi-mass model fed by a simple droop controlled torque. The result is shown in Figure 87. As turbine dynamics are slow compared to the interharmonic effects this simplification shouldn't affect the outcome in any significant manner.

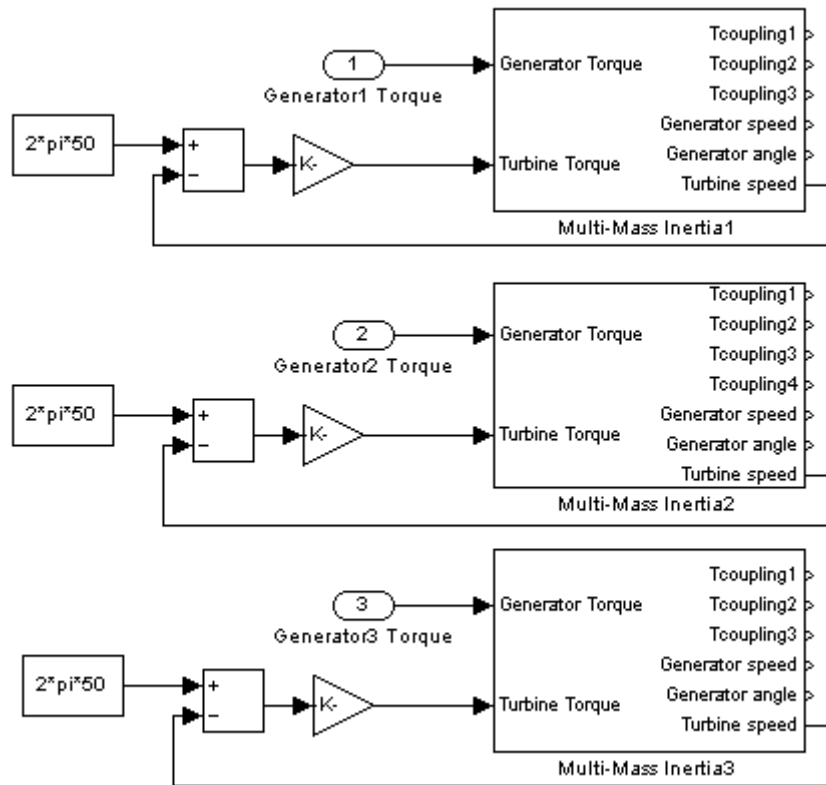


Figure 87: Simplified total system Simulink implementation

4.6 Compressor Model

The compressor is not extensively modeled as it has very little effect on the resonance phenomena on the generator side. What is important however is how its torque and speed relate. This way the effect of speed variations can be accurately modeled and the start-up of the machine can be accurately modeled.

A centrifugal compressor has a torque speed characteristic of:

$$T = C \cdot \omega^2 \tag{46}$$

As the nominal power and speed are known, nominal torque can also be calculated as:

$$T_{nom} = \frac{P_{nom}}{\omega_{nom}} \tag{47}$$

Therefore, with nominal power and speed known, C can also be calculated. With $P_{nom} = 80\text{MW}$ and $\omega_{nom} = 2 \cdot \pi \cdot 56.37\text{Hz} = 354\text{rad/s}$ this results in $C = 1.80$.

An inertia factor J is applied on the difference between the motor torque and the torque fed back by the compressor. This can then be integrated to a speed which can be integrated again to obtain the angle. A value of 12000 is chosen for J as this corresponds to the compressor getting up to running speed from standstill in roughly 15 seconds on nominal torque, which is a realistic value. This is for the case when the throttle of the compressor is fully open and no gas is compressed, so ideally all the torque is used to increase the speed. The inertia of the motor and compressor are combined in J.

The Simulink implementation is shown in Figure 88.

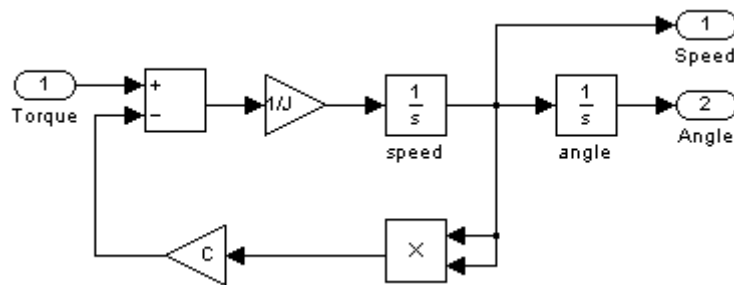


Figure 88: Compressor Simulink implementation

4.7 Grid

The characteristics of the grid will have a strong effect on interharmonics content. Especially the inductances can attenuate interharmonics quite drastically. It is therefore important to include the transformers and cables in the system model.

4.7.1 Transformer

As we are looking at interharmonics, the series impedance of the transformer is the point of interest. Therefore, the transformer is modeled as ideal transformer with a resistance and inductance in series. As the signals of interest are not 50Hz, it is important to use the inductance instead of impedance. The resulting single phase transformer model is shown in Figure 89.

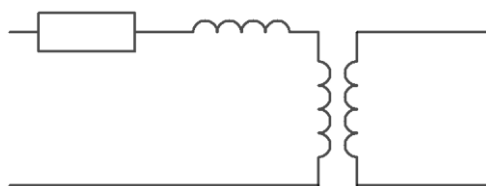


Figure 89: Transformer model

The three-phase transformers are modeled by combining three of these models.

The LCI input transformers are modeled slightly different as shown in the single line model in Figure 90.

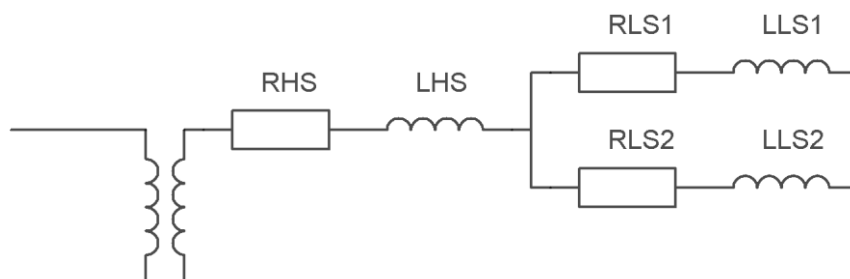


Figure 90: LCI input transformer model

Furthermore a 30° phase shift is introduced in one of the secondary windings to get the required behavior. A positive phase shift is generated by using the rotation matrix:

$$R_{pos} = \frac{2}{3} \cdot \begin{bmatrix} \cos\left(\frac{\pi}{6}\right) & \cos\left(\frac{5 \cdot \pi}{6}\right) & \cos\left(\frac{9 \cdot \pi}{6}\right) \\ \cos\left(\frac{9 \cdot \pi}{6}\right) & \cos\left(\frac{\pi}{6}\right) & \cos\left(\frac{5 \cdot \pi}{6}\right) \\ \cos\left(\frac{5 \cdot \pi}{6}\right) & \cos\left(\frac{9 \cdot \pi}{6}\right) & \cos\left(\frac{\pi}{6}\right) \end{bmatrix} \quad (48)$$

A negative phase shift is generated by using the rotation matrix:

$$R_{neg} = \frac{2}{3} \cdot \begin{bmatrix} \cos\left(-\frac{\pi}{6}\right) & \cos\left(-\frac{9 \cdot \pi}{6}\right) & \cos\left(-\frac{5 \cdot \pi}{6}\right) \\ \cos\left(-\frac{5 \cdot \pi}{6}\right) & \cos\left(-\frac{\pi}{6}\right) & \cos\left(-\frac{9 \cdot \pi}{6}\right) \\ \cos\left(-\frac{9 \cdot \pi}{6}\right) & \cos\left(-\frac{5 \cdot \pi}{6}\right) & \cos\left(-\frac{\pi}{6}\right) \end{bmatrix} \quad (49)$$

These phase shifts are implemented in the LCI model instead of in the network model, as the LCI model could otherwise not function in setups without this network (for small scale studies).

The parameters of the actual transformers are given in

	Pri. Voltage (kV)	Sec. Voltage (kV)	Rating (MVA)	Impedance (%)	X/R ratio
Generator Step-up transformer	15	225	225	14.5%	47
220kv to 132kv	220	145	220	12.5%	45

Table 7: Transformer parameters

These values have to be transformed into a series resistance and inductance before they can be used in the model. This can be done using equations 50 to 53. The results are shown in Table 8.

$$Z_{Base} = \frac{3 \cdot V^2}{S} \quad (50)$$

$$\varphi = \tan^{-1}(X/R) \quad (51)$$

$$R = Z_{Base} \cdot Z \cdot \cos(\varphi) \quad (52)$$

$$L = \frac{Z_{Base} \cdot Z \cdot \sin(\varphi)}{2 \cdot \pi \cdot f} \quad (53)$$

	Z _{base}	ϕ	Resistance	Inductance
Generator Step-up transformer	3Ω	88.78°	9.26mΩ	1.38mH
220kv to 132kv	660Ω	88.73°	1.83Ω	263mH

Table 8: Transformer model values

The LCI input transformer has the parameters given in Table 9. The short circuit reactances are relatively high. The reason for this is a combination of the power level and limitation of short circuit currents when the rectifier misses commutation.

Rating	103MVA
Primary Voltage	132kV
Secondary Voltage	2x 9.7kV
Short circuit reactance HV to LV1	28-42%
Short circuit reactance HV to LV2	28-42%

Short circuit reactance LV1 to LV2	42-56%
------------------------------------	--------

Table 9: LCI input transformer parameters

These parameters can be converted into R_{HS} , L_{HS} , R_{LS1} , L_{LS1} , R_{LS2} and L_{LS2} by using the equation 54 to 56 and 50 to 53.

$$Z_{HS} = \frac{1}{2} \cdot [Z_{HV-LV1} + Z_{HV-LV2} - Z_{LV1-LV2}] \quad (54)$$

$$Z_{LS1} = \frac{1}{2} \cdot [Z_{HV-LV1} + Z_{LV1-LV2} - Z_{HV-LV2}] \quad (55)$$

$$Z_{LS2} = \frac{1}{2} \cdot [Z_{HV-LV2} + Z_{LV1-LV2} - Z_{HV-LV1}] \quad (56)$$

The X/R ratio is assumed to be 50 and the lowest reactance value is chosen as this minimizes damping and is therefore the worst case scenario. The resulting values are shown in Table 10.

R_{HS}	3.84m Ω
L_{HS}	0.60mH
R_{LS1}	11.6m Ω
L_{LS1}	1.83mH
R_{LS2}	11.6m Ω
L_{LS2}	1.83mH

Table 10: LCI input transformer model values

4.7.2 Cables

Cables are modeled using the π -model depicted in Figure 91. Only the cables between the generator step-up transformers and the substation on the 220kV bus and from that substation to the 220kV to 132kV transformer are modeled. These are the only connections which have sufficient length to be of significance.

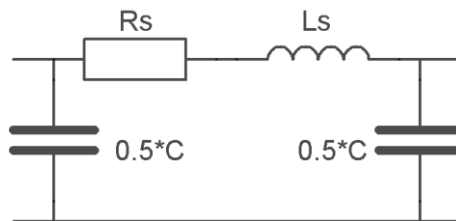


Figure 91: Cable Model

The parameters for the different cables are given in Table 11. The lengths of the different cables and their corresponding values are given in Table 12.

	Resistance (m Ω /km)	Inductance (mH/km)	Capacitance (nF/km)
TR1-3 to substation	38.5	0.767	149
Substation to TR4-5	16.8	0.538	208

Table 11: Cable parameters

	Length (m)	R_s (m Ω)	L_s (mH)	C (nF)
TR1 to substation	130	5.0	0.100	19.4
TR2 to substation	165	6.4	0.127	24.6
TR3 to substation	280	10.8	0.215	41.7

Substation to TR4	670	11.3	0.360	139
Substation to TR5	670	11.3	0.360	139

Table 12: Cable model values

4.7.3 Network

Combining the earlier models into the network as already shown in Figure 50 we arrive at the network as depicted in Figure 92.

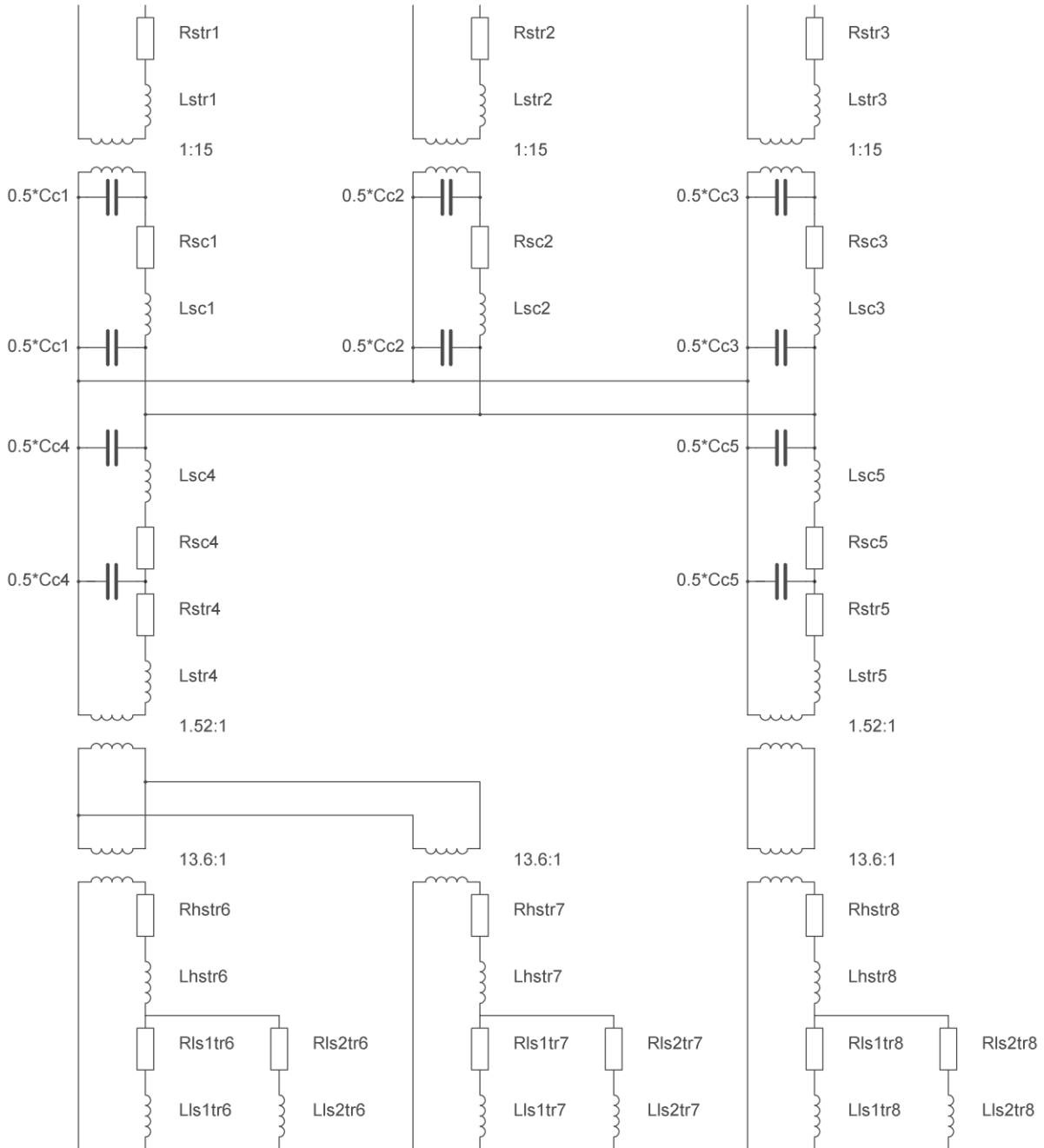


Figure 92: System network

When shifting all transformers to the inputs, we arrive at the simpler network as shown in Figure 93. Of course the component values have to change along with the transformer shift.

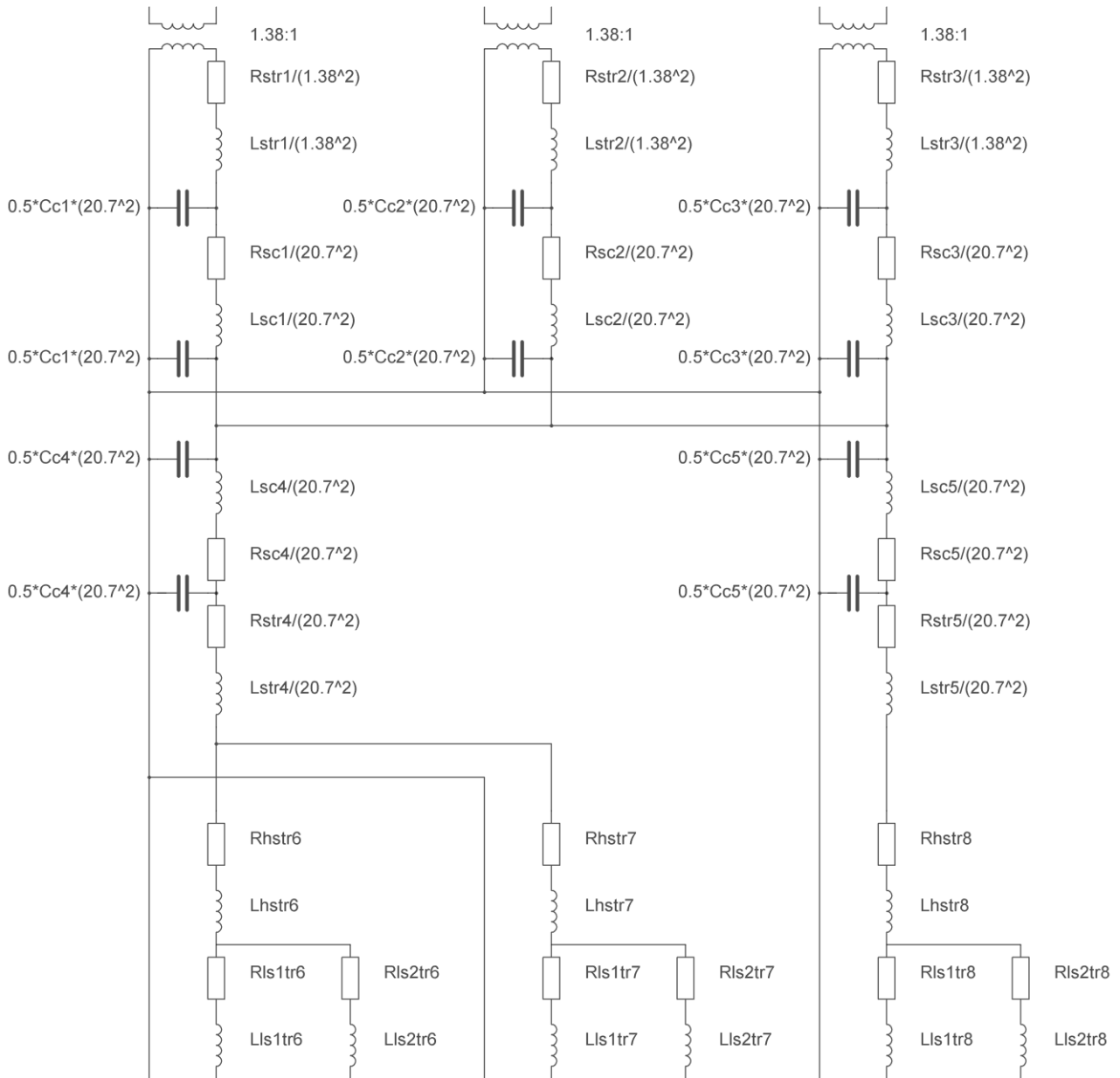


Figure 93: Network with transformers shifted to the input

After combining series connected elements the network can be even further simplified as shown in Figure 94.

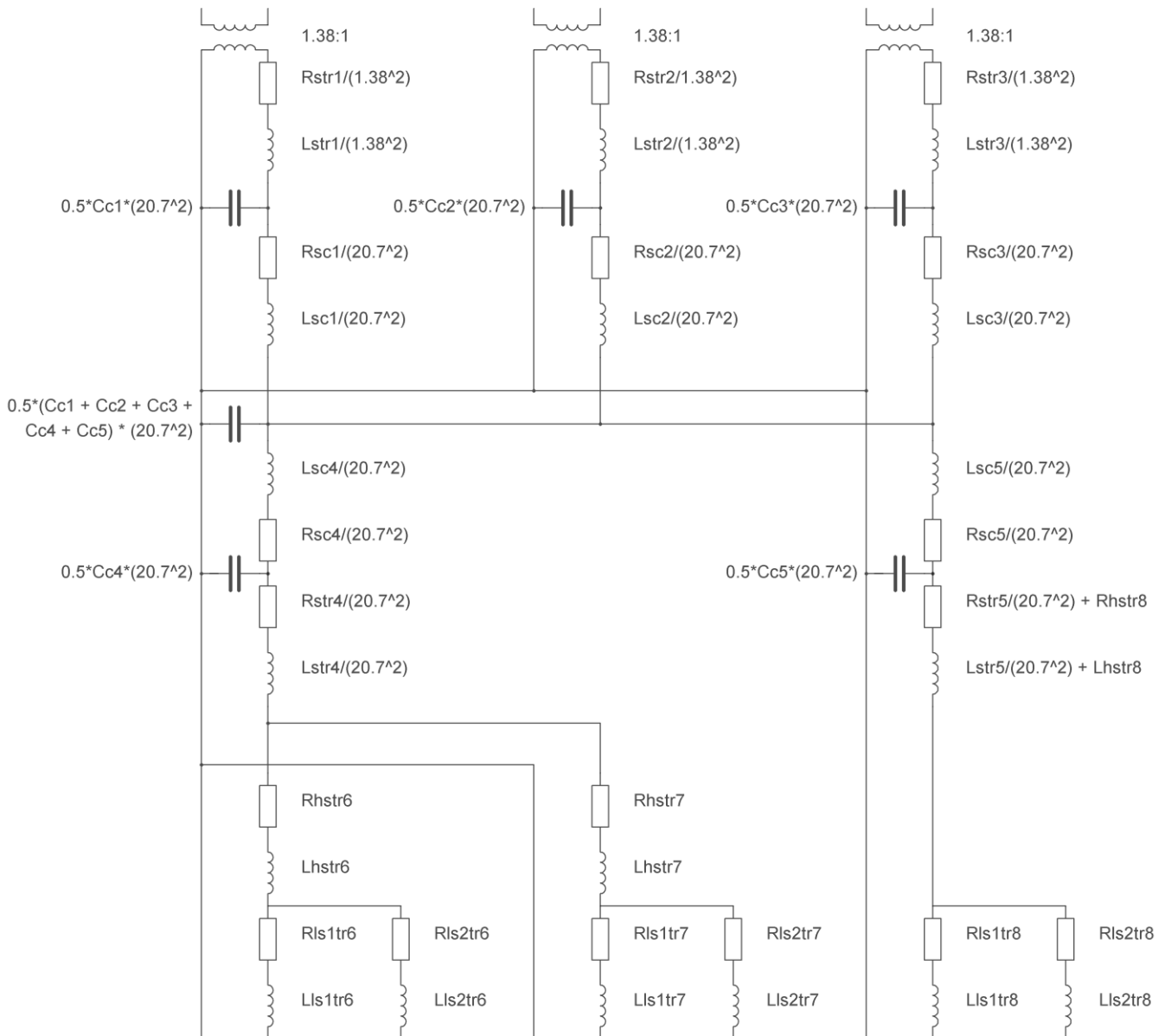


Figure 94: Simplified network

To model this, state-space equations are used [42]. As the generator model gives a current output and the LCI model also returns a current value, both sides of the network can be seen as current inputs. To be able to use state-space modeling, small capacitors, in the order of the parasitic capacitances present in practice, are added to all inputs, outputs and nodes with multiple inductors connected to it, so the voltage on them can be readily determined.

The main matrix, or A matrix in the state-space equations will be $N \times N$ in size, where N is the number of state variables which is equal to the number of inductors and capacitors. With the network of Figure 94 this would result in 36 state variables, so a 36×36 matrix resulting in 1296 elements. Beside the time consuming nature of determining this matrix, the chances of errors in the implemented model are also very large.

To overcome these issues a further simplified model is proposed. First step is to move all cable capacitances to one side, the common 220KV bus. As the transformer inductances are a factor 1000

larger than the cable inductances, the effect of moving the capacitance is negligible. By reducing the number of capacitance and being able to combine inductances, the number of state variables is reduced to 26. The second step is to reduce the 12-pulse transformer model. By combining the two secondary windings into one, the voltage on the rectifier inputs will be distorted by the current drawn by the other rectifier. As the secondary inductances are relatively large, this is not a negligible effect. However, the current that we are interested in, the ones fed back to the generator, are not significantly altered by this change. After applying these two steps, the network is reduced to the one in Figure 95 which needs only 15 state variables.

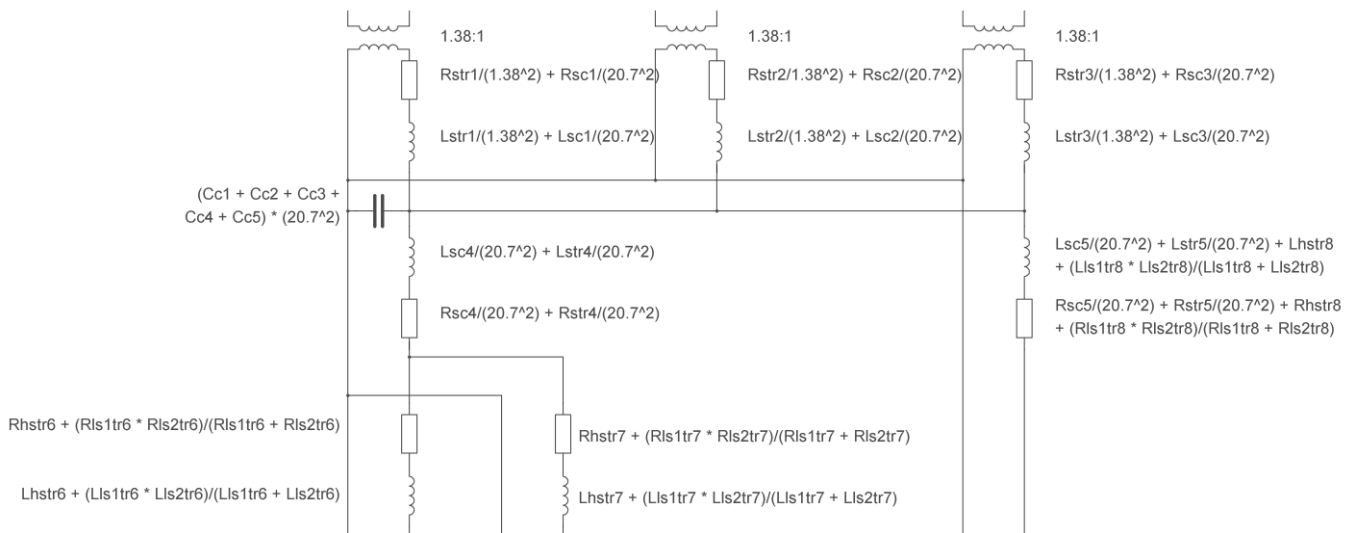


Figure 95: Network after applying two simplification steps

With the network of Figure 95 we can start determining the state-space equations. First the “parasitic” capacitances mentioned before are added and the components are given simpler names to keep the calculations clear. The cleaned up network is shown in Figure 96 with the values as shown in Table 13. The value of $1\mu\text{F}$ for the “parasitic” capacitances may seem large, but as they are more than a hundred times smaller than the main capacitance they shouldn’t influence the characteristics significantly, and larger values slow simulations down. The capacitors on the LCI side are even $500\mu\text{F}$. This is necessary to keep the system stable, in practice there will also be large capacitance of up to $500\mu\text{F}$ included in the harmonic filtering and power factor compensation circuit. Unfortunately this results in resonance between the inductor and capacitor (for instance L4 and C6), causing problems with the rectifier. To solve this, the resistors R4, R6 and R7 are all increased in value in the model. They are implemented a factor 10 larger than in Table 13, which has significant effect on the voltages in the network. The effect on interharmonic currents is however small which is verified by comparing the input current off the LCI with the generator current. This makes increasing these resistance values acceptable for this research.

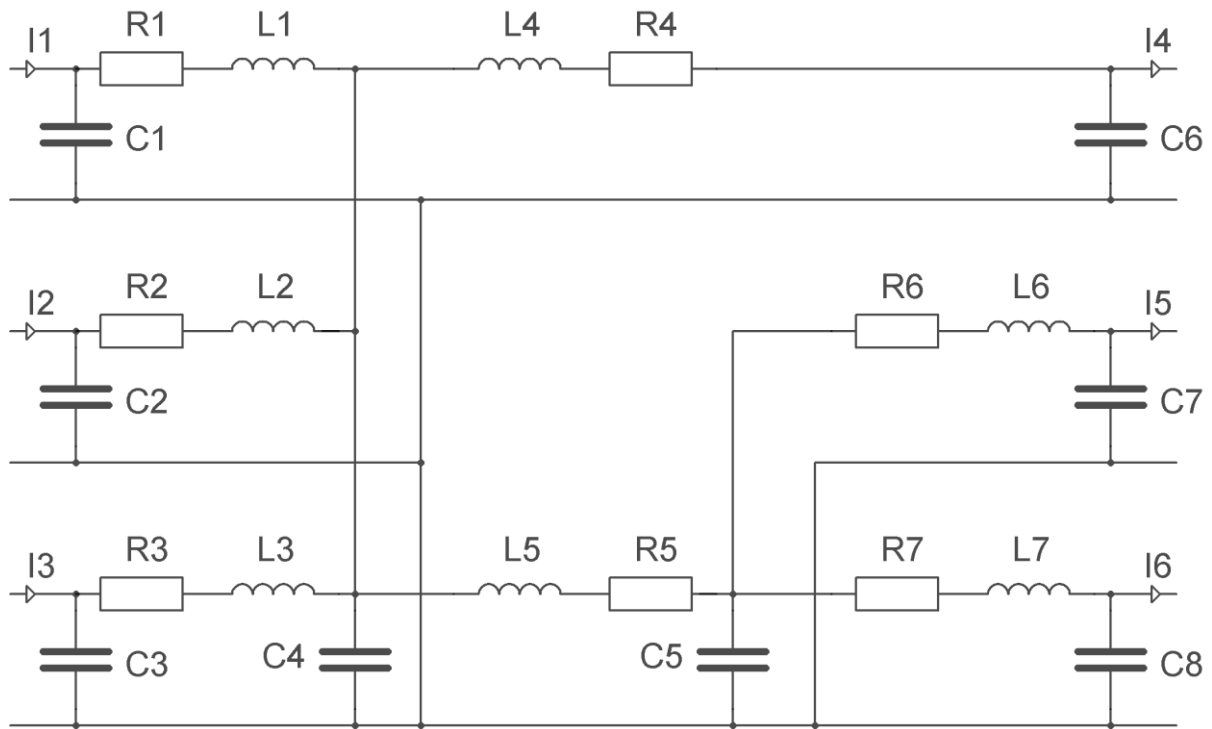


Figure 96: State Space Network

R1	$\frac{R_{str1}}{1.38^2} + \frac{R_{sc1}}{20.7^2}$	4.87mΩ
R2	$\frac{R_{str2}}{1.38^2} + \frac{R_{sc2}}{20.7^2}$	4.88mΩ
R3	$\frac{R_{str3}}{1.38^2} + \frac{R_{sc3}}{20.7^2}$	4.89mΩ
R4	$\frac{R_{str5}}{20.7^2} + \frac{R_{sc5}}{20.7^2} + R_{hstr8} + \frac{R_{ls1tr8} \cdot R_{ls2tr8}}{R_{ls1tr8} + R_{ls2tr8}}$	7.55mΩ
R5	$\frac{R_{str4}}{20.7^2} + \frac{R_{sc4}}{20.7^2}$	4.34mΩ
R6	$R_{hstr6} + \frac{R_{ls1tr6} \cdot R_{ls2tr6}}{R_{ls1tr6} + R_{ls2tr6}}$	3.21mΩ
R7	$R_{hstr7} + \frac{R_{ls1tr7} \cdot R_{ls2tr7}}{R_{ls1tr7} + R_{ls2tr7}}$	3.21mΩ
L1	$\frac{L_{str1}}{1.38^2} + \frac{L_{sc1}}{20.7^2}$	725μH
L2	$\frac{L_{str2}}{1.38^2} + \frac{L_{sc2}}{20.7^2}$	725μH
L3	$\frac{L_{str3}}{1.38^2} + \frac{L_{sc3}}{20.7^2}$	725μH
L4	$\frac{L_{str5}}{20.7^2} + \frac{L_{sc5}}{20.7^2} + L_{hstr8} + \frac{L_{ls1tr8} \cdot L_{ls2tr8}}{L_{ls1tr8} + L_{ls2tr8}}$	1.12mH
L5	$\frac{L_{str4}}{20.7^2} + \frac{L_{sc4}}{20.7^2}$	615μH
L6	$L_{hstr6} + \frac{L_{ls1tr6} \cdot L_{ls2tr6}}{L_{ls1tr6} + L_{ls2tr6}}$	505μH
L7	$L_{hstr7} + \frac{L_{ls1tr7} \cdot L_{ls2tr7}}{L_{ls1tr7} + L_{ls2tr7}}$	505μH

C1	“parasitic”	1μF
C2	“parasitic”	1μF
C3	“parasitic”	1μF
C4	$(C_{c1} + C_{c2} + C_{c3} + C_{c4} + C_{c5}) \cdot 20.7^2$	156μF
C5	“parasitic”	1μF
C6	“parasitic”	500μF
C7	“parasitic”	500μF
C8	“parasitic”	500μF

Table 13: Network parameters

We start by defining the state variables as the capacitor voltages and inductor currents. The inductor current derivatives are given by equations 57 to 63.

$$\frac{dI_{L1}}{dt} = \frac{1}{L_1} \cdot V_{L1} \quad (57)$$

$$\frac{dI_{L2}}{dt} = \frac{1}{L_2} \cdot V_{L2} \quad (58)$$

$$\frac{dI_{L3}}{dt} = \frac{1}{L_3} \cdot V_{L3} \quad (59)$$

$$\frac{dI_{L4}}{dt} = \frac{1}{L_4} \cdot V_{L4} \quad (60)$$

$$\frac{dI_{L5}}{dt} = \frac{1}{L_5} \cdot V_{L5} \quad (61)$$

$$\frac{dI_{L6}}{dt} = \frac{1}{L_6} \cdot V_{L6} \quad (62)$$

$$\frac{dI_{L7}}{dt} = \frac{1}{L_7} \cdot V_{L7} \quad (63)$$

The derivatives of the capacitor voltages are given by equations 64 to 71.

$$\frac{dV_{C1}}{dt} = \frac{1}{C_1} \cdot I_{C1} \quad (64)$$

$$\frac{dV_{C2}}{dt} = \frac{1}{C_2} \cdot I_{C2} \quad (65)$$

$$\frac{dV_{C3}}{dt} = \frac{1}{C_3} \cdot I_{C3} \quad (66)$$

$$\frac{dV_{C4}}{dt} = \frac{1}{C_4} \cdot I_{C4} \quad (67)$$

$$\frac{dV_{C5}}{dt} = \frac{1}{C_5} \cdot I_{C5} \quad (68)$$

$$\frac{dV_{C6}}{dt} = \frac{1}{C_6} \cdot I_{C6} \quad (69)$$

$$\frac{dV_{C7}}{dt} = \frac{1}{C_7} \cdot I_{C7} \quad (70)$$

$$\frac{dV_{C8}}{dt} = \frac{1}{C_8} \cdot I_{C8} \quad (71)$$

The next step is to determine the inductor voltages and capacitor currents. The inductor voltages are given by equations 72 to 78.

$$V_{L1} = V_{C1} - V_{C4} - R_1 \cdot I_{L1} \quad (72)$$

$$V_{L2} = V_{C2} - V_{C4} - R_2 \cdot I_{L2} \quad (73)$$

$$V_{L3} = V_{C3} - V_{C4} - R_3 \cdot I_{L3} \quad (74)$$

$$V_{L4} = V_{C4} - V_{C6} - R_4 \cdot I_{L4} \quad (75)$$

$$V_{L5} = V_{C4} - V_{C5} - R_5 \cdot I_{L5} \quad (76)$$

$$V_{L6} = V_{C5} - V_{C7} - R_6 \cdot I_{L6} \quad (77)$$

$$V_{L7} = V_{C5} - V_{C8} - R_7 \cdot I_{L7} \quad (78)$$

The capacitor currents are given by equations 79 to 86.

$$I_{C1} = I_1 - I_{L1} \quad (79)$$

$$I_{C2} = I_2 - I_{L2} \quad (80)$$

$$I_{C3} = I_3 - I_{L3} \quad (81)$$

$$I_{C4} = I_{L1} + I_{L2} + I_{L3} - I_{L4} - I_{L5} \quad (82)$$

$$I_{C5} = I_{L5} - I_{L6} - I_{L7} \quad (83)$$

$$I_{C6} = I_{L4} - I_4 \quad (84)$$

$$I_{C7} = I_{L6} - I_5 \quad (85)$$

$$I_{C8} = I_{L7} - I_6 \quad (86)$$

The input and output voltages are simply defined by equations 87 to 92.

$$V_1 = V_{C1} \quad (87)$$

$$V_2 = V_{C2} \quad (88)$$

$$V_3 = V_{C3} \quad (89)$$

$$V_4 = V_{C6} \quad (90)$$

$$V_5 = V_{C7} \quad (91)$$

$$V_6 = V_{C8} \quad (92)$$

The last step is to rewrite these equations into the matrix form of equations 93 and 94 where x is the state variable vector, u the input vector and y the output vector.

$$\dot{x} = A \cdot x + B \cdot u \quad (93)$$

$$y = C \cdot x + D \cdot u \quad (94)$$

The matrices for this network are given by equations 95 to 98.

$$A = \begin{bmatrix} \frac{-R_1}{L_1} & 0 & 0 & 0 & 0 & 0 & 0 & \frac{1}{L_1} & 0 & 0 & \frac{-1}{L_1} & 0 & 0 & 0 & 0 \\ 0 & \frac{-R_2}{L_2} & 0 & 0 & 0 & 0 & 0 & 0 & \frac{1}{L_2} & 0 & \frac{-1}{L_2} & 0 & 0 & 0 & 0 \\ 0 & 0 & \frac{-R_3}{L_3} & 0 & 0 & 0 & 0 & 0 & 0 & \frac{1}{L_3} & \frac{-1}{L_3} & 0 & 0 & 0 & 0 \\ 0 & 0 & 0 & \frac{-R_4}{L_4} & 0 & 0 & 0 & 0 & 0 & 0 & \frac{1}{L_4} & 0 & \frac{-1}{L_4} & 0 & 0 \\ 0 & 0 & 0 & 0 & \frac{-R_5}{L_5} & 0 & 0 & 0 & 0 & 0 & \frac{1}{L_5} & \frac{-1}{L_5} & 0 & 0 & 0 \\ 0 & 0 & 0 & 0 & 0 & \frac{-R_6}{L_6} & 0 & 0 & 0 & 0 & 0 & \frac{1}{L_6} & 0 & \frac{-1}{L_6} & 0 \\ 0 & 0 & 0 & 0 & 0 & 0 & \frac{-R_7}{L_7} & 0 & 0 & 0 & 0 & \frac{1}{L_7} & 0 & 0 & \frac{-1}{L_7} \\ \frac{-1}{C_1} & 0 & 0 & 0 & 0 & 0 & 0 & 0 & 0 & 0 & 0 & 0 & 0 & 0 & 0 \\ 0 & \frac{-1}{C_2} & 0 & 0 & 0 & 0 & 0 & 0 & 0 & 0 & 0 & 0 & 0 & 0 & 0 \\ 0 & 0 & \frac{-1}{C_3} & 0 & 0 & 0 & 0 & 0 & 0 & 0 & 0 & 0 & 0 & 0 & 0 \\ \frac{1}{C_4} & \frac{1}{C_4} & \frac{1}{C_4} & \frac{-1}{C_4} & \frac{-1}{C_4} & 0 & 0 & 0 & 0 & 0 & 0 & 0 & 0 & 0 & 0 \\ 0 & 0 & 0 & 0 & \frac{1}{C_5} & \frac{-1}{C_5} & \frac{-1}{C_5} & 0 & 0 & 0 & 0 & 0 & 0 & 0 & 0 \\ 0 & 0 & 0 & \frac{1}{C_6} & 0 & 0 & 0 & 0 & 0 & 0 & 0 & 0 & 0 & 0 & 0 \\ 0 & 0 & 0 & 0 & 0 & \frac{1}{C_7} & 0 & 0 & 0 & 0 & 0 & 0 & 0 & 0 & 0 \\ 0 & 0 & 0 & 0 & 0 & 0 & \frac{1}{C_8} & 0 & 0 & 0 & 0 & 0 & 0 & 0 & 0 \end{bmatrix} \quad (95)$$

$$B = \begin{bmatrix} 0 & 0 & 0 & 0 & 0 & 0 \\ 0 & 0 & 0 & 0 & 0 & 0 \\ 0 & 0 & 0 & 0 & 0 & 0 \\ 0 & 0 & 0 & 0 & 0 & 0 \\ 0 & 0 & 0 & 0 & 0 & 0 \\ 0 & 0 & 0 & 0 & 0 & 0 \\ 0 & 0 & 0 & 0 & 0 & 0 \\ \frac{1}{C_1} & 0 & 0 & 0 & 0 & 0 \\ 0 & \frac{1}{C_2} & 0 & 0 & 0 & 0 \\ 0 & 0 & \frac{1}{C_3} & 0 & 0 & 0 \\ 0 & 0 & 0 & 0 & 0 & 0 \\ 0 & 0 & 0 & 0 & 0 & 0 \\ 0 & 0 & 0 & \frac{-1}{C_6} & 0 & 0 \\ 0 & 0 & 0 & 0 & \frac{-1}{C_7} & 0 \\ 0 & 0 & 0 & 0 & 0 & \frac{-1}{C_8} \end{bmatrix} \quad (96)$$

$$C = \begin{bmatrix} 0 & 0 & 0 & 0 & 0 & 0 & 0 & 0 & 1 & 0 & 0 & 0 & 0 & 0 & 0 \\ 0 & 0 & 0 & 0 & 0 & 0 & 0 & 0 & 0 & 1 & 0 & 0 & 0 & 0 & 0 \\ 0 & 0 & 0 & 0 & 0 & 0 & 0 & 0 & 0 & 0 & 1 & 0 & 0 & 0 & 0 \\ 0 & 0 & 0 & 0 & 0 & 0 & 0 & 0 & 0 & 0 & 0 & 0 & 1 & 0 & 0 \\ 0 & 0 & 0 & 0 & 0 & 0 & 0 & 0 & 0 & 0 & 0 & 0 & 0 & 1 & 0 \\ 0 & 0 & 0 & 0 & 0 & 0 & 0 & 0 & 0 & 0 & 0 & 0 & 0 & 0 & 1 \end{bmatrix} \quad (97)$$

$$D = \begin{bmatrix} 0 & 0 & 0 & 0 & 0 & 0 \\ 0 & 0 & 0 & 0 & 0 & 0 \\ 0 & 0 & 0 & 0 & 0 & 0 \\ 0 & 0 & 0 & 0 & 0 & 0 \\ 0 & 0 & 0 & 0 & 0 & 0 \\ 0 & 0 & 0 & 0 & 0 & 0 \end{bmatrix} \quad (98)$$

The matrices can then be used as an input for the built in state-space model in Simulink.

Of course the transformer that was shifted to the inputs has to be implemented as well, which is done by a simple gain in both voltage and current signals. The phase shift of the LCI input transformer is actually implemented in the LCI model itself.

4.8 Controller

When dynamic operation is simulated, it is important to have some form of controller. Speed is controlled by controlling the motor torque as it is also done in reality. When speed is too low torque is increased and vice versa.

If the speed controller would directly control the firing angle, the DC-link current could get either too high or too low, resulting in commutation problems or overloading of the system. Therefore the speed controller gives a desired DC current as its output, which is limited. A current controller controls the rectifier firing angle, again with limits on the minimum and maximum firing angle. The feedback signal of the DC-link current has to be filtered as this has severe fluctuations, which would otherwise cause fluctuations in the firing angle signal, possibly exciting resonance issues.

Both controllers are implemented as simple PI controllers and are tuned by hand to ensure proper operation of the system. The Simulink implementation of the entire model is shown in Figure 97. The two subsystems are shown in Figure 98 and Figure 99, and the parameters given in Table 14.

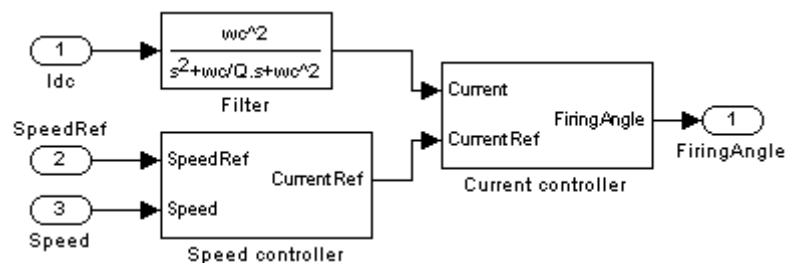


Figure 97: Controller Simulink implementation

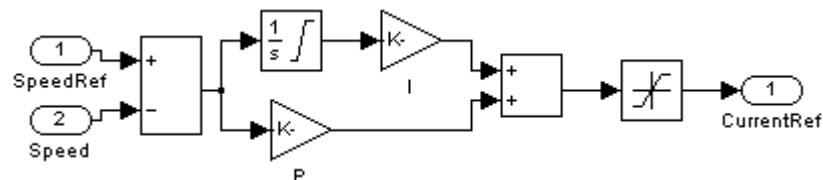


Figure 98: Speed controller Simulink implementation

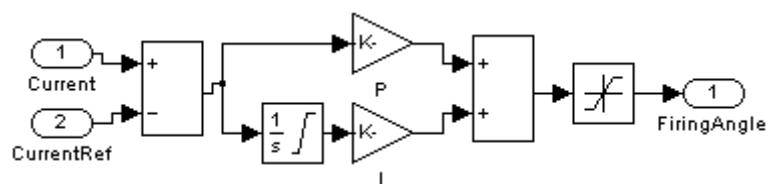


Figure 99: Current controller Simulink implementation

Speed P	5000
Speed I	10000
Max current	3400
Min current	500
Current P	0.002
Current I	0.04
Max firing angle	85°
Min firing angle	25°

Table 14: Controller Parameters

The inverter firing angle is kept constant in this model. It should be chosen low enough to avoid failure of commutation, but as high as possible to maximize power output.

The field voltage is controlled as a function of the motor speed, to obtain a constant V/F. This is common practice to keep the magnetic field at an acceptable level, but will also reduce the risk of commutation failure. The Simulink implementation of the field voltage regulation is shown in Figure 100.

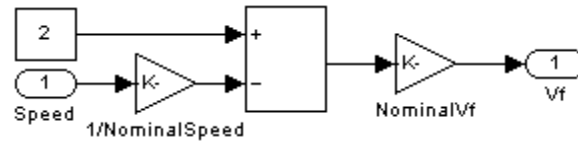


Figure 100: Field voltage controller Simulink implementation

4.9 Validation

With all subsystems of the model completed and combined it is important to see whether the model displays the expected behavior. The first test is to see if the interharmonics with the correct frequency are created and transported to the generator. Next the amplitude of these interharmonics are verified against other simulations of similar cases to verify their amplitude. Finally, the DC-link inductance is doubled. The interharmonics are expected to decrease by a factor two as a result. Figure 101 and Figure 102 show the interharmonic frequency spectra of the current on the generator output and on the LCI input with the standard 5mH DC-link inductance. Figure 103 and Figure 104 show the same interharmonic frequency spectra but now with a 10mH DC-link inductance.

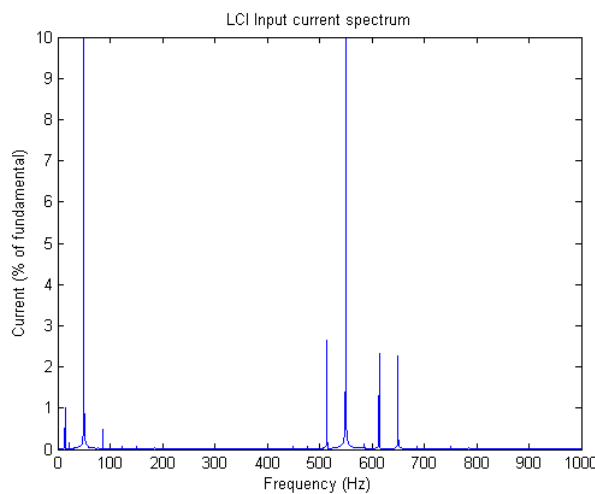


Figure 101: LCI input spectrum with 5mH DC-link inductance

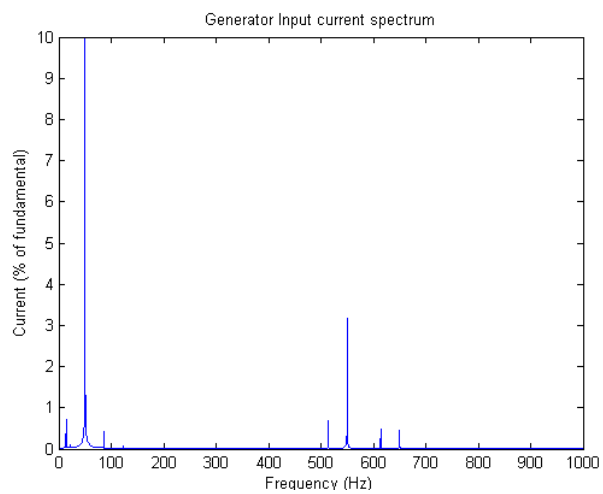


Figure 102: Generator input spectrum with 5mH DC-link inductance

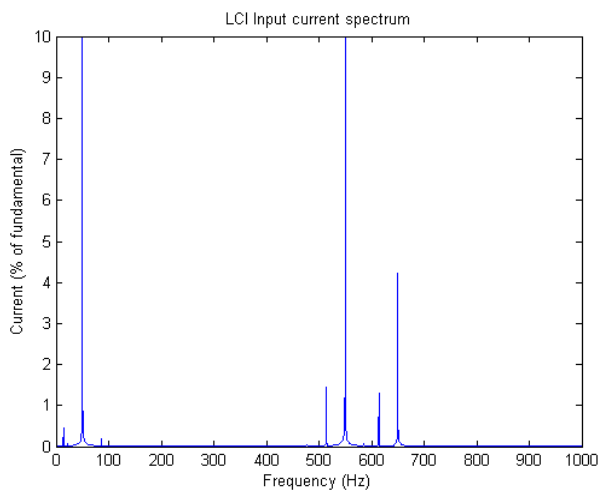


Figure 103: LCI input spectrum with 10mH DC-link inductance

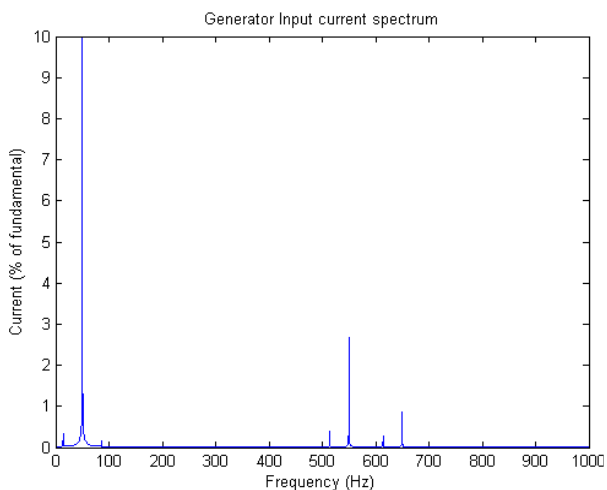


Figure 104: Generator input spectrum with 10mH DC-link inductance

The frequency spectra show components with the expected frequency. Doubling the DC-link inductance indeed decreases the interharmonics by a factor of two. The amplitude of the 14Hz and 86Hz interharmonic provided by Siemens for this machine under similar conditions are 0.60% and 0.40% respectively, which corresponds with Figure 102. This is also confirmed simulations done by Mott MacDonald to verify the outcomes of the Siemens simulations. Unfortunately, no

measurements of a built setup are available. However, as three independent simulations show similar results it may be assumed that the model is a correct representation of a real setup.

4.10 Results

Now the model is fully built and validated it is important to see how the system responds without any mitigation systems attached.

Both the controller (filter) and network model prevent the system from starting in a steady state. To avoid instability by commutation problems in the rectifier the DC-link inductance is increased by a factor of 100 for the first 100ms. This prevents the current in the DC-link from responding to these irregularities. After 100ms it is set to its normal value. The system is then allowed to stabilize for 1s before starting the plots.

First a simple and standard test is done where the system is constantly excited on the frequency that produces problematic interharmonics. The motor frequency should be 48.75Hz. The strongest resulting interharmonics is then -35.03Hz which when interacting with the main 50Hz torque component results in an actual torque component of 14.97Hz being applied to the multi-mass model, exciting the most susceptible resonance frequency.

It turned out that due to the droop control, the frequency was only 49.99Hz. This translates in the created interharmonic being 0.1Hz off which has great influence on the created resonance. The motor speed was therefore change to 48.74Hz. Figure 105 and Figure 106 show the generator current spectrum and the torque on the coupling between element two and three of the GTG. Due to the time consuming nature of these simulations only 5 seconds of operation is simulated.

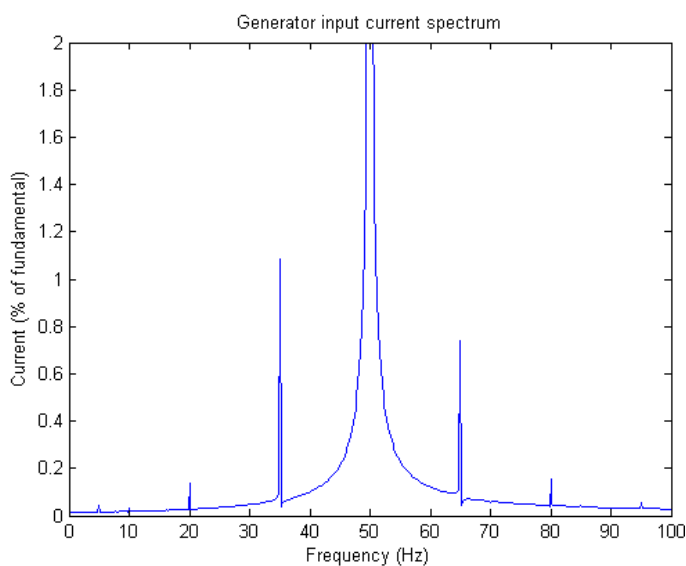


Figure 105: Generator current spectrum all drives at 48.74Hz

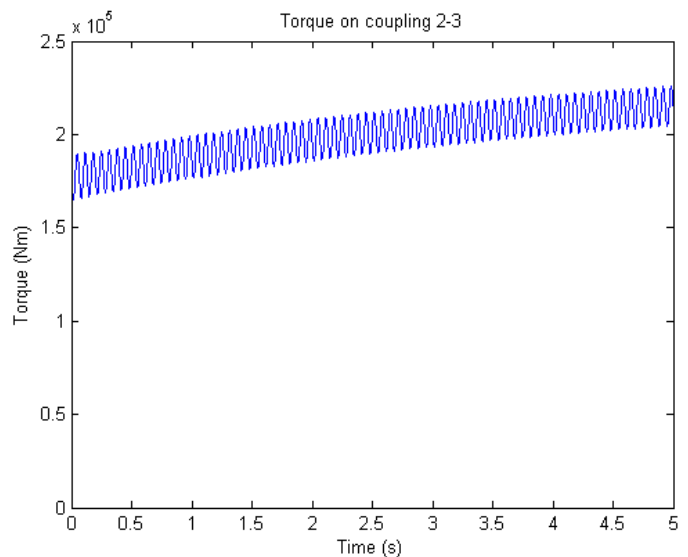


Figure 106: Torque on coupling 2-3 all drives at 48.74Hz

The increase in torque is due to a change in distribution over the different generators.

The created oscillating torques seem very modest when compared to other tests with only the multi-mass model or the later presented test with both the LCI and the multi-mass model. This is due to a number of factors:

1. The network connecting all components damps the interharmonics; this is slightly aggravated by the increased resistance.
2. The generator loading angle will change due to the resonance causing a damping effect.

3. The current drawn by the LCIs interact with each other. All interharmonics having the same phase is the worst case which should be considered here.
4. The damping effect of the two GTGs interacting with each other
5. A shift in frequency response has occurred due to the extra elements attached. This was confirmed by doing a sweep.

Point one and two aren't modeling issues but physical effects. To overcome point three and four a reduced model is used where all LCIs and both GTG behave exactly equal. This is done by using one model to simulate the behavior and connect its feedback signals to the different connections on the network. This also reduces the complexity of the model thereby decreasing simulation time allowing longer simulations. The output speed is set to 48.85Hz which was found to be frequency showing the largest torque response. To show how the torque builds up the motor is initially ran at a frequency that doesn't excite the resonance (48.5Hz). At $t = 0.5s$ the signal to the speed controller is changed to 48.85Hz. The result of this simulation is shown in Figure 107 and Figure 108. The increased torque between $t = 0.5s$ and $t = 1.4s$ is due to the extra current drawn by the drives to speed the motor up. The torque resonance will build up over a period of 2s before damping and excitation match each other. The vibration may seem acceptable at first glance, but it should be kept in mind that a torsional vibration of one third of the tensile strength will already cause fatigue problems in steel.

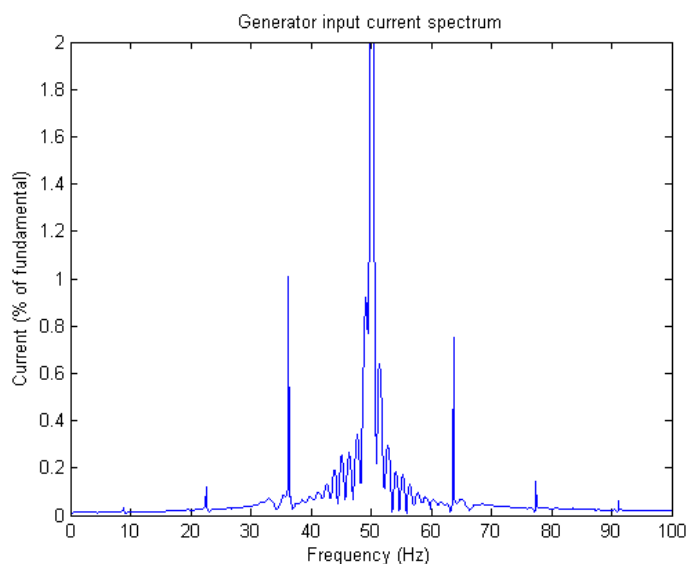


Figure 107: Generator current spectrum all drives on 48.85Hz

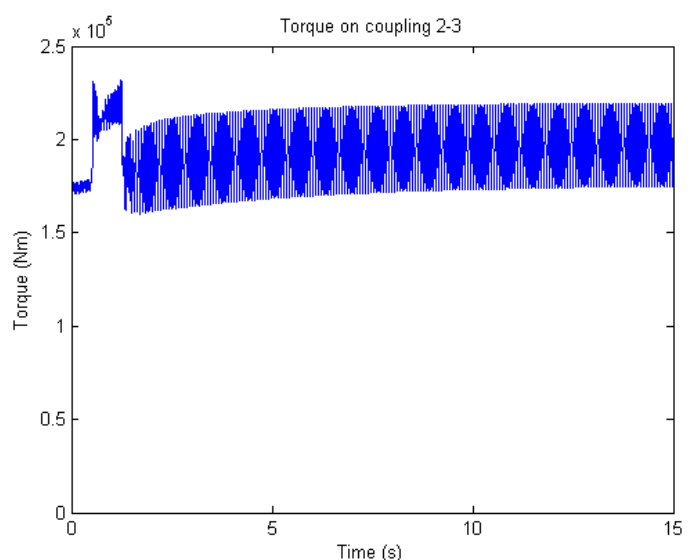


Figure 108: Torque on coupling 2-3 all drives on 48.85Hz

5 Solution simulations

With the LNG plant model complete the new solutions can be tested. However, running these simulations is very time consuming due to the size of the model. Therefore two small scale models are used for initial testing.

The first model is just the basic multi-mass model already introduced in section 2.3. This model can be used to evaluate how resonance is built up when different forms of disturbance are applied.

The second model shown in Figure 109 uses the LCI, motor, compressor and multi-mass model. A sinusoidal 3-phase source is used as supply. The d-component of the current is scaled to obtain an approximation of the torque. The damping in the multi-mass model is increased by a factor ten to speed simulations up by the same amount. The resulting torque would therefore be ten times higher in reality. When the solutions are incorporated in this model, a good approximation of the actual behavior is acquired without requiring much simulation time.

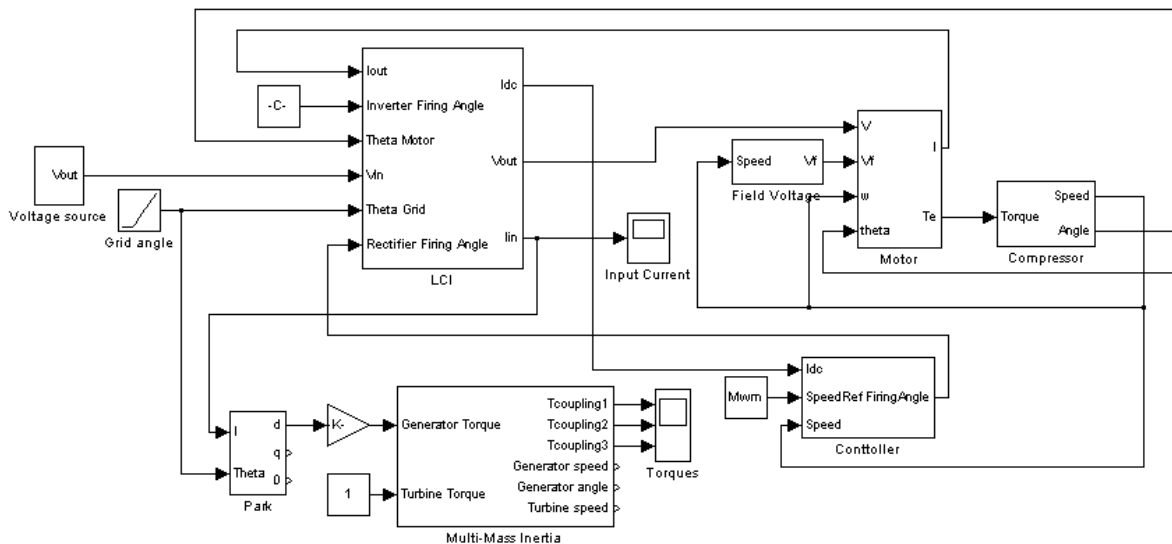


Figure 109: Second test model

After the study of different solutions two solutions were selected for further research: sloppy speed control and varying firing angles. Both try to change the interharmonic frequencies slightly as a function of time to avoid constant excitation. As seen in section 2.3 and section 3.11, deviating from the exact resonance frequency by just a small amount can be enough to significantly reduce torques.

5.1 Constant sinusoidal frequency variations

The first test is how resonance changes when the interharmonics are varied in time. For this purpose a torque is given directly onto the multi-mass model to see how it responds. As a reference the response of the model to the constant excitation of Figure 110 is repeated in Figure 111.

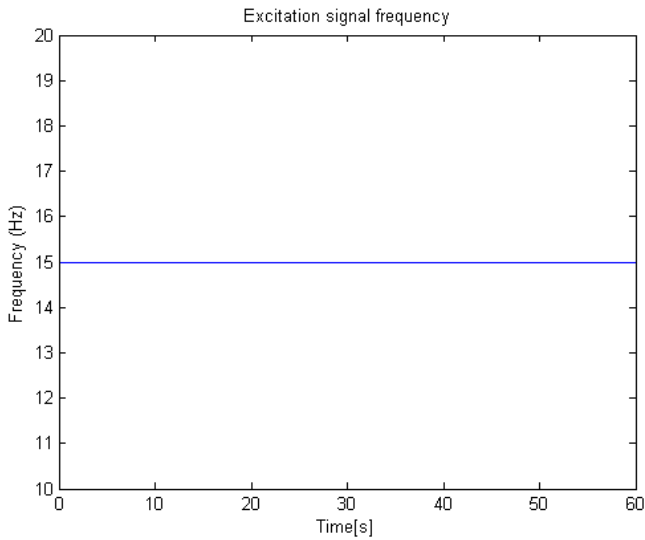


Figure 110: Constant excitation signal (14.973Hz)

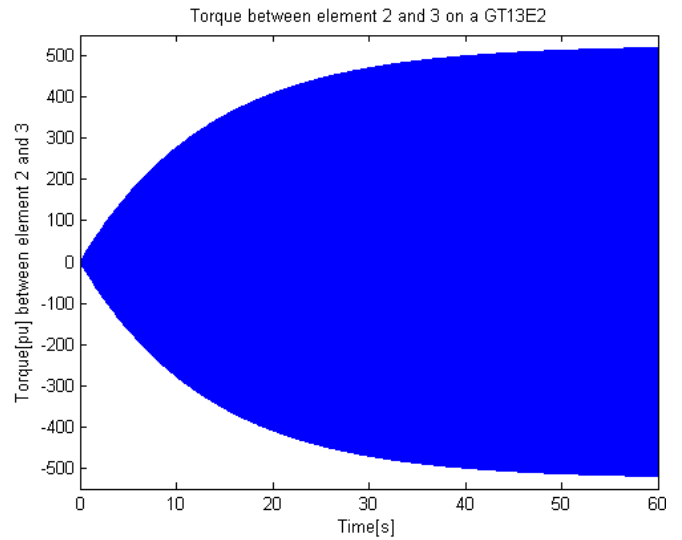


Figure 111: Torque with constant excitation

The basic idea is to avoid constant excitation of a resonance point. This will ensure that instead of constantly amplifying the torque by adding a torque with the same phase, the torque will subsequently be amplified and attenuated as the phase of the applied torque and torque in the coupling varies over time.

First the simple sinusoidal change in frequency of Figure 112 is applied. The result is shown in Figure 113 which with an 11 times torque reduction is very promising. However for a slightly different frequency, with a non changing frequency as in Figure 114, the resulting torque used to stay quite low as in Figure 115. Applying the same variation in frequency the signal of Figure 116 is created which will respond into the resonance of Figure 117. It is therefore clear that although simply applying a variation to the interharmonics can decrease resonance at certain frequencies, it will aggravate the problem at others. So attention has to be paid to the full operating range and not just problematic frequencies.

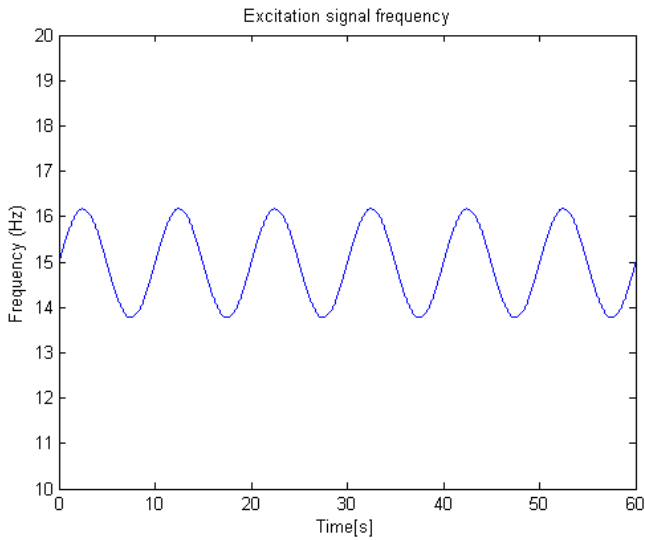


Figure 112: Sloppy excitation signal (1,2Hz variation, 10s period)

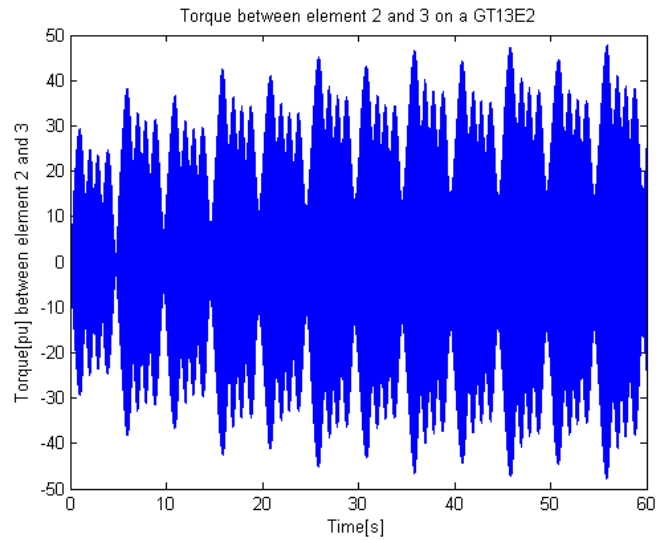


Figure 113: Torque with sloppy excitation

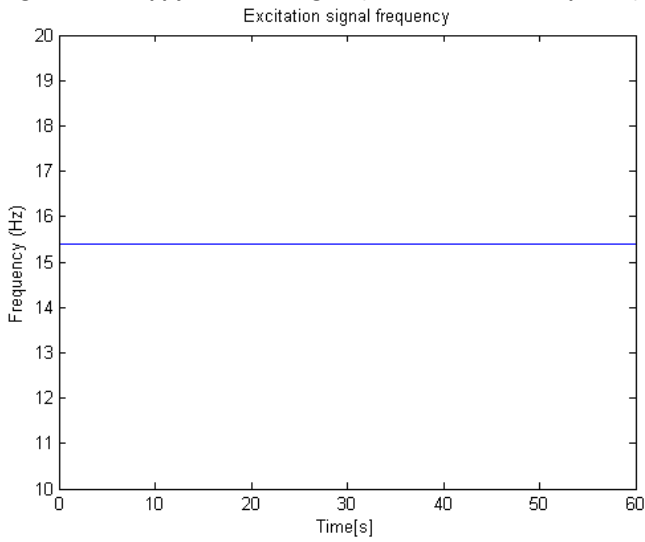


Figure 114: Constant excitation signal (15.4Hz)

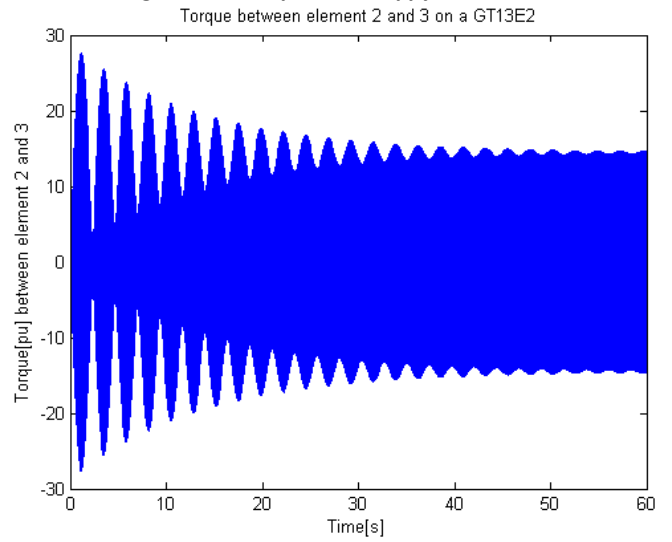


Figure 115: Torque with constant excitation

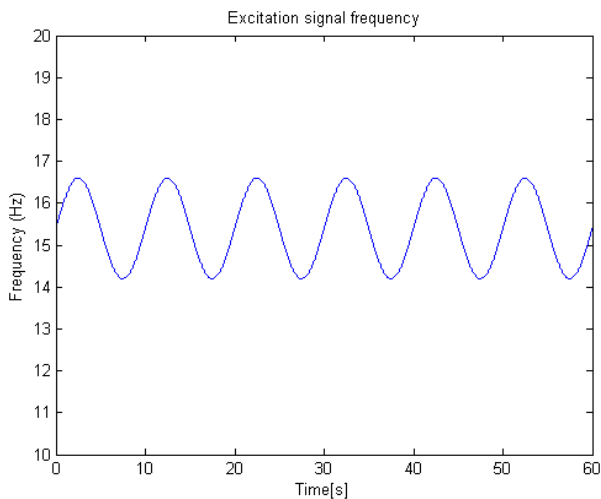


Figure 116: Sloppy excitation signal (1,2Hz variation, 10s period)

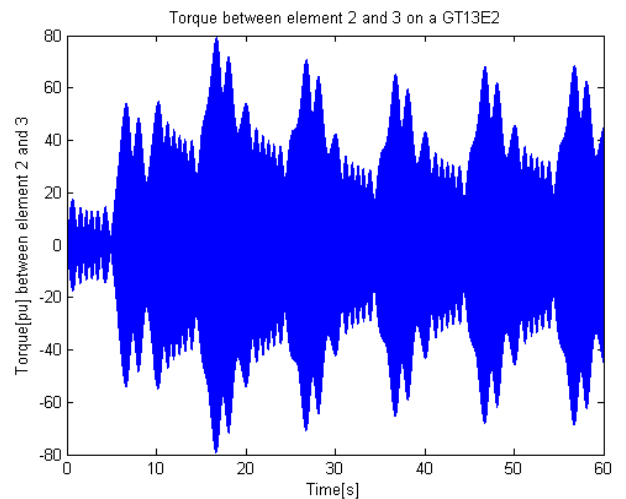


Figure 117: Torque with sloppy excitation

5.2 Frequency variations: other waveforms

Until now, sinusoidal disturbances were made. It is however interesting to see how other waveforms would perform. Therefore, simulations are done using triangular and square wave waveforms. Figure 118 to Figure 121 show their effect on the resonance frequency.

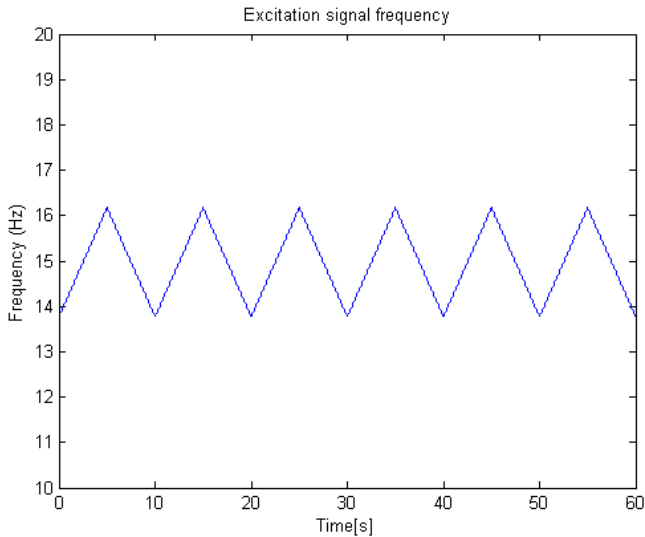


Figure 118: Excitation signal with triangular disturbance

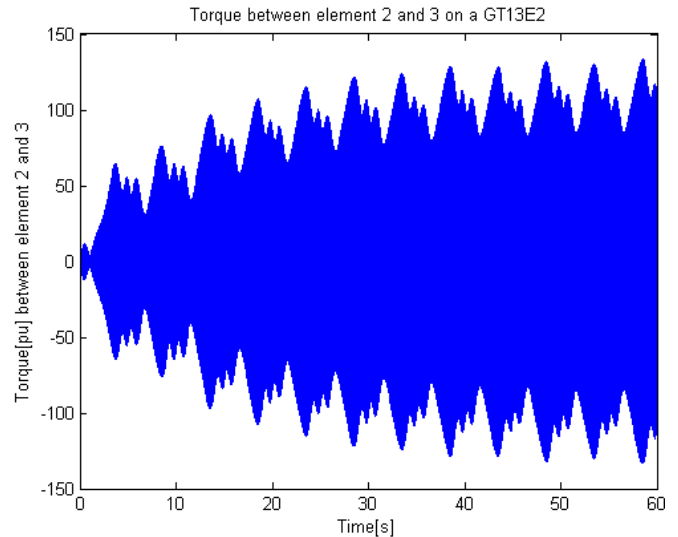


Figure 119: Torque with triangular disturbance

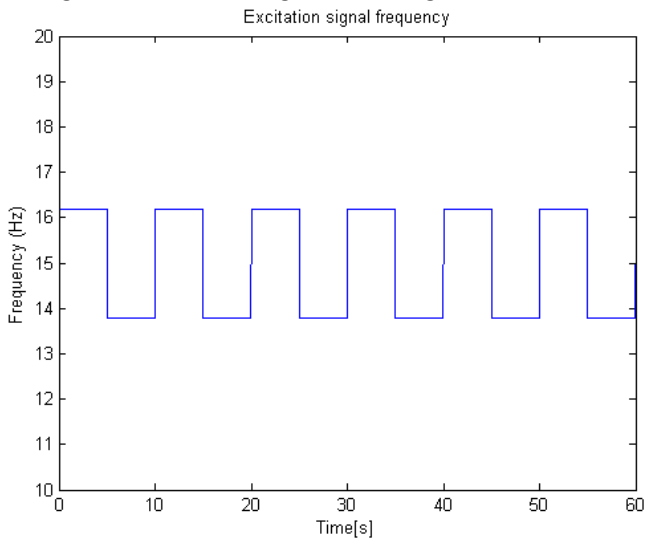


Figure 120: Excitation signal with square wave disturbance (1,2Hz variation, 10s period)

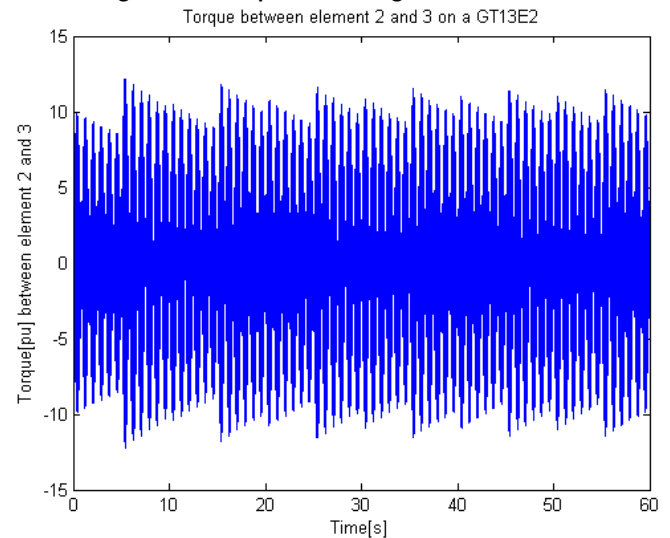


Figure 121: Torque with square wave disturbance

While the triangular waveform doesn't perform very well, the square wave produces very promising results. It has to be noted however that a square wave disturbance can't be achieved by disturbances on the speed controller, as the machine speed can't vary instantly. The inverter firing angle can however be varied instantly.

As it was already concluded that problems may arise at other frequencies, so the square wave is tested for a range of frequencies with the results in Figure 122.

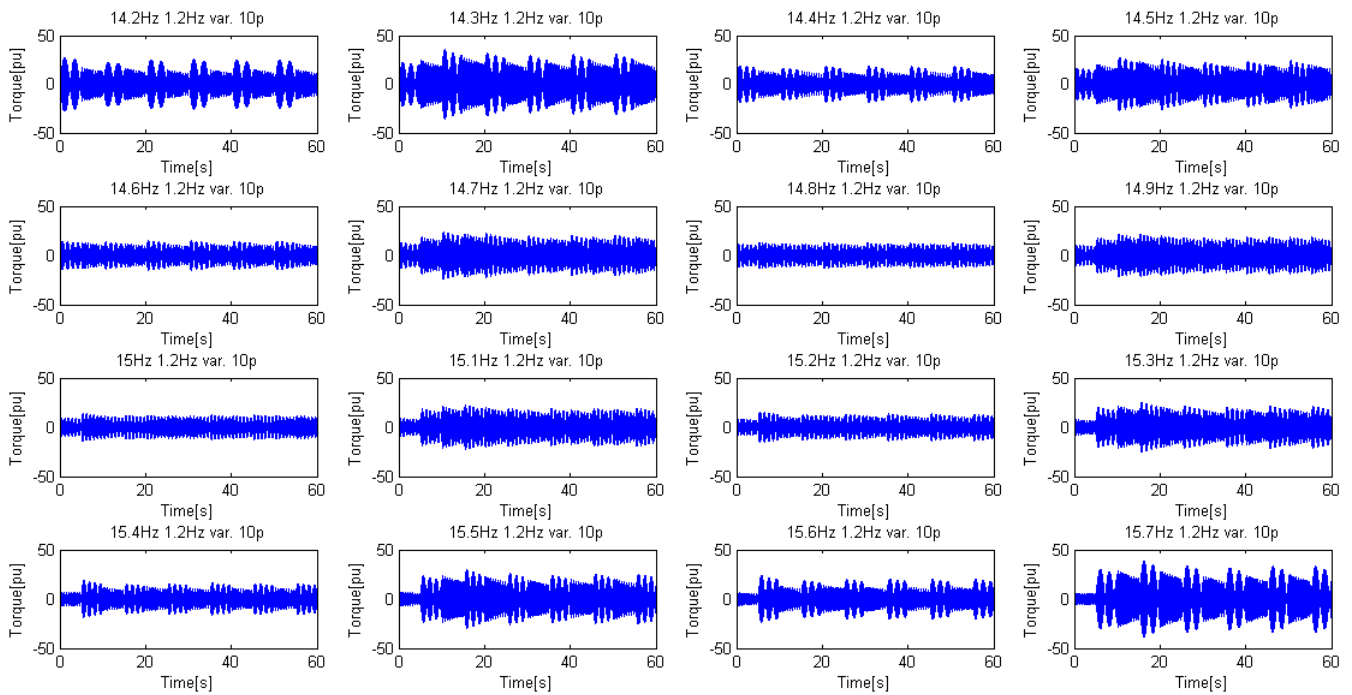


Figure 122: Torque with square wave disturbance for various frequencies

5.3 Dynamic frequency variations

With all forms of disturbances both the amount of change in frequency and the period of this disturbance can be changed to obtain the best possible results. It also varies which frequencies get negatively affected by applying a disturbance.

For the sinusoidal disturbance many simulations have been done to find a set of values that reduce torques to acceptable levels for all frequencies. Although no such set of values was found, it was noted that for every frequency the values can be chosen to limit torque sufficiently. A system that dynamically changes these parameters based on the frequency (so in practice on the drive output frequency) could therefore reach very good results as shown in Figure 123. Above each graph, the frequency is shown along with the amount of change applied to it and the period over which this is changed.

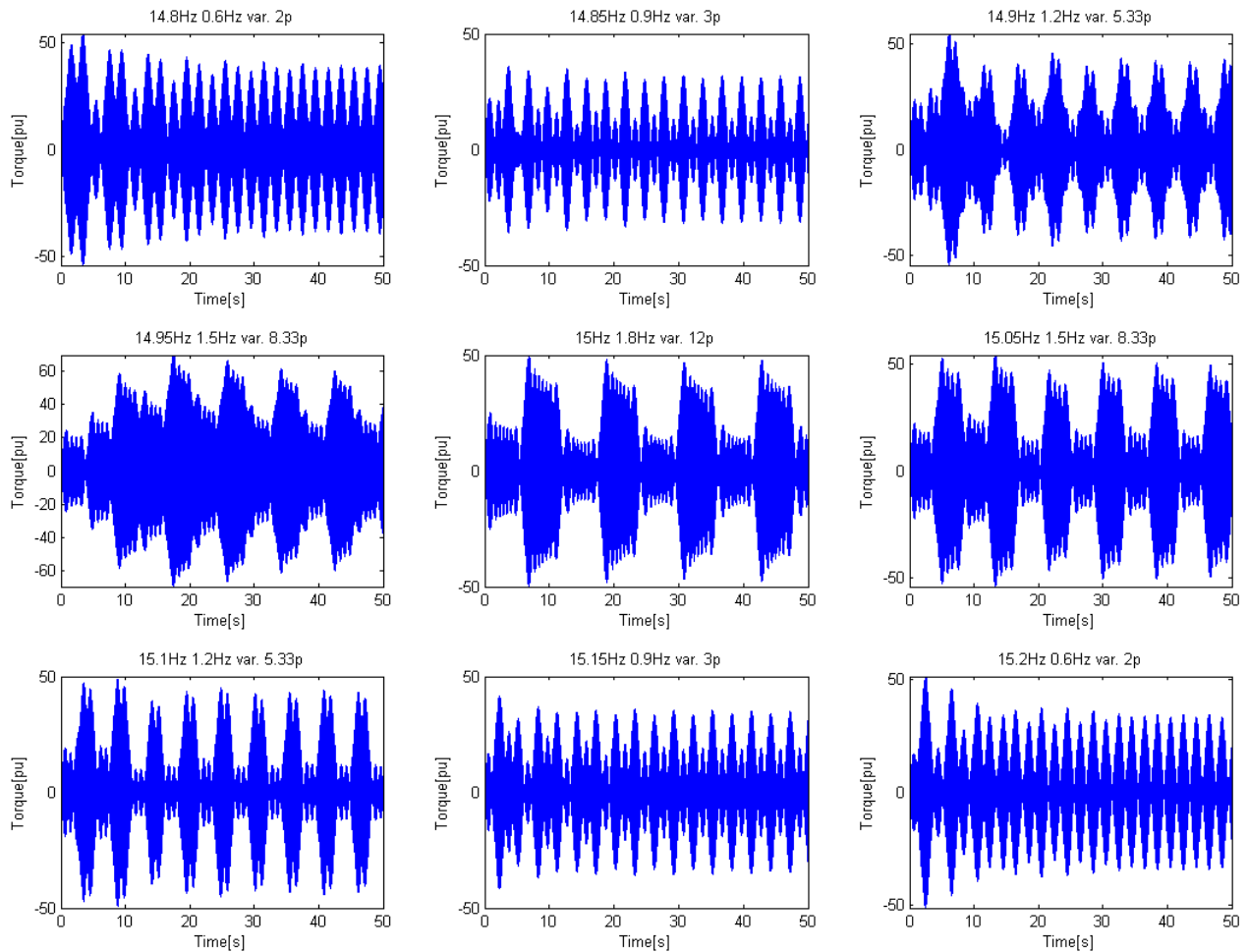


Figure 123: Torques with sinusoidal disturbances with dynamic parameters

5.4 Torque feedback

Moving away from the exact resonance frequency by as little as 0.1Hz can have a large effect as we already saw comparing Figure 16 and Figure 15. As these resonance points can shift large safety regions have to be taken into account when planning to just avoid these band as mentioned in section 3.9. This can be avoided using the feedback of a torque sensor. The simplest form would be a torque sensor that directly can give a (limited) increase in speed to the speed controller.

Figure 124 shows a very slow sweep passed the resonance point without any mitigation measures. As can be expected, the torque builds up to large values.

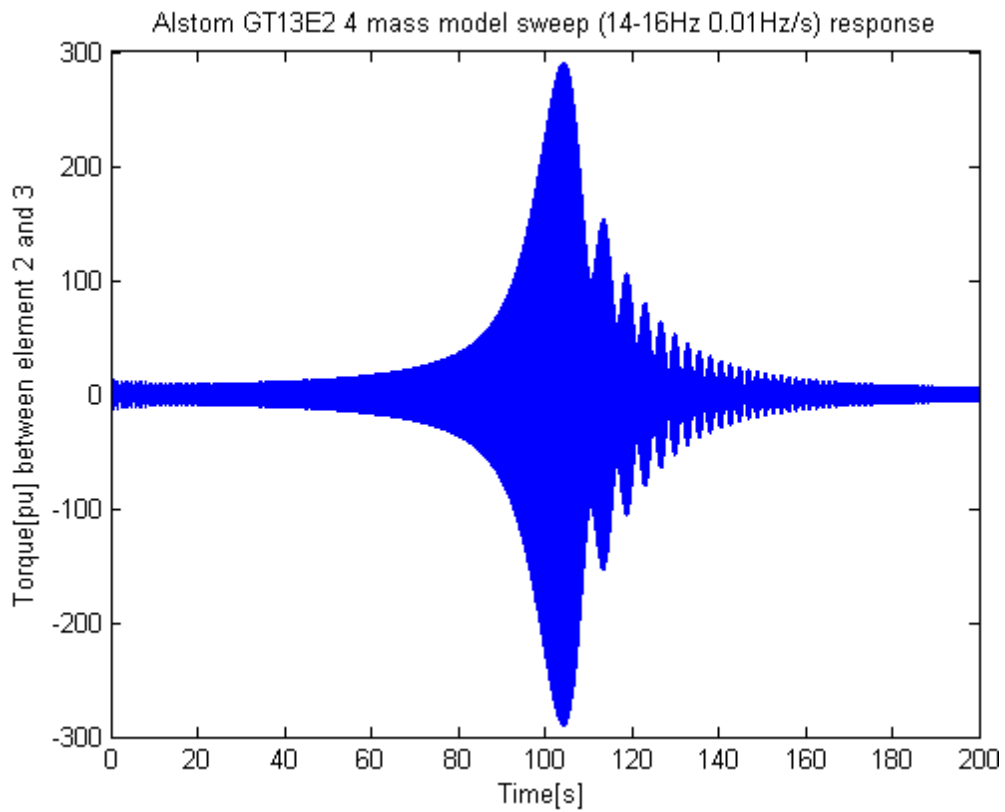


Figure 124: Sweep without mitigation measures

Figure 125 shows the same very slow sweep passed the resonance point but this time with the simple torque feedback. The result is a much lower torque.

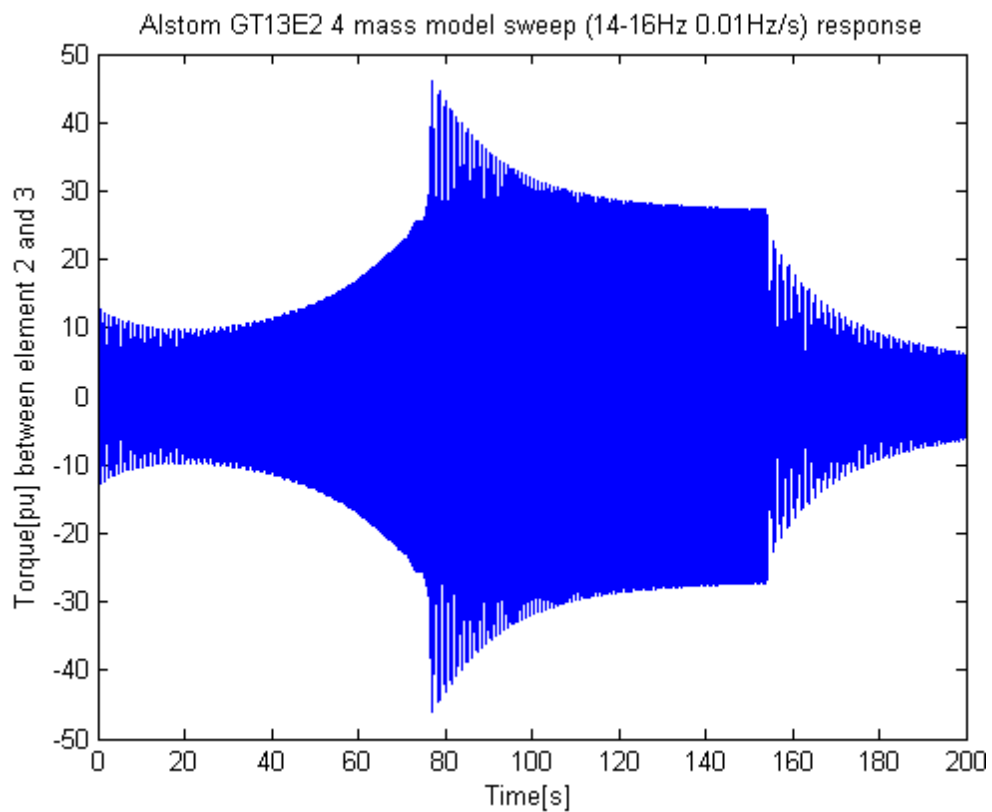


Figure 125: Sweep with torque feedback

The results of this simple test are very promising. However, practical application is only possible when a torque sensor can be installed in the system. This is not an easy task to achieve inside a GT. However, research is being done on new types of torque sensors that may solve this problem in the near future.

5.5 Effect of speed variations

The tests directly on the multi-mass model give insight in what may work. The next step is to test if the solutions work when applied to the LCI. Therefore the model that was already presented in Figure 109 is used in combination with the selected solutions. First a simulation has to be done to determine what would happen when no measures are taken. Figure 126 shows the input current spectrum of the LCI which clearly shows the interharmonics. Figure 127 shows the torque on coupling 2-3 of the multi-mass model which is the most sensitive to this frequency.

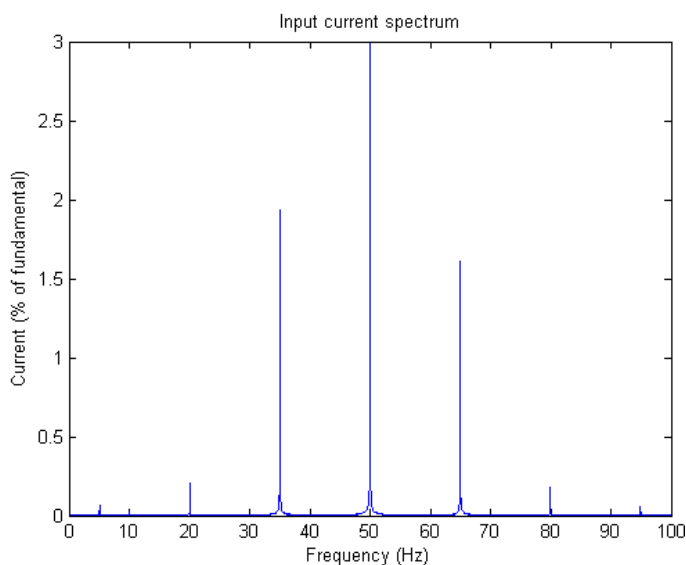


Figure 126: LCI input current spectrum without mitigation

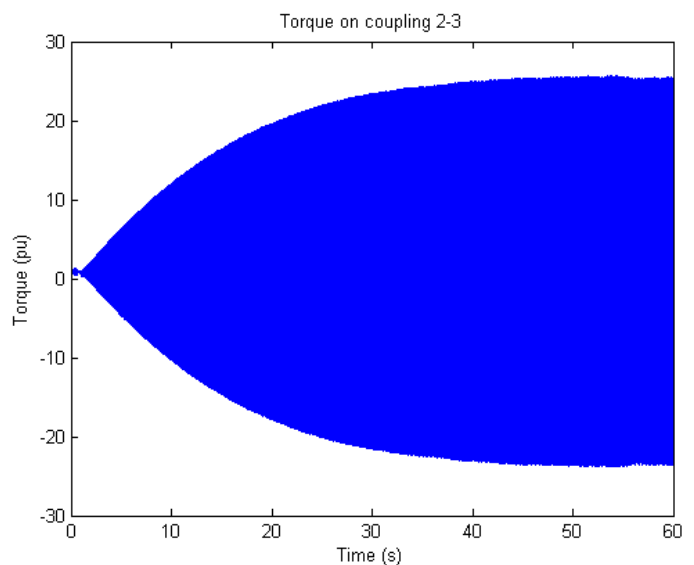


Figure 127: Torque on coupling 2-3 without mitigation

Figure 126 shows sharp excitation of the problematic frequencies. Figure 127 shows resonance on this coupling which causes torques to reach up to 25pu. To accomplish the same sinusoidal frequency variation of 1.2Hz over a 10 second period on the interharmonics, a 0.1Hz variation over a 10 second period is offered to the speed controller. The results are as in Figure 128 and Figure 129. The torque stays below 6pu here which is an improvement by a factor of 4.

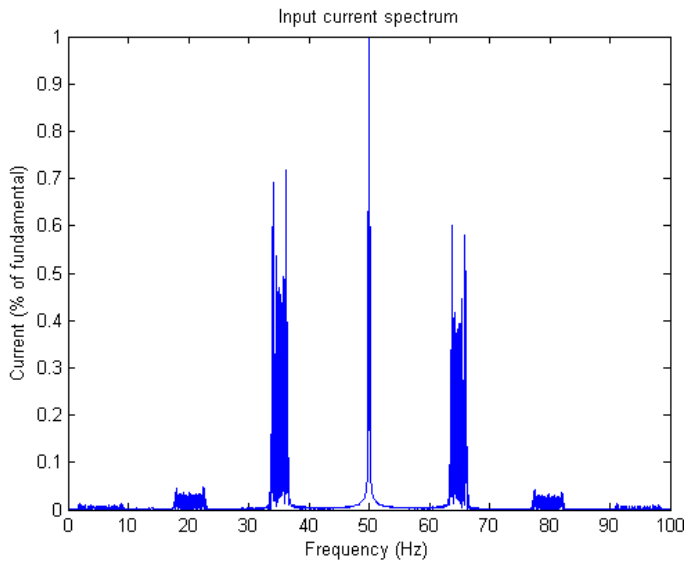


Figure 128: LCI input current spectrum with sinusoidal speed variation

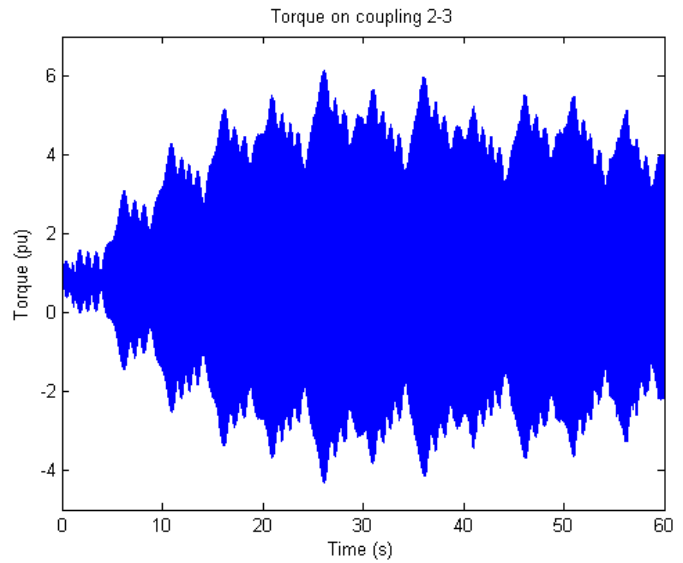


Figure 129: Torque on coupling 2-3 with sinusoidal speed variation

The motor speed can keep track of a slow changing sinusoidal speed variation. Due to the inertia it is impossible to vary the speed as a step. When a square wave is offered to the speed controller the resulting speed change and therefore the created interharmonic frequencies will not have a square wave form as they did in Figure 120. However, the results are still very good as shown in Figure 130 and Figure 131, where the torque stays below 2pu (except for a small starting transient) so a factor of 12.5 is achieved.

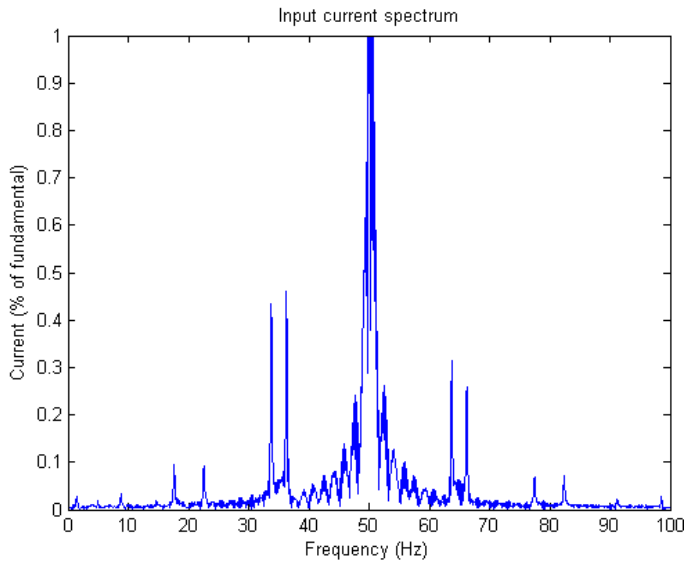


Figure 130: LCI input current spectrum with square wave speed variation

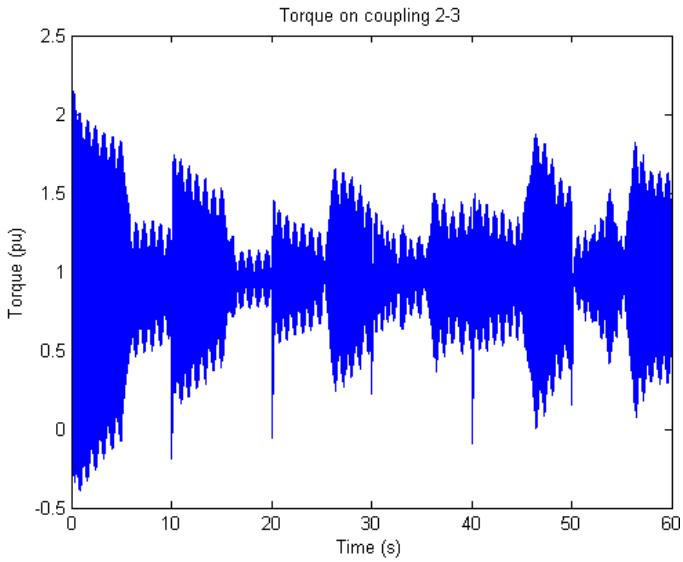


Figure 131: Torque on coupling 2-3 with square wave speed variation

5.6 Effect of firing angle variations

Another way to ensure the phase of the interharmonics changes in time is by altering the inverter firing angle in time. Changing the firing angle will affect the power output, but as long as variations are small, the speed controller will be able to handle this. A large advantage is that the inverter firing

angle can be changed instantly thereby allowing a square wave variation. Tests show that this is again the most effective waveform.

To test the influence of the inverter firing angle the model of Figure 109 is used where a square waveform is applied to the inverter firing angle input. After some short test to find a good signal, the amplitude of this signal is chosen to be 2° with a 1 second period. The motor speed is set at 48.75Hz which should excite a resonance on the coupling between element 2 and 3. The input current spectrum and the resulting torque are shown in Figure 132 and Figure 133. These figures show that changing the firing angle will indeed reduce the torque, but not as effectively as changes in the speed will do.

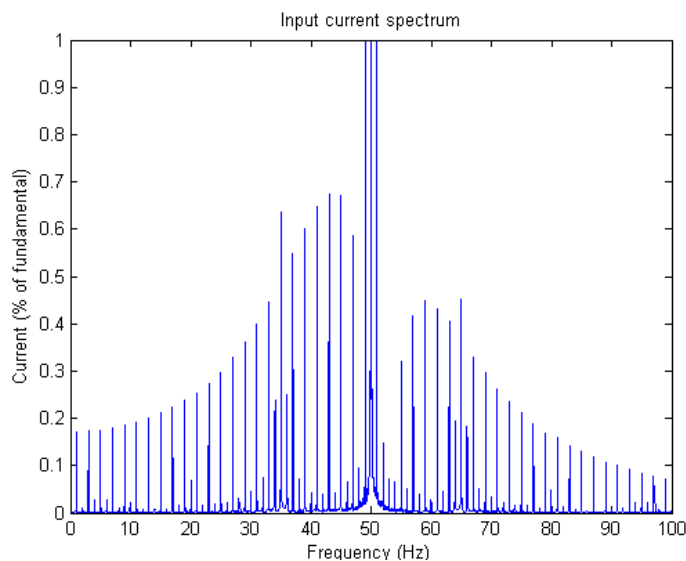


Figure 132: LCI input current spectrum with square wave inverter firing angle variation

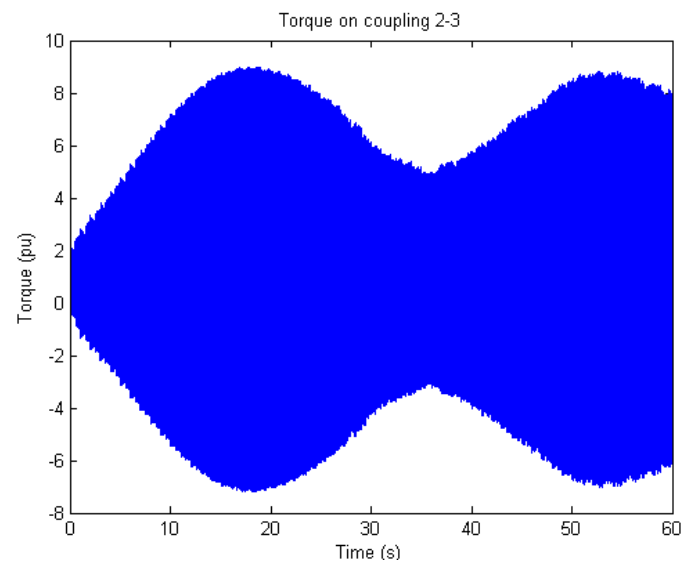


Figure 133: Torque on coupling 2-3 with square wave inverter firing angle variation

5.7 Total system result

Applying a speed reference with a square wave distortion proved to be the most effective solution in the small scale tests. This solution is therefore applied to the full scale model.

The system is again constantly excited on the frequency that produces problematic interharmonics in a similar way as in section 4.10. As the torque build up faster in the full model, the distortion signal will also have to be faster to be able to act when the torque is still building up. Furthermore, the sharp current variations due to the square wave signal turned out to cause torsional vibrations so the smoother sine wave was chosen despite its lower performance in the small scale tests. The signal has a 0.1Hz variation with a 2s period. Figure 134 and Figure 135 show the generator current spectrum and the torque on the coupling between element two and three of the GTG when the motors are run at 48.85 Hz.

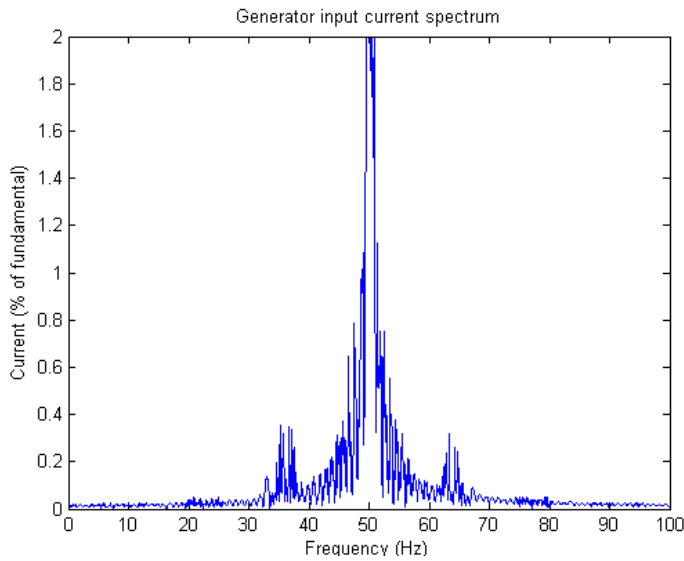


Figure 134: Generator current spectrum all drives at 48.85Hz

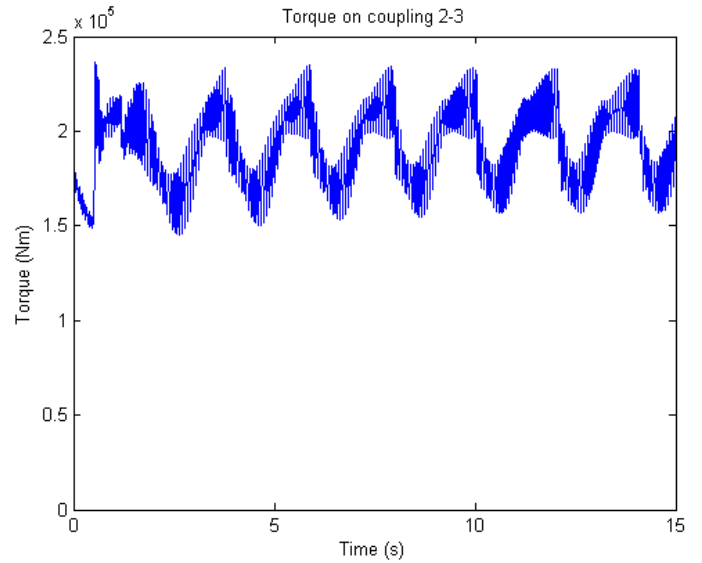


Figure 135: Torque on coupling 2-3 all drives at 48.85Hz

The effect of the speed changes, both at $t = 0.5s$ (from 48.5Hz to 48.85Hz) and implemented speed variations are reflected in the torque. The torque levels are 30-60% of the torque levels for continuous operation. Unfortunately the speed can't be increased faster, but it is expected that if this could be done, for instance by a more sophisticated controller, that torque can be reduce even further. Furthermore the waveform used here is probably not the most optimal waveform so even more improvement can be gained here. However, both these changes are outside the scope of this research.

6 Conclusion

In this thesis interharmonics and solutions to them were studied. To do this properly a lot of factors have to be taken into account. Not only the VSD that creates them, but also the motors, generators, controllers, turbines and grid have to be taken into account. A thorough understanding of the resonance issue is also essential.

After understanding the interharmonic issues, possible solutions were considered and carefully reviewed. It was chosen to prevent the resonance from building up to its maximal value by avoiding constant excitation of a resonance point. Both changes to the inverter firing angle and the motor speed have been considered with different waveforms. Applying a square wave distortion to the motor speed turned out to be the most effective solution on small scale. Using feedback of torque sensors could further improve the effectiveness of these solutions. However, these sensors are too complicated to implement currently.

After modeling each part of a realistic LNG setup, the effect of this solution could be verified. As this simulation has shown torque can be reduced by 40%, which is impressive when the simplicity of the system is considered. Another benefit of this system is that it is not very sensitive to the value of mechanical damping, which is not reliably available. Smaller damping will increase the maximum torques slightly as the resonance can build up slightly faster, but it won't increase linearly with the damping as is the case with most solutions.

When selecting the compressor and motor it is still advisable to keep interharmonics in mind. When the operation speed bands are chosen correctly, interharmonic problems can be avoided. In most cases 12-pulse converters are already applied for the power levels considered here. When this is combined with the solutions proposed here, interharmonics won't be a problem for most cases.

As this solution will have a slight impact on the output speed, it is important to verify whether this presents problems on either the rotating equipment or process side.

The extra disturbance on the motor could cause new problems. When discussing this solution with the rotating equipment group inside Shell, their view is that fatigue on the motor side due to the disturbance is not expected as the variations are small and slow.

Another concern would be that the slight speed variations may interfere with the overall process. Discussion with Process Engineers for Gas and LNG revealed that the 6rpm changes over a 2 second period will not cause any problems. GT drivers in conventional setups have much more speed fluctuations so from a process point of view this is still considered to be fixed speed. Furthermore a Mixed Refrigerant cooler has a time constant of around 20-30 minutes, so the 2 second period is too fast to be noticeable on the process.

Due to the many aspects connected to the subject of interharmonics, there is much more research that could be done on the subject. Following are a number of recommendations.

The network model used here is not very well suited for this purpose. For further research it should be considered to use a different model or even different modeling software.

The effect of LCIs and generators interacting with each other was briefly considered in this research. Further research should be done to see how these interactions can be used to avoid amplification of interharmonics or even to attenuate them.

The disturbance of 6 rpm on a 2 second period was selected after testing several different parameters. Future research should be done to find the most optimal distortion. This could further improve the effectiveness of this solution.

As VSIs are being developed with ever higher power levels, a similar study should be done to find a solution with similar or even better results than presented here. The carrier inversion discussed in section 3.11 would be a good starting point for this.

Appendix 1 References

- [1] Ambra Sannino, Lars Liljestr nd, Bengt Rothman, Tom Nestli, Martin Kj ll-Ohlsson and Per-Erik Holsten, "All-electric LNG liquefaction plants," in *Conference Record of the 2007 IEEE Industry Applications Conference 42nd IAS Annual Meeting.*, 2007, pp. 2407 - 2413.
- [2] U.S. Department of Energy. (2005) Liquefied Natural Gas: Understanding the Basic Facts. [Online]. http://fossil.energy.gov/programs/oilgas/publications/lng/LNG_primerupd.pdf
- [3] ABB. (2006) ABB.com. [Online]. <http://www05.abb.com/global/scot/scot216.nsf/veritydisplay/f36f7c833c88986bc1257244003ce293/>
- [4] TMEIC GE. (2009, Aug.) tmeicge.com. [Online]. http://www.tmeicge.com/upload/library_docs/english/TMG-1220-Oil-Gas_2009_Final_HIGH-RES_1291392480.pdf
- [5] Duro Basic, "Input Current Interharmonics of Variable-Speed Drives due to Motor Current Imbalance," *IEEE Transactions on Power Delivery*, pp. 2797 - 2806, 2010.
- [6] Erich W. Gunther, "Interharmonics – Recommended Updates to IEEE 519," in *IEEE Power Engineering Society Summer Meeting*, 2004, pp. 950 - 954.
- [7] K.S. Smith and L. Ran, "Torsional Resonance Risk Management in Islanded," in *Conference Record of the Industry Applications Conference, 42nd IAS Annual Meeting*, 2007.
- [8] Thavatchai Tayjasanant and Wilsun Xu, "A Case Study of Flicker/Interharmonic Problems Caused by a Variable Frequency Drive," in *11th Conference on Harmonics and Quality of Power*, 2004, pp. 72 - 76.
- [9] Volker H tten, Rainer M. Zurowski and Martin Hilsher, "Torsional Interharmonic Interaction Study of 75MW Direct-Driven VSD Motor Compressor Trains for LNG Duty," in *Proceedings of the thirty-seventh rubomachinery symposium*, 2008, pp. 57 - 66.
- [10] Siemens. (2008) siemens.com. [Online]. <https://www.automation.siemens.com/mcms/infocenter/dokumentencenter/Id/Documentsu20Catalogs/mv-umrichter/d12-en.zip>
- [11] Joseph Song-Manguelle, Jean-Maurice Nyobe-Yome and Gabriel Ekemb, "Pulsating Torques in PWM Multi-Megawatt Drives for Torsional Analysis of Large Shafts," *Transactions on Industry Applications*, vol. 46, no. 1, pp. 130 - 138, 2010.
- [12] Yu Yu, Kai-pei Liu, Bo Fu and Yang Zhao, "Harmonic and Interharmonic Currents generated by the VSI-Fed Adjustable Speed Drive," in *IEEE 6th International Power Electronics and Motion Control Conference*, 2009, pp. 2464 - 2467.
- [13] Hiromi Hosoda and Steven Peak, "Multi-Level Converters for Large Capacity Motor Drive," in *International Power Electronics Conference*, 2010, pp. 516 - 522.

- [14] Undeland, Robbin Mohan, *Power Electronics*. Hoboken: John Wiley & Sons Inc., 2003.
- [15] Tatiana Ravani von Ow, "Milling - Energy Intensive And High Maintenance, Overcoming The Challenges Using Frequency Converters," in *MAPLA*, 2009, pp. 207 - 218.
- [16] ABB. (2011) ABB.com. [Online].
<http://www05.abb.com/global/scot/scot216.nsf/veritydisplay/413cdb84f7f999b8c125785b0045167a/>
- [17] J.-J. Simond, A. Sapin, M. Tu Xuan, R. Wetter and P. Burmeister, "12-Pulse Lci Synchronous Drive For A 20 Mw Compressor Modeling, Simulation And Measurements," in *IAS 2005*, 2005, pp. 2302 - 2308.
- [18] B. Singh, S. Singh and S.P. Hemanth Chender, "Power quality improvement in load commutated inverter-fed synchronous motor drives," *IET Power Electronics*, vol. 3, no. 3, pp. 411 - 428, 2008.
- [19] Pablo Aravena, Luis Morán, Juan Dixon and José Espinoza, "A New Hybrid Filter Topology for Sub and Inter-harmonic Attenuation in Cycloconverter-Fed Drives Applications," in *Industry Applications Society Annual Meeting*, 2009, pp. 1 - 7.
- [20] Alexandre B. Nassif and Wilsun Xu, "Passive Harmonic Filters for Medium-Voltage Industrial Systems: Practical Considerations and Topology Analysis," in *39th North American Power Symposium*, 2007, pp. 301 - 307.
- [21] D. Basic, V.S. Ramsden and P.K. Muttik, "Performance Of Combined Power Filters In Harmonic Compensation Of High-Power Cycloconverter," in *Seventh International Conference on Power Electronics and Variable Speed Drives*, 1998, pp. 674 - 679.
- [22] Peng and Fang Zheng, "Application Issues of Active Power Filters," *IEEE Industry Applications Magazine*, vol. 4, no. 5, pp. 21 - 30, 1998.
- [23] E. J. Delaney and R. E. Morrison, "Minimisation of Interharmonic Currents from a Current Source A.C. Drive by Means of a Selective D.C. Side Active Filter," *IEEE Transactions on Power Delivery*, vol. 10, no. 3, pp. 1584 - 1590, 1994.
- [24] F.M. Pkrez-Hidalgo, J.L. Duran-Paz and J.R. Heredia Larrubia, "DC side harmonic reduction in rectifiers by direct ripple reinjection," *Electronics Letters*, vol. 35, no. 20, pp. 1698 - 1700, 1999.
- [25] Luis Morán, José Espinoza, Mauricio Ortíz, José Rodríguez and Juan Dixon, "Practical Problems Associated With The Operation Of ASDS Based On Active Front End Converters In Power Distribution Systems," in *39th Industry Applications Conference Annual Meeting.*, vol. 4, 2004, pp. 2568 - 2572.
- [26] Mott MacDonald, "Voltage Source Drives Technology Review Part 2," 2007.
- [27] E.A. Klingshirn, "High Phase Order Induction Motors Part 1," *IEEE Transactions on Power Apparatus and Systems*, pp. 47 - 53, 1983.
- [28] Sandy Smith and Steve Williamson, "Pulsating Torque and Losses in Multiphase Induction Machines,"

Transactions on Industry Applications, vol. 39, no. 4, pp. 986 - 993, 2003.

- [29] E. Levi, R. Bojoi, F. Profumo, H.A. Toliyat and S. Williamson, "Multiphase induction motor drives – a technology status review," *IET Electric Power Applications*, pp. 489 - 516, 2007.
- [30] P.C. Sen, *Principles of Electric Machines and Power Electronics*.: John Wiley & Sons Inc., 1997.
- [31] A. Tessarolo, G. Zocco and C. Tonello, "Design and Testing of a 45-MW 100-Hz Quadruple-Star Synchronous Motor for a Liquefied Natural Gas Turbo-Compressor Drive," in *IEEE Transactions on Industry Applications*, vol. 47, 2011, pp. 1210 - 1219.
- [32] William R. Finley, Mark M. Hodowanec and Warren G. Holter, "An Analytical Approach To Solving Motor Vibration Problems," in *Industry Applications Society 46th Annual Petroleum and Chemical Industry Conference*, 1999, pp. 217 - 232.
- [33] Michael van der Giet, Kay Hameyer and Stephan Risse, "Induction motor with pole-changing winding for variable supply frequency," in *IEEE International Electric Machines & Drives Conference*, 2007, pp. 1484 - 1489.
- [34] D. Inácio, S. Inácio, J. Pina, S. Valtchev, M. Ventim Neves, J. F. A. Martins and A. Leão Rodrigues, "Conventional and HTS Disc motor with pole variation control," in *International Conference on Power Engineering, Energy and Electrical Drives*, 2009, pp. 513 -518.
- [35] Robert W. Wieseman, "A Two-Speed Salient-Pole Synchronous Motor," *Transactions of the American Institute of Electrical Engineers*, vol. XLIV, p. 436, 1925.
- [36] X. Ojeda, X. Miningert, M. Gabsit and M. Lecrivain, "Noise Cancellation of 6/4 Switched Reluctance Machine by Piezoelectric Actuators: Optimal Design and Placement using Genetic Algorithm," in *4th IET Conference on Power Electronics, Machines and Drives*, 2008, pp. 611 - 615.
- [37] Joseph Song-Manguelle, Christof Sihler and Simon Schramm, "A General Approach of Damping Torsional Resonance Modes in Multi-Megawatt Applications," in *Energy Conversion Congress and Exposition*, 2010, pp. 772 - 779.
- [38] M.J. Hoeijmakers, *Modelling of AC Machines*. Delft: TUdelft, 2004.
- [39] Prabha Kundur, *Power System Stability and Control*. New York: McGraw-Hill Inc., 1993.
- [40] W.J.Rowan, "Simplified Mathematical Representations of Heavy-Duty Gas Turbines," *Journal of Engineering for Power*, October 1983.
- [41] Q. Zhang and P.L. So, "Dynamic modelling of a combined cycle plant for power system stability studies," in *Power Engineering Society Winter Meeting*, 2000, p. 1538.
- [42] DeCarlo and Lin, *Linear Circuit Analysis*. New York: Oxford University Press, 2001.

Appendix 2 Rectifier MATLAB code

```
function out = Rectifier(in)

global var;

%in = [Vina, Vinb, Vinc, Iout, Fangle, Theta, Iina, Iinb, Iinc, T1i, T2i, T3i, T4i, T5i, T6i]
%out = [Vout+, Vout-, Iina, Iinb, Iinc, T1o, T2o, T3o, T4o, T5o, T6o]
%
%

Vina = in(1);
Vinb = in(2);
Vinc = in(3);
Iout = in(4)/2;
Fangle = in(5);
Theta = mod(in(6), 2*pi);
Iina = in(7);
Iinb = in(8);
Iinc = in(9);
T1i = round(in(10));
T2i = round(in(11));
T3i = round(in(12));
T4i = round(in(13));
T5i = round(in(14));
T6i = round(in(15));

FangleA = mod(2*pi*Fangle/360 + 5*pi/6, 2*pi);
FangleB = mod(2*pi*Fangle/360 + 9*pi/6, 2*pi);
FangleC = mod(2*pi*Fangle/360 + 13*pi/6, 2*pi);

%positive thyristors
if (Theta >= FangleA && Theta <= (FangleA + (10*pi*var.Fsupply*var.dt)))
    T2i = 1;
end
if (Theta >= FangleB && Theta <= (FangleB + (10*pi*var.Fsupply*var.dt)))
    T3i = 1;
end
if (Theta >= FangleC && Theta <= (FangleC + (10*pi*var.Fsupply*var.dt)))
    T1i = 1;
end

FangleA = mod(2*pi*Fangle/360 + 11*pi/6, 2*pi);
FangleB = mod(2*pi*Fangle/360 + 15*pi/6, 2*pi);
FangleC = mod(2*pi*Fangle/360 + 19*pi/6, 2*pi);
%negative thyristors
if (Theta >= FangleA && Theta <= (FangleA + (10*pi*var.Fsupply*var.dt)))
    T5i = 1;
end
if (Theta >= FangleB && Theta <= (FangleB + (10*pi*var.Fsupply*var.dt)))
    T6i = 1;
end
if (Theta >= FangleC && Theta <= (FangleC + (10*pi*var.Fsupply*var.dt)))
    T4i = 1;
end

if (-0.1*Iout <= Iina && Iina <= 0.1*Iout) %statement to prevent deviantions round zero
    dIina = -Iina/var.dt;
else
    dIina = 0;
end

if (-0.1*Iout <= Iinb && Iinb <= 0.1*Iout) %statement to prevent deviantions round zero
    dIinb = -Iinb/var.dt;
else
    dIinb = 0;
end

if (-0.1*Iout <= Iinc && Iinc <= 0.1*Iout) %statement to prevent deviantions round zero
    dIinc = -Iinc/var.dt;
else
    dIinc = 0;
end
```

```

%positive output, one thyristor conducting
if (T1i==1 && T2i==0 && T3i==0)           %A conducting
    Voutp = Vina;
    dIina = (Iout - Iina)/var.dt;
    T1o = 1;
    T2o = 0;
    T3o = 0;
elseif (T1i==0 && T2i==1 && T3i==0)       %B conducting
    Voutp = Vinb;
    dIinb = (Iout - Iinb)/var.dt;
    T1o = 0;
    T2o = 1;
    T3o = 0;
elseif (T1i==0 && T2i==0 && T3i==1)       %C conducting
    Voutp = Vinc;
    dIinc = (Iout - Iinc)/var.dt;
    T1o = 0;
    T2o = 0;
    T3o = 1;

%positive output, two thyristors conducting
elseif (T1i==1 && T2i==1 && T3i==0)       %A & B conducting
    if (Vina >= Vinb)
        Voutp = Vina;
        if (Iinb > 0)
            dIina = (Vina - Vinb)/var.Lsystem;
            dIinb = (Vinb - Vina)/var.Lsystem;
        end
    else
        Voutp = Vinb;
        if (Iina > 0)
            dIina = (Vina - Vinb)/var.Lsystem;
            dIinb = (Vinb - Vina)/var.Lsystem;
        end
    end
    T1o = isposrealscalar(Iina);
    T2o = isposrealscalar(Iinb);
    T3o = 0;

elseif (T1i==0 && T2i==1 && T3i==1)       %B & C conducting
    if (Vinb >= Vinc)
        Voutp = Vinb;
        if (Iinc > 0)
            dIinb = (Vinb - Vinc)/var.Lsystem;
            dIinc = (Vinc - Vinb)/var.Lsystem;
        end
    else
        Voutp = Vinc;
        if (Iinb > 0)
            dIinb = (Vinb - Vinc)/var.Lsystem;
            dIinc = (Vinc - Vinb)/var.Lsystem;
        end
    end
    T1o = 0;
    T2o = isposrealscalar(Iinb);
    T3o = isposrealscalar(Iinc);

elseif (T1i==1 && T2i==0 && T3i==1)       %C & A conducting
    if (Vinc >= Vina)
        Voutp = Vinc;
        if (Iina > 0)
            dIinc = (Vinc - Vina)/var.Lsystem;
            dIina = (Vina - Vinc)/var.Lsystem;
        end
    else
        %if Phase A voltage higher than Phase C
        %output voltage equals phase C voltage
        %if full current in C (commutation from C to A), no changes in both
        %currents, if current in A (commutation from A to C or current in A
        %not fully decreased)
    end
    T1o = 1;
    T2o = 0;
    T3o = 1;
end

```

```

Voutp = Vina; %output voltage equals phase A voltage
if (Iinc > 0) %if full current in A (commutation from A to C), no changes in both
               %currents, if current in C (commutation from C to A or current in A
               %not fully decreased)
    dIinc = (Vinc - Vina)/var.Lsystem;
    dIina = (Vina - Vinc)/var.Lsystem;
end
end
T1o = isposrealscalar(Iina); %switch off when current becomes zero
T2o = 0;
T3o = isposrealscalar(Iinc); %switch off when current becomes zero

else
Voutp = 0;
T1o = var.Thyrec0(1);
T2o = var.Thyrec0(2);
T3o = var.Thyrec0(3);
end

%negative output, one thyristor conducting
if (T4i==1 && T5i==0 && T6i==0) %A conducting
    Voutn = Vina;
    dIina = (-Iout - Iina)/var.dt;
    T4o = 1;
    T5o = 0;
    T6o = 0;
elseif (T4i==0 && T5i==1 && T6i==0) %B conducting
    Voutn = Vinb;
    dIinb = (-Iout - Iinb)/var.dt;
    T4o = 0;
    T5o = 1;
    T6o = 0;
elseif (T4i==0 && T5i==0 && T6i==1) %C conducting
    Voutn = Vinc;
    dIinc = (-Iout - Iinc)/var.dt;
    T4o = 0;
    T5o = 0;
    T6o = 1;

%negative output, two thyristors conducting
elseif (T4i==1 && T5i==1 && T6i==0) %A & B conducting
    if (Vina <= Vinb) %if Phase A voltage lower than Phase B
        Voutn = Vina; %output voltage equals phase A voltage
        if (Iinb < 0) %if full current in A (commutation from A to B), no changes in both
                     %currents, if current in B (commutation from B to A or current in B
                     %not fully decreased)
            dIina = (Vina - Vinb)/var.Lsystem;
            dIinb = (Vinb - Vina)/var.Lsystem;
        end
    else %if Phase B voltage higher than Phase A
        Voutn = Vinb; %output voltage equals phase B voltage
    end
if (Iina < 0) %if full current in B (commutation from B to A), no changes in
              %both currents, if current in A (commutation from A to B or current
              %in B not fully decreased)
    dIina = (Vina - Vinb)/var.Lsystem;
    dIinb = (Vinb - Vina)/var.Lsystem;
end
end
T4o = not(isposrealscalar(Iina)); %switch off when current becomes zero
T5o = not(isposrealscalar(Iinb)); %switch off when current becomes zero
T6o = 0;

elseif (T4i==0 && T5i==1 && T6i==1) %B & C conducting
    if (Vinb <= Vinc) %if Phase B voltage higher than Phase C
        Voutn = Vinb; %output voltage equals phase B voltage
        if (Iinc < 0) %if full current in B (commutation from B to C), no changes in both
                     %currents, if current in C (commutation from C to B or current in C
                     %not fully decreased)
            dIinb = (Vinb - Vinc)/var.Lsystem;
            dIinc = (Vinc - Vinb)/var.Lsystem;
        end
    else %if Phase C voltage higher than Phase B
        Voutn = Vinc; %output voltage equals phase C voltage
    end
end

```

```

    if (Iinb < 0)                                %if full current in C (commutation from C to B), no changes in both
                                                %currents, if current in C (commutation from B to C or current in C
                                                %not fully decreased)
        dIinb = (Vinb - Vinc)/var.Lsystem;
        dIinc = (Vinc - Vinb)/var.Lsystem;
    end
end
T4o = 0;
T5o = not(isposrealscalar(Iinb));              %switch off when current becomes zero
T6o = not(isposrealscalar(Iinc));              %switch off when current becomes zero

elseif (T4i==1 && T5i==0 && T6i==1)            %C & A conducting
    if (Vinc <= Vina)                            %if Phase C voltage higher than Phase A
        Voutn = Vinc;                            %output voltage equals phase C voltage
        if (Iina < 0)                            %if full current in C (commutation from C to A), no changes in both
                                                %currents, if current in A (commutation from A to C or current in A
                                                %not fully decreased)
            dIinc = (Vinc - Vina)/var.Lsystem;
            dIina = (Vina - Vinc)/var.Lsystem;
        end
    else
        Voutn = Vina;                            %if Phase A voltage higher than Phase C
                                                %output voltage equals phase A voltage
        if (Iinc < 0)                            %if full current in A (commutation from A to C), no changes in both
                                                %currents, if current in A (commutation from C to A or current in A
                                                %not fully decreased)
            dIinc = (Vinc - Vina)/var.Lsystem;
            dIina = (Vina - Vinc)/var.Lsystem;
        end
    end
end
T4o = not(isposrealscalar(Iina));              %switch off when current becomes zero
T5o = 0;
T6o = not(isposrealscalar(Iinc));              %switch off when current becomes zero

else
Voutn = 0;
T4o = var.Thyrec0(4);
T5o = var.Thyrec0(5);
T6o = var.Thyrec0(6);
end

out = [Voutp, Voutn, dIina, dIinb, dIinc, T1o, T2o, T3o, T4o, T5o, T6o];

end

```

Appendix 3 Inverter MATLAB Code

```
function out = Inverter(in)

global var;

%in = [Iouta, Ioutb, Ioutc, Iin, Theta, Fangle, Vouta, Voutb, Voutc, T1i, T2i, T3i, T4i, T5i, T6i, T7i, T8i, T9i,
T10i, T11i, T12i]
%out = [Vin+, Vin-, dVouta, dVoutb, dVoutc, T1o, T2o, T3o, T4o, T5o, T6o, T7o, T8o, T9o, T10o, T11o, T12o]

Ioutfal = in(1);
Ioutfb1 = in(2);
Ioutfc1 = in(3);
Iin = in(4)/2;
Theta = mod((in(5)-var.theta0)*var.p, 2*pi);
Theta2 = mod((in(5)+ pi/6)-var.theta0)*var.p, 2*pi);
Fangle = in(6);
Voutfal = in(7);
Voutfb1 = in(8);
Voutfc1 = in(9);
T1i = round(in(10));
T2i = round(in(11));
T3i = round(in(12));
T4i = round(in(13));
T5i = round(in(14));
T6i = round(in(15));
T7i = round(in(16));
T8i = round(in(17));
T9i = round(in(18));
T10i = round(in(19));
T11i = round(in(20));
T12i = round(in(21));

FangleA = mod(2*pi*Fangle/360 - 1*pi/6, 2*pi);
FangleB = mod(2*pi*Fangle/360 + 3*pi/6, 2*pi);
FangleC = mod(2*pi*Fangle/360 + 7*pi/6, 2*pi);

%positive thyristors
if (Theta >= FangleA && Theta <= (FangleA + (10*pi*50*var.dt)))
    T2i = 1;
end
if (Theta >= FangleB && Theta <= (FangleB + (10*pi*50*var.dt)))
    T3i = 1;
end
if (Theta >= FangleC && Theta <= (FangleC + (10*pi*50*var.dt)))
    T1i = 1;
end
if (Theta2 >= FangleA && Theta2 <= (FangleA + (10*pi*50*var.dt)))
    T8i = 1;
end
if (Theta2 >= FangleB && Theta2 <= (FangleB + (10*pi*50*var.dt)))
    T9i = 1;
end
if (Theta2 >= FangleC && Theta2 <= (FangleC + (10*pi*50*var.dt)))
    T7i = 1;
end

FangleA = mod(2*pi*Fangle/360 + 5*pi/6, 2*pi);
FangleB = mod(2*pi*Fangle/360 + 9*pi/6, 2*pi);
FangleC = mod(2*pi*Fangle/360 + 1*pi/6, 2*pi);
%negative thyristors
if (Theta >= FangleA && Theta <= (FangleA + (10*pi*50*var.dt)))
    T5i = 1;
end
if (Theta >= FangleB && Theta <= (FangleB + (10*pi*50*var.dt)))
    T6i = 1;
end
if (Theta >= FangleC && Theta <= (FangleC + (10*pi*50*var.dt)))
    T4i = 1;
end
if (Theta2 >= FangleA && Theta2 <= (FangleA + (10*pi*50*var.dt)))
    T11i = 1;
end
end
```

```

if (Theta2 >= FangleB && Theta2 <= (FangleB + (10*pi*50*var.dt)))
    T12i = 1;
end
if (Theta2 >= FangleC && Theta2 <= (FangleC + (10*pi*50*var.dt)))
    T10i = 1;
end

theta1 = 2*pi*30/360;
theta2 = 2*pi*150/360;
theta3 = -2*pi*90/360;

angle = 2*pi/3;

Rotp = (2/3)*[cos(theta1), cos(theta2), cos(theta3);
             cos(theta1 - angle), cos(theta2 - angle), cos(theta3 - angle);
             cos(theta1 + angle), cos(theta2 + angle), cos(theta3 + angle)];

theta1 = -2*pi*30/360;
theta2 = 2*pi*90/360;
theta3 = -2*pi*150/360;

Rotn = (2/3)*[cos(theta1), cos(theta2), cos(theta3);
             cos(theta1 - angle), cos(theta2 - angle), cos(theta3 - angle);
             cos(theta1 + angle), cos(theta2 + angle), cos(theta3 + angle)];

Ioutf2 = Rotp * [Ioutfa1; Ioutfb1; Ioutfc1];
Voutf2 = Rotp * [Voutfa1; Voutfb1; Voutfc1];

Ioutfa2 = Ioutf2(1);
Ioutfb2 = Ioutf2(2);
Ioutfc2 = Ioutf2(3);

Voutfa2 = Voutf2(1);
Voutfb2 = Voutf2(2);
Voutfc2 = Voutf2(3);

F12 = 1 + sqrt(1/3);
Ioff = Iin/sqrt(3);

%without phase shift
Iouta1 = 0;
Ioutb1 = 0;
Ioutc1 = 0;

%positive output, one thyristor conducting
if (T1i==1 && T2i==0 && T3i==0)           %A conducting
    Vinp1 = Voutfa1;
    Iouta1 = Iin;
    T1o = 1;
    T2o = 0;
    T3o = 0;
elseif (T1i==0 && T2i==1 && T3i==0)       %B conducting
    Vinp1 = Voutfb1;
    Ioutb1 = Iin;
    T1o = 0;
    T2o = 1;
    T3o = 0;
elseif (T1i==0 && T2i==0 && T3i==1)       %C conducting
    Vinp1 = Voutfc1;
    Ioutc1 = Iin;
    T1o = 0;
    T2o = 0;
    T3o = 1;

%positive output, two thyristors conducting
elseif (T1i==1 && T2i==1 && T3i==0)       %A & B conducting
    Iouta1 = F12*Iin - Ioutfb1;           %Voltage equals deviation in current times expected
                                          %inductance
    Ioutb1 = F12*Iin - Ioutfa1;           %voltage equals vouta (parralel)
    Vinp1 = Voutfa1;                       %voltage equals outputs voltages
    T1o = isposrealscalar(Ioutfa1 - Ioff); %switch off when current becomes zero
    T2o = isposrealscalar(Ioutfb1 - Ioff); %switch off when current becomes zero
    T3o = 0;
elseif (T1i==0 && T2i==1 && T3i==1)       %B & C conducting

```

```

Ioutb1 = F12*Iin - Ioutfc1; %Voltage equals deviation in current times expected
                                inductance
Ioutc1 = F12*Iin - Ioutfb1; %voltage equals voutb (parralel)
Vinp1 = Voutfb1; %voltage equals outputs voltages
T1o = 0;
T2o = isposrealscalar(Ioutfb1 - Ioff); %switch off when current becomes zero
T3o = isposrealscalar(Ioutfc1 - Ioff); %switch off when current becomes zero
elseif (T1i==1 && T2i==0 && T3i==1) %C & A conducting
    Ioutc1 = F12*Iin - Ioutfal; %Voltage equals deviation in current times expected
                                inductance
    Iouta1 = F12*Iin - Ioutfc1; %voltage equals voutc (parralel)
    Vinp1 = Voutfc1; %voltage equals outputs voltages
    T1o = isposrealscalar(Ioutfal - Ioff); %switch off when current becomes zero
    T2o = 0;
    T3o = isposrealscalar(Ioutfc1 - Ioff); %switch off when current becomes zero
else
    Vinp1 = 0;
    T1o = 0;
    T2o = 0;
    T3o = 0;
end

%negative output, one thyristor conducting
if (T4i==1 && T5i==0 && T6i==0) %A conducting
    Vinn1 = Voutfal;
    Iouta1 = -Iin;
    T4o = 1;
    T5o = 0;
    T6o = 0;
elseif (T4i==0 && T5i==1 && T6i==0) %B conducting
    Vinn1 = Voutfb1;
    Ioutb1 = -Iin;
    T4o = 0;
    T5o = 1;
    T6o = 0;
elseif (T4i==0 && T5i==0 && T6i==1) %C conducting
    Vinn1 = Voutfc1;
    Ioutc1 = -Iin;
    T4o = 0;
    T5o = 0;
    T6o = 1;

%negative output, two thyristors conducting
elseif (T4i==1 && T5i==1 && T6i==0) %A & B conducting
    Iouta1 = -F12*Iin - Ioutfb1; %Voltage equals deviation in current times expected
                                inductance
    Ioutb1 = -F12*Iin - Ioutfal; %voltage equals vouta (parralel)
    Vinn1 = Voutfal; %voltage equals outputs voltages
    T4o = not(isposrealscalar(Ioutfal + Ioff)); %switch off when current becomes zero
    T5o = not(isposrealscalar(Ioutfb1 + Ioff)); %switch off when current becomes zero
    T6o = 0;
elseif (T4i==0 && T5i==1 && T6i==1) %B & C conducting
    Ioutb1 = -F12*Iin - Ioutfc1; %Voltage equals deviation in current times expected
                                inductance
    Ioutc1 = -F12*Iin - Ioutfb1; %voltage equals voutb (parralel)
    Vinn1 = Voutfb1; %voltage equals outputs voltages
    T4o = 0;
    T5o = not(isposrealscalar(Ioutfb1 + Ioff)); %switch off when current becomes zero
    T6o = not(isposrealscalar(Ioutfc1 + Ioff)); %switch off when current becomes zero
elseif (T4i==1 && T5i==0 && T6i==1) %C & A conducting
    Ioutc1 = -F12*Iin - Ioutfal; %Voltage equals deviation in current times expected
                                inductance
    Iouta1 = -F12*Iin - Ioutfc1; %voltage equals voutc (parralel)
    Vinn1 = Voutfc1; %voltage equals outputs voltages
    T4o = not(isposrealscalar(Ioutfal + Ioff)); %switch off when current becomes zero
    T5o = 0;
    T6o = not(isposrealscalar(Ioutfc1 + Ioff)); %switch off when current becomes zero
else
    Vinn1 = 0;
    T4o = 0;
    T5o = 0;
    T6o = 0;
end

%with phase shift
Iouta2 = 0;
Ioutb2 = 0;

```

```

Ioutc2 = 0;

%positive output, one thyristor conducting
if (T7i==1 && T8i==0 && T9i==0) %A conducting
    Vinp2 = Voutfa2;
    Iouta2 = Iin;
    T7o = 1;
    T8o = 0;
    T9o = 0;
elseif (T7i==0 && T8i==1 && T9i==0) %B conducting
    Vinp2 = Voutfb2;
    Ioutb2 = Iin;
    T7o = 0;
    T8o = 1;
    T9o = 0;
elseif (T7i==0 && T8i==0 && T9i==1) %C conducting
    Vinp2 = Voutfc2;
    Ioutc2 = Iin;
    T7o = 0;
    T8o = 0;
    T9o = 1;

%positive output, two thyristors conducting
elseif (T7i==1 && T8i==1 && T9i==0) %A & B conducting
    Iouta2 = F12*Iin - Ioutfb2; %Voltage equals deviation in current times expected
                                inductance
    Ioutb2 = F12*Iin - Ioutfa2; %voltage equals vouta (parralel)
    Vinp2 = Voutfa2; %voltage equals outputs voltages
    T7o = isposrealscalar(Ioutfa2 - Ioff); %switch off when current becomes zero
    T8o = isposrealscalar(Ioutfb2 - Ioff); %switch off when current becomes zero
    T9o = 0;
elseif (T7i==0 && T8i==1 && T9i==1) %B & C conducting
    Ioutb2 = F12*Iin - Ioutfc2; %Voltage equals deviation in current times expected
                                inductance
    Ioutc2 = F12*Iin - Ioutfb2; %voltage equals voutb (parralel)
    Vinp2 = Voutfb2; %voltage equals outputs voltages
    T7o = 0;
    T8o = isposrealscalar(Ioutfb2 - Ioff); %switch off when current becomes zero
    T9o = isposrealscalar(Ioutfc2 - Ioff); %switch off when current becomes zero
elseif (T7i==1 && T8i==0 && T9i==1) %C & A conducting
    Ioutc2 = F12*Iin - Ioutfa2; %Voltage equals deviation in current times expected
                                inductance
    Iouta2 = F12*Iin - Ioutfc2; %voltage equals voutc (parralel)
    Vinp2 = Voutfc2; %voltage equals outputs voltages
    T7o = isposrealscalar(Ioutfa2 - Ioff); %switch off when current becomes zero
    T8o = 0;
    T9o = isposrealscalar(Ioutfc2 - Ioff); %switch off when current becomes zero
else
    Vinp2 = 0;
    T7o = 0;
    T8o = 0;
    T9o = 0;
end

%negative output, one thyristor conducting
if (T10i==1 && T11i==0 && T12i==0) %A conducting
    Vinn2 = Voutfa2;
    Iouta2 = -Iin;
    T10o = 1;
    T11o = 0;
    T12o = 0;
elseif (T10i==0 && T11i==1 && T12i==0) %B conducting
    Vinn2 = Voutfb2;
    Ioutb2 = -Iin;
    T10o = 0;
    T11o = 1;
    T12o = 0;
elseif (T10i==0 && T11i==0 && T12i==1) %C conducting
    Vinn2 = Voutfc2;
    Ioutc2 = -Iin;
    T10o = 0;
    T11o = 0;
    T12o = 1;

%negative output, two thyristors conducting
elseif (T10i==1 && T11i==1 && T12i==0) %A & B conducting

```

```

Iouta2 = -F12*Iin - Ioutfb2; %Voltage equals deviation in current times expected
                                inductance
Ioutb2 = -F12*Iin - Ioutfa2; %voltage equals vouta (parralel)
Vinn2 = Voutfa2; %voltage equals outputs voltages
T10o = not(isposrealscalar(Ioutfa2 + Ioff)); %switch off when current becomes zero
T11o = not(isposrealscalar(Ioutfb2 + Ioff)); %switch off when current becomes zero
T12o = 0;
elseif (T10i==0 && T11i==1 && T12i==1) %B & C conducting
    Ioutb2 = -F12*Iin - Ioutfc2; %Voltage equals deviation in current times expected
                                inductance
    Ioutc2 = -F12*Iin - Ioutfb2; %voltage equals voutb (parralel)
    Vinn2 = Voutfb2; %voltage equals outputs voltages
    T10o = 0;
    T11o = not(isposrealscalar(Ioutfb2 + Ioff)); %switch off when current becomes zero
    T12o = not(isposrealscalar(Ioutfc2 + Ioff)); %switch off when current becomes zero
elseif (T10i==1 && T11i==0 && T12i==1) %C & A conducting
    Ioutc2 = -F12*Iin - Ioutfa2; %Voltage equals deviation in current times expected
                                inductance
    Iouta2 = -F12*Iin - Ioutfc2; %voltage equals voutc (parralel)
    Vinn2 = Voutfc2; %voltage equals outputs voltages
    T10o = not(isposrealscalar(Ioutfa2 + Ioff)); %switch off when current becomes zero
    T11o = 0;
    T12o = not(isposrealscalar(Ioutfc2 + Ioff)); %switch off when current becomes zero
else
    Vinn2 = 0;
    T10o = 0;
    T11o = 0;
    T12o = 0;
end

Iout2r = Rotn * [Iouta2; Ioutb2; Ioutc2];

Vouta = var.Lmotor*((Iouta1 + Iout2r(1))-Ioutfa1)/var.dt;
Voutb = var.Lmotor*((Ioutb1 + Iout2r(2))-Ioutfb1)/var.dt;
Voutc = var.Lmotor*((Ioutc1 + Iout2r(3))-Ioutfc1)/var.dt;

Vinp = (Vinp1 + Vinp2);
Vinn = (Vinn1 + Vinn2);

out = [Vinp, Vinn, Vouta, Voutb, Voutc, T1o, T2o, T3o, T4o, T5o, T6o, T7o, T8o, T9o, T10o, T11o, T12o];
end

```